Universidad de Huelva

Departamento de Ciencias de la Tierra

Hydrogeochemical and mineralogical study of the ecological treatment of phosphogypsum leachates

Memoria para optar al grado de doctor
presentada por:

Ricardo Millán Becerro

Fecha de lectura: 31 de mayo de 2022

Bajo la dirección de los doctores:

Rafael Pérez López

Francisco Macías Suárez

Huelva, 2022

Universidad de Huelva

Departamento de Ciencias de la Tierra

Hydrogeochemical and mineralogical study of the ecological treatment of phosphogypsum leachates

Memoria para optar al grado de doctor
presentada por:

Ricardo Millán Becerro

Fecha de lectura: May 2022

Bajo la dirección de:

Dr. Rafael Pérez López

Dr. Francisco Macías Suárez

Huelva, 2022

University of Huelva

Department of Earth Sciences

Hydrogeochemical and mineralogical study of the ecological treatment of phosphogypsum leachates

Conducted by:

Ricardo Millán Becerro

May 2022

Supervised by:

Dr. Rafael Pérez López

Dr. Francisco Macías Suárez

This Doctoral thesis has been carried out within the framework of the Official Doctoral Program in Industrial and Environmental Science and Technology to obtain the degree of International Doctor in Earth Sciences at the University of Huelva.

FINANCIACIÓN

La presente tesis doctoral ha sido cofinanciada por la Junta de Andalucía a través del proyecto de investigación FOREVER "Fosfoyesos: de su evaluación ambiental como residuo a su revalorización como recurso" (Ref.: P12-RNM-2260) y por el Ministerio de Economía y Competitividad de España (MINECO) a través del proyecto de investigación CAPOTE "Contaminación asociada a la actividad minera que se transfiere al Océano Atlántico: Procesos geoquímico en el Estuario Odiel-Tinto" (Ref.: CGL2017-86050-R).

El doctorando estuvo contratado durante 18 meses con cargo al Proyecto de Excelencia de la Consejería de Economía y Conocimiento de la Junta de Andalucía Ref.: P12-RNM-2260 "Fosfoyeso: de su evaluación ambiental como residuo a su revalorización como recurso" (FOREVER). Actualmente, el doctorando es financiado por el Ministerio de Ciencia e Innovación a través de su programa de ayudas para contratos predoctorales para la formación de doctores (FPI; PRE2018-085765), vinculada al proyecto CAPOTE (Ref.: CGL2017-86050-R).

AGRADECIMIENTOS

Ahora que comienzo a vislumbrar la luz al final del túnel, me gustaría tener mis primeras palabras de agradecimiento para mi director de tesis Rafael Pérez López, quien me ha hecho de lazarillo durante todos estos años de duro trabajo, señalándome el camino y la meta final. Aún recuerdo, cuando comezaba el trabajo fin de grado, y me hablabas por las noches para comentarme algunos resultados de los análisis que nos habían mandado de los laboratorios del CIDERTA. Esta vinculación siguió con la realización del trabajo fin de máster y posteriormente la presente tesis. Gracias por ser un referente para mí en este mundillo de la investigación en el que comencé hace unos años a dar mis primeros pasos y en el que espero no tener techo. Perdona por no considerarte ya mi profesor o director, sino un amigo. En segundo lugar, me gustaría agradecer la ayuda prestada por mi otro director Francisco Macías Suárez, tu afán de aprender y de adquirir nuevos conocimientos no tiene límites y ha de ser así, ya que los humanos morimos cuando dejamos de aprender. Que nunca se deje de oír por los pasillos esa fracesilla de "illo que guapo!!". Gracias José Miguel Nieto Liñán por ser el faro que guía al grupo GeoEnvi y por estar siempre dispuesto a resolver preguntas que para el resto parecen no tener respuestas.

Por otra parte me gustaría dar las gracias a Carlos Ruíz Cánovas, pese a que tu nombre no aparece como director de esta tesis, es sabido que tú has sido también mi director. Muchas gracias por toda la ayuda prestada. Ahora que parece que va llegando el final, he de decirte que en más de una ocasión, cuando me acercaba a tu despacho y comenzabas a recitarme tecnicismos como si ya fuese postdoc, yo asentaba con la cabeza y decía en voz baja; "madre mía donde me he metido!!". Muchas gracias María de los Dolores Basallote Sanchez por estar siempre ahí, dispuesta a resolverme cualquier pregunta que se me pasara por la cabeza.

Gracias al grupo de curritos compuesto por Rafael León Cortegano, Raul Moreno Gonzalez, José María Fuentes López y Jonatan Romero Matos, en el que me incluyo y del que nunca parece que podré salir, sin ustedes este tiempo nada habría sido igual. Rafa te recuerdo que el día que dejamos el coche del grupo sepultado en barro, me prometiste que aparecería como autor en una de tus publicaciones…Ha pasado más de un año, ponte las pilas!!

Finalmente, dar las gracias a mi madre, mi pareja Carmen y resto de familiares por darme la estabilidad necesaria y por ser un pilar básico en el dia a dia. El logro de esta nueva meta también es gracias a ti, mira donde está llegando tu campeón.

ABSTRACT

The production of phosphoric acid in the phosphate fertilizer industry, via the wet chemical attack of phosphate rock with sulfuric acid, generates an unwanted by-product known as phosphogypsum. This waste is mainly composed of gypsum ($CaSO_4 \cdot 2H_2O$) and contains high amounts of metal(loid)s, radionuclides and a residual fraction of free acids. Despite the high content of toxic impurities, most of phosphogypsum wastes generated around the world are stored in stacks close to coastal areas and exposed to continuous weathering processes. Thus, approximately 100 million tons of phosphogypsum wastes were stockpiled onto salt-marsh soils of the Tinto River estuary (Huelva, SW Spain). This phosphogypsum stack is a continuous source of pollution to the estuarine environment due to the existence of two types of highly acidic and polluted waters; on the one hand, the process water stored in surface ponds on the stack, which was used to transport the waste as a slurry from the industry, and on the other hand, the polluted groundwater contained in the stack that is drained outside through numerous sources of contamination, known as edge outflows. The main objective of this research work is to develop an effective treatment system for acidic and polluted effluents from the phosphogypsum stack, since it is assumed to be the only viable option to minimize its impact on the surrounding environment.

Firstly, edge outflows were sampled around the whole perimeter of the phosphogypsum stack during four sampling campaigns under different hydrological conditions, in order to study their seasonal and spatial hydrochemical variability. In addition, water-table variations within the phosphogypsum stack were analyzed, in order to know the hydrological response of the system to the different weathering agents. For this purpose, a CTD-Diver was installed in a bore-hole within the profile of the phosphogypsum pile. In periods with absence of rains, the water-table of the stack remained almost constant most of the time (± 2 cm) and only oscillated with the tidal fluctuations. Nevertheless, during the rainy events, the water-table level of the pile increased up to 20 cm and subsequently decreased, defining peaks that coincided with rainfalls. The hydraulic response of the phosphogypsum stack, similar to that of a coastal karst aquifer, and the geochemical characteristics of the leachates pointed to an estuarine origin for the edge outflows. With respect to the hydrochemical behavior of edge leachates, the concentration of most contaminants (e.g., PO_4, F, Al, Zn, U or Cd) suffered a slight decrease from the dry-warm to the rainy period, due to a dilution effect by rainwater recharge. These leachates discharge high loads of pollutants to the estuary, e.g., PO_4, F,

As and U (average values of 5000 tons/yr, 300 tons/yr, 6.9 tons/yr and 3.0 tons/yr, respectively).

Secondly, a titration experiment was performed to assess the feasibility of a potential alkaline treatment system for phosphogypsum leachates. The experiment was based on the addition of a $Ca(OH)_2$ solution to different types of phosphogypsum-related acidic leachates. The alkaline addition provoked an efficient removal of most dissolved pollutants. In fact, removal values close to 100% were achieved for PO_4, Fe, Al, Cr, Zn Cd, and U. However, it was not so effective for As (removal of 57–82%) due probably to competition between As (in the form of oxyanion) and anionic P species for the same binding sites in the newly-formed solids. The removal of elements in solution occurred by co-precipitation and/or adsorption with phosphate phases, as well as by fluoride precipitation. The newly-formed precipitates during the treatment were subjected to two standardized leaching tests (EN 12457-2 from the European Union and TCLP from the United States) for their classification and management according to their hazardousness. In this sense, some of the solids precipitated during the treatment should be classified as hazardous wastes due to the high concentrations of As released.

Thirdly, column experiments were performed in the laboratory to simulate the passive treatment of edge outflows using the dispersed alkaline substrate (DAS) technology. Passive treatment was chosen given the orphan site condition of some zones of the phosphogypsum stack. The experiment consisted of flowing the acid leachates through columns loaded with a mixture of an alkaline reagent (i.e., limestone, barium carbonate (whiterite, $BaCO_3$), biomass ash, fly ash, MgO, $Mg(OH)_2$ or $Ca(OH)_2$) and an inert matrix. The $Ca(OH)_2$-DAS and MgO-DAS treatment systems were the most effective, achieving near total removal for PO_4, F, Fe, Zn, Cu, Al, Cr, and U. However, the total removal of As was only reached in the $Ca(OH)_2$-DAS treatment. The removal of contaminants was mainly due to the precipitation of phosphate minerals.

Once the high effectiveness of the MgO-DAS and $Ca(OH)_2$-DAS treatment systems was demonstrated, these treatments were replicated under equal conditions in order to collect solid samples for their mineralogical and geochemical characterization, as well as to evaluate their potential environmental risk. These DAS treatments generated significant amounts of metal-rich wastes. Therefore, the hazardousness of these solids must be evaluated prior to their disposal in a landfill, in order to avoid potential environmental

impacts. To this end, the DAS wastes were subjected to the European Union EN 12457-2 and United State TCLP leaching tests. According to European Union legislation, some of these solids should be classified as hazardous wastes due to the release of high concentrations of SO_4 or Sb. However, according to United States regulation, all DAS wastes are considered as non-hazardous material. In addition, the solid wastes from DAS treatment systems could be considered a secondary source of critical raw materials.

Finally, batch experiments were carried out in the laboratory to simulate the treatment of phosphogypsum-related leachates by adding an alkaline industrial waste (biomass ash), in order to design a combined system of sustainable treatment and metal recovery. These experiments consisted of batch reactions between biomass ash and phosphogypsum leachates at different solid-liquid (S:L) ratios (i.e., 1:2.5, 1:5, and 1:10). The alkaline treatment at a S:L ratio of 1:2.5 showed a high success in the elimination of contaminants, reaching removal values close to 100% for F, Fe, Zn, Al, Cr, U, Cu and Cd. These results are comparable to those achieved during the treatment with a conventional reactive (i.e., $Ca(OH)_2$). The precipitation of phosphate and fluoride phases was the main mechanism responsible for the depletion of pollutants during the treatments. In addition, the solids precipitated during the treatments contained high concentration of elements of high economic interest such as rare earth elements plus Y (REY), Sc, Be, V, Ga or U, with concentrations of up to 3992 mg/kg, 164 mg/kg, 7.0 mg/kg, 2974 mg/kg, 40 mg/kg and 2963 mg/kg, respectively. The potential recovery of these valuable elements contained in the newly-formed solids could help to offset the costs associated with the passive treatment.

RESUMEN

La producción de ácido fosfórico en la industria de fertilizantes fosfatados, a través del ataque químico húmedo de rocas fosfatadas con ácido sulfúrico, genera un subproducto no deseado conocido como fosfoyeso. Este residuo están compuesto principalmente por yeso ($CaSO_4 \cdot 2H_2O$) y contienen altas cantidades de metal(oide)s, radionúclidos y una fracción residual de ácidos libres. A pesar del alto contenido en impurezas tóxicas, la mayoría de los fosfoyesos generados en todo el mundo se almacenan en pilas cercanas a zonas costeras y están expuestos a continuos procesos de meteorización. Así, aproximadamente 100 millones de toneladas de fosfoyesos fueron depositados en balsas sobre los suelos de las marismas saladas del estuario del Río Tinto (Huelva, SO de España). Esta balsa de fosfoyesos es una fuente continua de contaminación al medio estuarino debido a la existencia de dos tipos de aguas altamente ácidas y contaminadas; por un lado, el agua de proceso que se almacena en estanques sobre la superficie de la balsa, la cual fue utilizada para transportar el residuo en forma de lodo desde la industria, y por otro lado, el agua subterránea contaminada contenida en la balsa que es drenada al exterior a través de numerosos focos de contaminación, conocidos como salidas de borde. El objetivo principal de este trabajo de investigación es desarrollar un sistema de tratamiento efectivo para los efluentes ácidos y contaminados procedentes de la balsa de fosfoyesos, ya que se asume que es la única opción viable para minimizar su impacto sobre el medio ambiente circundante.

En primer lugar, se muestrearon las salidas de borde alrededor de todo el perímetro de la balsa de fosfoyesos durante cuatro campañas de muestreo bajo diferentes condiciones hidrológicas, a fin de estudiar su variabilidad hidroquímica estacional y espacial. Además, se analizaron las variaciones del nivel freático dentro de la balsa de fosfoyesos, con el fin de conocer la respuesta hidrológica del sistema a los diferentes agentes de meteorización. Para este propósito, se instaló un CTD-Diver en un sondeo dentro del perfil de la pila de fosfoyesos. En períodos con ausencia de lluvias, el nivel freático de la balsa se mantuvo casi constante la mayor parte del tiempo (± 2 cm) y solo osciló con las fluctuaciones de las mareas. Sin embargo, durante los eventos lluviosos, el nivel freático de la pila aumentó hasta 20 cm y posteriormente disminuyó, definiendo picos que coincidieron con las lluvias. La respuesta hidráulica de la balsa de fosfoyesos, es similar a la de un acuífero kárstico costero, y las características geoquímicas de los lixiviados apuntaron a un origen estuarino para las salidas de borde. Con respecto al comportamiento hidroquímico de los lixiviados de borde, las concentraciones de la

mayoría de los contaminantes (e.g., PO_4, F, Al, Zn, U o Cd) sufrieron una ligera disminución desde el período seco-cálido al lluvioso, debido a un efecto de dilución por recarga de agua de lluvia. Estos lixiviados descargan una alta carga de contaminantes al estuario, e.g., PO_4, F, As y U (valores medios de 5000 toneladas/año, 300 toneladas/año, 6.9 toneladas/año y 3.0 toneladas/año, respectivamente).

En segundo lugar, se realizó un experimento de valoración para evaluar la viabilidad de un posible sistema de tratamiento alcalino para los lixiviados de fosfoyesos. El experimento se basó en la adición de una solución de $Ca(OH)_2$ a diferentes tipos de lixiviados ácidos relacionados con los fosfoyesos. La adición alcalina provocó una eliminación eficiente de la mayoría de los contaminantes disueltos. De hecho, se lograron valores de retención cercanos al 100% para PO_4, Fe, Al, Cr, Zn Cd y U. Sin embargo, éste no fue tan efectivo para As (eliminación del 57–82%) debido probablemente a la competencia entre As (en forma de oxianión) y especies aniónicas de P por los mismos sitios de unión en los sólidos neoformados. La retención de elementos en solución ocurrió por co-precipitación y/o adsorción con fases fosfatadas, así como por precipitación de fluoruros. Los precipitados neoformados durante el tratamiento fueron sometidos a dos tests de lixiviación estandarizados (EN 12457-2 de la Unión Europea y TCLP de Estados Unidos) para su clasificación y gestión de acuerdo a su peligrosidad. En este sentido, algunos de los sólidos precipitados durante el tratamiento deberían ser clasificados como residuos peligrosos debido a las altas concentraciones de As liberadas.

En tercer lugar, se realizaron experimentos en columnas en el laboratorio para simular el tratamiento pasivo de las salidas del borde utilizando la tecnología sustrato alcalino disperso (DAS). Se optó por el tratamiento pasivo dada la condición de sitio huérfano de algunas zonas de la balsa de fosfoyesos. El experimento consistió en hacer fluir el lixiviado ácido a través de columnas rellenas con una mezcla de un reactivo alcalino (i.e., caliza, carbonato de bario (witherita, $BaCO_3$), cenizas de biomasa, cenizas volantes, MgO, $Mg(OH)_2$ o $Ca(OH)_2$) y una matriz inerte. Los sistemas de tratamiento DAS-$Ca(OH)_2$ y DAS-MgO fueron los más efectivos, logrando una eliminación casi total de PO_4, F, Fe, Zn, Cu, Al, Cr y U. Sin embargo, la retención total de As sólo fue alcanzada con el tratamiento DAS-$Ca(OH)_2$. La retirada de contaminantes fue debida principalmente a la precipitación de minerales fosfatados.

Una vez demostrada la alta efectividad de los sistemas de tratamiento DAS-MgO y DAS-$Ca(OH)_2$, estos tratamientos fueron replicados en igualdad de condiciones con el fin de recoger muestras sólidas para su caracterización mineralógica y geoquímica, así como para evaluar su potencial riesgo ambiental. Estos tratamientos DAS generaron cantidades significativas de residuos ricos en metales. Por lo tanto, la peligrosidad de estos sólidos debe evaluarse antes de ser depositados en un vertedero, para evitar posibles impactos ambientales. Con este fin, los residuos DAS fueron sometidos a los tests de lixiviación EN 12457-2 de la Unión Europea y TCLP de Estados Unidos. Según la legislación de la Unión Europea, algunos de estos sólidos deben ser clasificados como residuos peligrosos debido a la liberación de altas concentraciones de SO_4 o Sb. Sin embargo, de acuerdo con la regulación de los Estados Unidos, todos los residuos DAS son considerados como material no peligroso. Además, los residuos sólidos procedentes de los sistemas de tratamiento DAS podrían ser considerados una fuente secundaria de materias primas críticas.

Finalmente, se llevaron a cabo experimentos batch en el laboratorio para simular el tratamiento de lixiviados relacionados con los fosfoyesos mediante la adición de un residuo industrial alcalino (cenizas de biomasa), con el fin de diseñar un sistema combinado de tratamiento sostenible y recuperación de metales. Estos experimentos consistieron en reacciones batch entre las cenizas de biomasa y el lixiviado de fosfoyeso en diferentes proporciones sólido-líquido (S:L) (i.e., 1:2.5, 1:5 y 1:10). El tratamiento alcalino en un ratio S:L de 1:2.5 mostró un alto éxito en la eliminación de contaminantes, alcanzando valores de retención cercanos al 100% para F, Fe, Zn, Al, Cr, U, Cu y Cd. Estos resultados son comparables a los obtenidos durante el tratamiento con un reactivo convencional (i.e., $Ca(OH)_2$). La precipitación de fases fosfatadas y fluoruros fue el principal mecanismo responsable de la retirada de los contaminantes durante los tratamientos. Además, los sólidos precipitados durante los tratamientos mostraron altas concentraciones de elementos de alto interés económico tales como elementos de tierras raras más Y (REY), Sc, Be, V, Ga o U, con concentraciones de hasta 3992 mg/kg, 164 mg/kg, 7,0 mg/kg, 2974 mg/kg, 40 mg/kg y 2963 mg/kg, respectivamente. La potencial recuperación de estos elementos valiosos contenidos en los sólidos neoformados podría ayudar a compensar los costes asociados con el tratamiento pasivo.

INDEX:

LIST OF FIGURES AND TABLES:

Chapter 1:

Chapter 2:

Chapter 3:

Chapter 4:

Chapter 6:

PUBLICACIONES

Los artículos publicados en los capítulos 3, 4 y 6, debido a restricciones relativas a derechos de autor, han sido retirados de la tesis. En sustitución de los artículos ofrecemos la siguiente información: referencia bibliográfica, enlace a la revista y resumen.

Capítulo 3:

Millán-Becerro, R., Pérez-López, R., Macías, F., Cánovas, C. R., Papaslioti, E.-M., & Dolores Basallote, M. (2019). Assessment of metals mobility during the alkaline treatment of highly acid phosphogypsum leachates. In Science of The Total Environment (Vol. 660, pp. 395–405). Elsevier BV. https://doi.org/10.1016/j.scitotenv.2018.12.305

Enlace al texto completo: https://doi.org/10.1016/j.scitotenv.2018.12.305

Resumen:

This research evaluates the feasibility of an alkaline treatment system for highly acid leachates from a phosphogypsum stack located in an estuarine environment degraded by such pollution. The presented methodology consists of the addition of a Ca(OH)2 solution to the different types of phosphogypsum-related acidic leachates with the aim to increase their pH and subsequently, to provoke the precipitation and immobilization of the dissolved contaminants. In fact, phosphates and fluorides reached removal of 100% and 90%, respectively. As regards metals, removal values close to 100% were reached for Fe, Al, Cr, Cd, U and Zn, whereas it did not seem to be totally effective for other elements such as As (removal of 57–82%) and Sb (4–36%). The decrease of contaminant concentrations was caused probably by co-precipitation and/or adsorption to phosphate phases, together with by fluoride precipitation. The solid phases formed during the treatment were subjected to two standard leaching tests (EN 12457-2 from the EU and TCLP from the US) in order to conduct a risk and management assessment. In this context, some of the precipitates formed during the treatment would be classified as hazardous wastes, due to the high concentration of As leached. Moreover, the potential economic costs of a convectional active treatment system were also explored. This study sets the basis for a new research line with the aim to minimise the impact of the phosphogypsum stacks worldwide to their adjacent environment.

Capítulo 4:

Millán-Becerro, R., Pérez-López, R., Macías, F., & Cánovas, C. R. (2020). Design and optimization of sustainable passive treatment systems for phosphogypsum leachates in an orphan disposal site. In Journal of Environmental Management (Vol. 275, p. 111251). Elsevier BV. https://doi.org/10.1016/j.jenvman.2020.111251

Enlace al texto completo: https://doi.org/10.1016/j.jenvman.2020.111251

Resumen:

The optimization of the dispersed alkaline substrate (DAS) technology was investigated to achieve the treatment of highly acidic and polluted effluents from a phosphogypsum pile in an orphan site of SW Spain. This phosphogypsum disposal area is located on the Tinto river marsh soils, where it acts as a source of pollution for the estuarine environment, releasing high concentrations of metal(loid)s and radionuclides, which degrade the surrounding waters. The methodology consists of flowing the leachates through columns loaded with a combination of a fine-grained alkaline reagent scattered in a non-reactive matrix to raise the water pH while decreasing the solubility of dissolved contaminants. Seven columns were built, one for each of the alkaline reagent used: limestone, barium carbonate, biomass ash, fly ash, MgO, Mg(OH)2, and Ca(OH)2. The Ca(OH)2-DAS and MgO-DAS treatment systems showed the highest effectiveness, reaching near-total removal for PO4, F, Fe, Zn, Cu, Al, Cr, and U with initial reagent mass:treated volume ratios of 36.3 g/L and 7.57 g/L, respectively. Total As removal was only achieved in the Ca(OH)2-DAS treatment. Phosphate precipitation was the main mechanism responsible for pollutants removal. Geochemical modeling using PHREEQC code and mineralogical evidence confirmed the precipitation of these minerals. This study forms the basis of an effective and environmentally sustainable treatment system for phosphogypsum leachates to reduce the impact of the fertilizer industry worldwide.

Capítulo 6:

Millán-Becerro, R., Cánovas, C. R., Pérez-López, R., Macías, F., & León, R. (2021). Combined procedure of metal removal and recovery of technology elements from fertilizer industry effluents. In Journal of Geochemical Exploration (Vol. 221, p. 106698). Elsevier BV. https://doi.org/10.1016/j.gexplo.2020.106698

Enlace al texto completo: https://doi.org/10.1016/j.gexplo.2020.106698

Resumen:

This study focuses on the search for a sustainable treatment and metal recovery system for acid discharges from a fertilizer industry in SW Spain. The methodology proposed involves the addition of two types of alkaline materials (an industrial waste and a commercial reagent) to neutralize the acidity and remove dissolved elements. In the first case, the treatment consisted on batch reactions between biomass ashes and phosphogypsum leachates at different solid-liquid ratios (i.e. 1:2.5, 1:5, and 1:10). On the other hand, a 0.01 M solution of Ca(OH)2 was used. The experiment with biomass ashes at a solid:liquid ratio of 1:2.5 showed a high effectiveness, reaching removal

percentages close to 100% for F, Fe, Zn, Al, Cr, U, Cu and Cd. The depletion of contaminants from solutions during the alkaline treatments occurred mainly by co-precipitation and/or adsorption onto phosphate phases, in addition to precipitation of fluorides. Moreover, the solids precipitated during the alkaline treatments contain elements of high economic interest such as rare earth elements plus Y (353–3992 mg/kg), Sc (21–164 mg/kg), Be (5.0–7.0 mg/kg), V (1036–2974 mg/kg), Ga (16–40 mg/kg) or U (721–2963 mg/kg). These values could make this by-product a promising source of technology metals. This study proposes an environmentally-friendly solution for these industrial leachates, removing selectively impurities and target elements and producing a promising exploitable metal concentrate. This research could lay the foundations for an effective and sustainable treatment system for acid leachates from phosphogypsum stacks. Furthermore, the costs related with the treatments could be covered by recovering the valuable elements contained in the newly-formed precipitates during the treatments.

CHAPTER 1. INTRODUCTION

1.1. PHOSPHATE FERTILIZER INDUSTRY AND PHOSPHOGYPSUM GENERATION

Phosphoric acid (H_3PO_4) is the main raw material employed in the manufacture of phosphate fertilizers, which are essential to maintain current levels of agricultural production worldwide. In this sense, agriculture provides a basic source of food in the human diet. According to the United Nations, a significant increase in the human population is expected in the next three decades, growing from the current 7800 million to around 9700 million in 2050. Thus, it seems obvious that agricultural production levels must be increased in the coming decades. However, the availability of arable land is limited, so the demand for phosphate fertilizers used to increase the productive capacity of these lands is expected to rise. The phosphate rock ore used to generate phosphoric acid, essential for the production of phosphate fertilizer, is predominantly composed of apatite (mainly fluorapatite ($Ca_5(PO_4)_3F$)). The phosphoric acid is usually obtained by the fertilizer industry through two different processes; by pyrometallurgy, using the method known as “thermal process”, which consists of the thermal reduction of phosphate ore in an electric furnace to generate elemental phosphorus, or by hydrometallurgy, via the wet chemical digestion of phosphate rock with sulfuric acid (H_2SO_4). The latter process, known as "wet digestion", is cheaper and generates around 90% of phosphoric acid worldwide (USGS, 2020). However, as a result of this wet manufacturing process, an unwanted waste, commonly known as phosphogypsum, is generated (Cánovas et al., 2018a). The reaction that summarizes the process is as follows (Eq. (1.1)):

$$Ca_5(PO_4)_3F + 5H_2SO_4 + 10H_2O \rightarrow 3H_3PO_4 + 5CaSO_4{\cdot}2H_2O + HF \qquad (1.1)$$

The industrial process generates around five tons of phosphogypsum for each ton of phosphorus pentoxide (P_2O_5) manufactured (El-Didamony et al., 2012). Thus, the annual worldwide phosphogypsum production is expected to be approximately 300 million tons (Yang et al., 2016). Phosphogypsum is mainly composed of gypsum ($CaSO_4{\cdot}2H_2O$) (around 95%), although it also contains other minor mineral phases (e.g., alkali fluorosilicates, fluorides, quartz, and feldspars), unreacted phosphate rock and organic substances (Cánovas et al., 2018a). In addition, phosphogypsum is enriched in metal(loid)s (e.g., As and Cd) and radionuclides from the ^{238}U decay series (i.e., U, Ra, and Rn), which are released from the raw materials used (mainly from the phosphate

rock but also from the sulfuric acid) and subsequently transferred to the generated waste (Macías et al., 2017a; Pérez-López et al., 2010; Rutherford et al., 1994). However, the chemical composition of phosphogypsum is variable and depends mainly on the nature of the phosphate rock and the type of wet chemical process carried out. According to Pérez-López et al. (2010), most of the metallic impurities contained in the phosphate rock ore are transferred into the waste in values of 2-12%. These transfer rates were even higher in the phosphogypsum studied by other authors, with values that ranged from 3% to 100% (i.e., Al-Masri et al., 2004; Rutherford et al., 1994). In this same sense, Macías et al. (2017a) pointed to the quality of the acid used to dissolve the phosphate rock during the industrial process as the main cause of the high concentrations of arsenic observed in the waste. Consequently, these toxic impurities limit the commercial usage of phosphogypsum. In fact, only around 15% of the phosphogypsum produced worldwide is recycled, its main uses being as a raw material for the production of building materials and as an amendment of agricultural soils (Cánovas et al., 2018a; Tayibi et al., 2009). With respect to the remaining 85%, it is often transported as an aqueous slurry along with a residual fraction of the reagents (i.e., sulfuric acid) and products (i.e., phosphoric and hydrofluoric acids) from the manufacturing process and then stored in stacks or piles, without any type of previous treatment, on large flat areas close to the phosphate fertilizer industries (Tayibi et al., 2009). The phosphogypsum is highly acidic because its interstitial space is filled with extremely-polluting residual acids. However, most of the phosphogypsum piles are located in coastal areas, where these wastes are usually exposed to strong weathering processes (El Samad et al., 2014; El Zrelli et al., 2016; Pérez-López et al., 2016; Sanders et al., 2013).

Nevertheless, solid phosphogypsum is not the only waste derived from the manufacture of phosphoric acid. The industrial process requires a large volume of water, known as process water, which is employed for slurry and transport the phosphogypsum to the stack in a closed-circuit system. Thus, the continuous reuse of process water in the closed-loop system yields a wastewater characterized by extremely low pH values and very high concentrations of phosphate, sulfate, fluoride, metal(loid)s and radionuclides (Cánovas et al., 2017; Lottermoser, 2010). Such waters require storage and isolation within the waste repository in central or lined ponds, and must be neutralized before their discharge to the surrounding water bodies.

On the other hand, the wastes derived from the manufacture of phosphoric acid (i.e., phosphogypsum and process water) also contains elevated concentrations of elements of high economic interest, so-called technology metals, such as rare earth elements (REE), Y, Sc, V, Be or Ga, among others (Cánovas et al., 2017). In general, the content of the valuable metals in these wastes is one or various order of magnitude lower than in conventional mineral deposits. However, the production of phosphoric acid generates huge amounts of wastes, which could turn them into potential secondary sources of metals of high economic interest (e.g., Cánovas et al., 2017; 2019; El-Didamony et al., 2012; 2013; Walawalkar et al., 2016). Thus, the potential recovery of the technology metals could help offset the costs associated with the management of these wastes.

1.2. HUELVA PHOSPHOGYPSUM STACK

During the 1960s, an industrial complex was built in the city of Huelva (SW Spain) to satisfy the needs of an increasingly developed and globalized population. The city of Huelva was selected as the ideal location to host at its vicinity this industrial complex due to a series of political, demographic and, mainly, geographical aspects. Huelva and the industrial complex are located near the Ría de Huelva estuary, formed by the confluence of the Tinto and Odiel Rivers (Fig. 1.1). This location is strategic since the estuary is a large and relatively flat area, with high water availability and close to the sea, which means an important communication route.

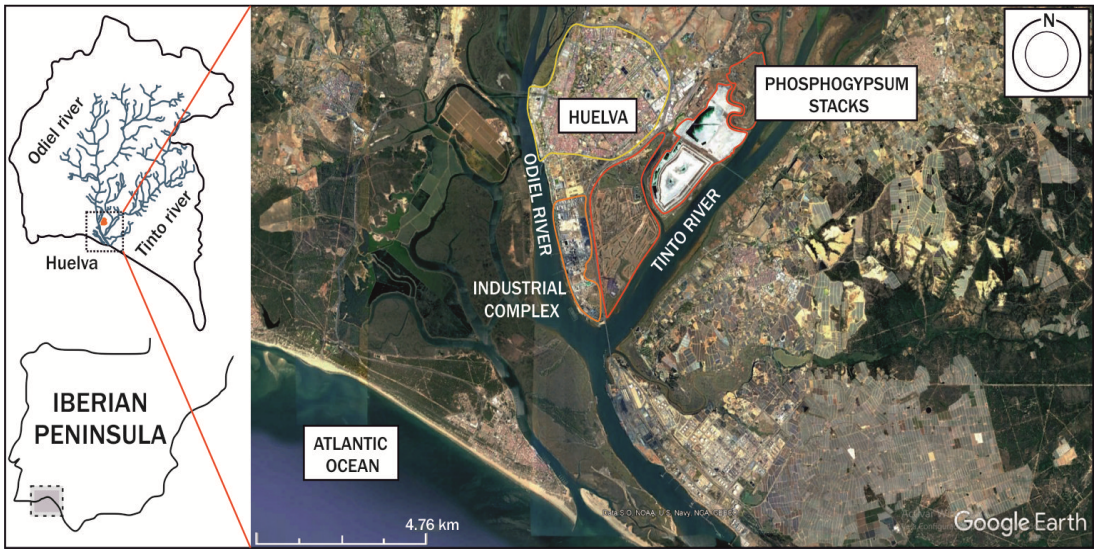

Figure 1.1. Geographical location of the phosphogypsum stack next to Huelva city (SW Spain).

The Huelva industrial complex comprises a series of chemical and petrochemical plants, where a large part of the industrial activity has been dedicated to the manufacture of phosphoric acid for the production of phosphate fertilizers through the wet process. The phosphate rock used by the fertilizer industry is of sedimentary origin and came mainly from Morocco. Since 1968 -when the industrial activity began- until its cessation in 2010, approximately 3 million tons of phosphogypsum were produced each year, resulting in a huge stack of 12 km^2 that contains around 100 million tons of phosphogypsum, less than 100 meters from the Huelva city (Fig. 1.1). This waste, classified as a hazardous material (Macías et al., 2017a) and considered a Naturally Occurring Radioactive Material (NORM) according to current EU legislation (EU, 2013; IAEA, 2003), was deposited directly onto the salt-marsh soils of Tinto River estuary with no barrier or liner to avoid infiltration. This phosphogypsum, together with the sulfides-rich wastes existing in the abandoned mining districts of the Iberian Pyrite Belt (IPB), are the main solid residues that act as a source of continuous pollution to the Ría de Huelva estuary. Instead, the salt-marshes of the Odiel River were declared a Biosphere Reserve by UNESCO in 1983 and a RAMSAR-NATURA wetlands zone in 1989.

From 1968 to 1997, the phosphogypsum was transported and deposited on four disposal areas using seawater, which was later discharged without any type of treatment to the estuary after waste decantation. Around 20% of the waste generated was also dumped directly into the Ría de Huelva estuary. The direct discharges of industrial wastes to the Ría de Huelva estuary worsened the quality of water and sediments (Bolívar et al., 2002; Martínez-Aguirre and García-León, 1991; Martínez-Aguirre et al., 1994; 1996). However, in 1997 a change in legislation forced the fertilizer company to present a new waste management project to avoid any direct discharge into the estuary (OSPAR, 2002; 2007). According to the new management policy, from 1997 to 2010, the waste was stored in a large pyramidal pile on a single zone already used previously. In addition, the transport and decantation of the phosphogypsum was carried out through a closed-loop system of freshwater, known as process waters, instead of the old open-circuit system of seawater used until then. These process waters (around 10 Mm^3) were stored in shallow ponds on the stack in order to promote evaporation as a measure to reduce its volume. At the end of 2010, the phosphate fertilizer industry was forced by

the Spanish National Court to cease dumping wastes on the salt-marshes of the Tinto River.

At present, the phosphogypsum stack is comprised of four different disposal modules (Fig. 1.2); while zones 1 and 4 are already considered as restored, zones 2 and 3 are currently pending restoration. The previous restoration of zones 1 and 4 consisted of adding a cover over the naked phosphogypsum to avoid its weathering. A more detailed description of each zone is shown as follows:

- Zone 1, situated in "Marismas del Pinar", is a 4.5 km^2 sector with an average thickness of phosphogypsum of 2-3 m. This area was closed and restored in the beginning of the 1990s, and the restoration measures consisted of the addition of a 25 cm thick layer natural soil with vegetation directly over the naked phosphogypsum (Más et al., 2006).

- Zone 2, located in "Marismas del Rincón", occupies an area of 2.7 km^2 and up to 30 m in height. This zone contains the large pyramidal phosphogypsum pile built after 1997 with the change of environmental legislation. This zone was active until phosphogypsum production in Huelva ceased in 2010.

- Zone 3, located also in "Marismas del Rincón", has an area of 1.8 km^2 and a thickness of 8-12 m. The phosphogypsum in this zone was deposited until 1997, this zone being used as of that date to store process water for the closed-loop system. Currently, zones 2 and 3 area unrestored, and the phosphogypsum is directly exposed to weathering processes. In these areas, central surface ponds with process water and perimeter channels were built with the aim of collecting water from runoff and infiltrations.

- Zone 4 is located in "Marismas de Medaña". This restored phosphogypsum disposal area has an extension of 3.0 km^2 with an average height of 8 m, where the waste was dumped before 1997. The restoration tasks were made in this zone at the beginning of the current century. Zone 4 has a more complex cover than that previously installed in zone 1, which consists of several layers (in ascending order): 1 m of construction debris, 2 m of inert industrial wastes and 30-50 cm of vegetable soil.

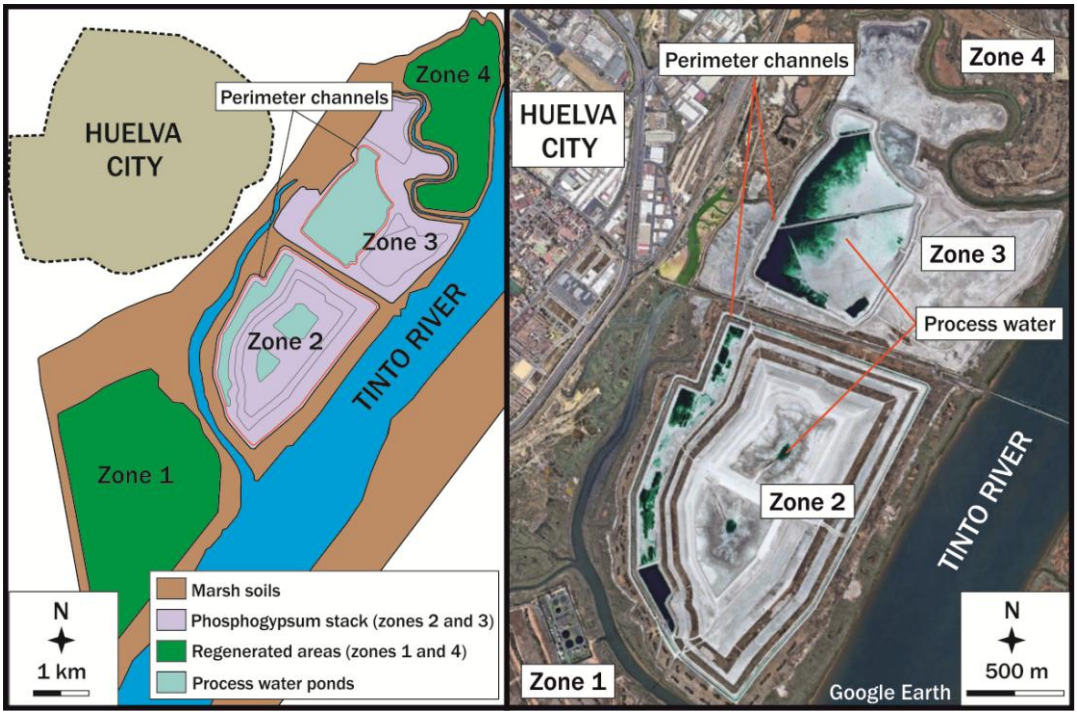

Figure 1.2. Location map of the phosphogypsum stack on the salt-marshes of the Tinto River and its division into disposal modules.

Due to its location in the tidal prism of the estuary, the phosphogypsum stack is exposed to varying weathering conditions significantly influenced by tidal action. This waste is a source of contamination due to the residual fraction of metal-bearing phosphoric acid that occupies the interstitial space between gypsum particles. The presence of acidic and polluted solutions trapped in the pores of the waste causes the stack to have a dynamic similar to that of an unconfined aquifer but, in this case, with highly-polluted groundwater (Pérez-López et al., 2011a). Three possible environmental scenarios could play an important role in the weathering processes and release of pollutants from the stack:

1) In the unsaturated zone, between the stack surface and the water-table, phosphogypsum is subjected to oxidizing conditions depending on the regional climate.

2) In the saturated zone, between the water-table and the marsh soil, stagnation or slow flow causes the water to be anoxic and the phosphogypsum to be subjected to reducing conditions.

3) In the intermediate zone, around the water-table, the water level could vary depending on the action of the tides and the phosphogypsum could undergo alternating and continuous oxidation-reduction cycles.

Previous studies showed that a relatively high proportion of pollutants (e.g., As, U, Zn and V) are mainly associated with the easily leachable fraction of phosphogypsum (Pérez-López et al., 2010). The regional climate is Mediterranean with a rainy season in winter and a dry-warm season in summer. In dry-warm periods, the high waste porosity (Rabi and Mohamad, 2006) could favor the continuous entry of atmospheric oxygen and water through the unsaturated zone, as well as the subsequent release of pollutants associated with the easily leachable fraction. These mobile pollutants could precipitate in the form of sulfate and phosphate evaporitic salts during this period, although these soluble salts would be subsequently washed, causing the releasing of contaminants to the surrounding environment, during the rainy periods (Pérez-López et al., 2010). On the other hand, the deepest zones of the stack below the water-table would be influenced by reducing conditions. The phosphogypsum stack is directly disposed on organic matter-rich marsh soils which favor sulfate-reduction processes and therefore the precipitation of metal sulfides driven by bacterial activity (Pérez-López et al., 2011a; 2018). This process immobilizes some trace elements (e.g., Zn, Cu, Ni, As or Cd), which would pass to the oxidizable fraction of phosphogypsum (Pérez-López et al., 2010).

Sulfide precipitation in the marsh contact could naturally attenuate the pollution and, therefore, the impact of the phosphogypsum stack on the estuarine environment. Nevertheless, the marsh soils do not have enough capacity to completely remove all the pollution. In fact, the muddy soils supporting the waste are highly impermeable, retaining the groundwater at depth and forcing its movement laterally until reaching the edge of the stack, resulting in the formation of superficial leakages, known as edge outflows, that discharge the pollution directly into the Ría de Huelva estuary (Fig. 1.3a,b,c) (Pérez-López et al., 2015; 2016). Another potential source of contamination to the estuarine environment is the extremely acidic and polluted process water stored in surface ponds on the stack (Fig. 1.3d). It should be highlighted that there is poor geochemical connection between the ponded process water and the edge outflows that emerge from the stack, i.e., the process water stored on the stack is not the main route of pollutant diffusion from phosphogypsum to the environment through its downward

infiltration (Pérez-López et al., 2016). In this sense, previous studies reported that the edge outflows have a geochemical fingerprint that indicates a predominantly estuarine origin (Papaslioti et al., 2018a; Pérez-López et al., 2016). These findings pointed to that the intertidal water access to the phosphogypsum stack through the secondary channels could act as one of the preferential paths that lead to the leaching mechanism. According to these studies, any restoration action that involves the elimination of the stored process water and the addition of a surface cover would not imply the cessation of the edge outflows. Indeed, despite the restoration measures implemented in disposal zones 1 and 4, edge outflows continue to be released, especially in zone 4 (Pérez-López et al., 2016). This situation turns zone 4 into an orphan site since this area returned to the government after the adoption of these measures, and the company is not required to pay for additional measures. On the other hand, similar restoration measures to those adopted in the restored zones are planned for unrestored zones 2 and 3. Therefore, it seems reasonable to expect the existence of pollutant edge outflows even after restoration actions, as is currently the case in the restored zones 1 and 4, and hence that the entire stack becomes an orphan site.

Numerous sources of pollution have been identified around the whole perimeter of the phosphogypsum stack. Pérez-López et al. (2016), estimate than the total volume of acid leachates emerging from the stack is around 335,000 m^3/yr, although this value must be higher due to the existence of diffuse edge outflows, difficult to quantify These leachates release large amounts of contaminants to the Ría de Huelva estuary, e.g., 42 tons/yr of Fe, 12 tons/yr of Zn, 6.9 tons/yr of As, 4.2 tons/yr of U, 3.5 tons/yr of Cr, 1.8 tons/yr of Cu, 1.6 tons/yr of Cd and 1.2 tons/yr of Ni, among others (Pérez-López et al., 2016). Most of the pollutants released including Co, Ni, Cu, Zn, As, Cd and Sb behave conservatively when mixed with seawater, remaining mobile in the estuarine waters and, finally, ending up the Atlantic Ocean (Papaslioti et al., 2018b). Therefore, it is highlighted the urgent need to design effective remediation strategies for these pollutant leachates before they reach the Ría de Huelva estuary.

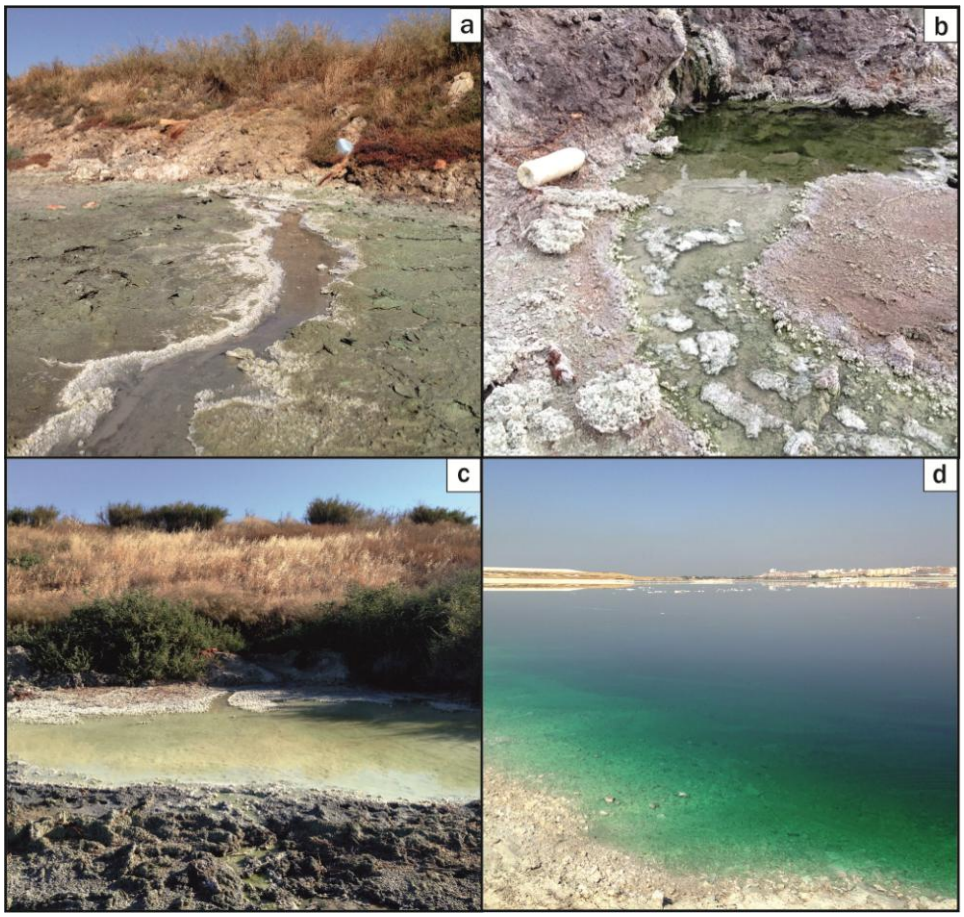

Figure 1.3. Example of edge outflow of zone 2 (a), edge outflow of zone 3 (b), edge outflow of zone 4 (c) and process water (d).

1.3. MOTIVATION AND OBJECTIVES

Industrial leachates are usually treated in active plants, where chemicals are added in controlled doses to precipitate the metals. These treatment systems require the continuous use of electrical energy and continuous addition of chemical reagents, as well as intensive monitoring and management of wastes. Therefore, active treatments are commonly unsuitable at orphan sites. An interesting substitute would be passive technologies, which may be an environmentally friendly and cost-effective alternative. Passive technologies are preferable to active treatments in orphan sites because they do not need energy consumption, continuous addition of chemicals or regular maintenance (Johnson and Hallberg, 2005). Passive treatment systems have been widely developed to treat acid mine drainage (AMD) (INAP, The International Network for Acid Prevention, 2021). In this context, given the similarities between AMD and phosphogypsum-related leachates (i.e., both are metal-rich and acidic waters), it would

seem reasonable to use the same guidelines to propose a similar passive treatment system in both cases. A promising passive technology to treat phosphogypsum-related waters could be the dispersed alkaline substrate (DAS), which is currently considered the best passive option to remediate highly polluted AMD based on environmental and economic criteria (Ayora et al., 2013; Martínez et al., 2019; Orden et al., 2021). The DAS system consists of a mixture of a fine-grained alkaline material with high neutralization potential (usually limestone) and an inert matrix to provide high porosity (commonly wood chips), avoiding therefore passivation and clogging problems associated with mineral precipitation (Ayora et al., 2016; Macías et al., 2012c).

The main objective of the current Doctoral Thesis is to develop an effective treatment system for discharges from phosphogypsum stack in order to minimize the pollutant load that reaches the Ría de Huelva estuary and subsequently the Atlantic Ocean. To achieve this goal, the following aims were proposed:

1. To identify and geochemically characterize all the acidic and polluted effluents from the Huelva phosphogypsum stack. This is a fundamental first step for any restoration plan, because a deeper knowledge of the spatial and temporal evolution of this pollution seems to be essential to achieve adequate environmental and economical results. The novelty with respect to previous works lies in considering the influence of possible seasonal variations both in the hydraulic response of the phosphogypsum stack and in the geochemistry of the edge outflows. This information will allow clarifying the weathering model of the pile and how restoration actions should be directed.

2. To study the behavior of acidity and the main contaminants present in phosphogypsum leachates during the addition of a conventional alkaline reagent (calcium hydroxide). To the best of our knowledge, it is the first time that a conventional alkaline neutralization has been proposed for metal-rich leachates based on three -sulfuric, hydrofluoric and mainly phosphoric- acids. The behavior of contaminants during neutralization must be clarified to optimize further treatment systems.

3. To evaluate the potential application of DAS technology for the passive treatment of phosphogypsum leachates and to select the most appropriate reagent. For this, several conventional alkaline reagents (limestone, magnesia, magnesium hydroxide or calcium hydroxide), non-conventional alkaline reactive (barium carbonate), and even alkaline wastes (biomass ash and fly ash) have

been used in the development of DAS technology for this type of waters. The idea is to check if this type of passive technologies, until now only tested for acid mine waters, are equally valid for other industrial facilities releasing acid wastewaters also in a state of orphan site.

4. To assess the potential environmental risks and the options of safe disposal of the pollutant-rich solid wastes generated during the passive treatment of fertilizer industry effluents with DAS technology. In the DAS technology, the dissolved pollution is pointedly retained within the reactive materials by newly-formed minerals precipitation. So, the DAS mixture should be replaced as soon as alkalinity drops. Hence, a proper characterization and management of these metal-rich solid wastes must be done. However, these high metal concentrations could lead to the possibility of reusing these wastes as a secondary source of metals of economic interests, which is addressed in the final objective.

5. To study the mobility of elements of high economic interest (i.e., rare earth elements (REE), Y, Sc, Be, V, Ga and U) during the alkaline neutralization of phosphogypsum leachates, and to evaluate the newly-formed solids as potential source of valuable elements. The valorization of these newly-formed metal-rich wastes could transform this residue into a valuable resource, which may constitute a promising step towards the zero waste goals and, at the same time, could offset the construction and maintenance costs of this technology, representing in turn a promising sustainable upcycling solution for the phosphate fertilizer industry.

1.4. THESIS OUTLINE

The doctoral thesis is composed of an introductory chapter (Chapter 1), five main chapters (Chapters 2 to 6) and a final chapter with general conclusions (Chapter 7). The five main chapters are structured in a short abstract, introduction, materials and methods, results and discussion, and conclusions. The chosen structure may be redundant, however, due to the variety of topics covered and approaches used in these five main chapters, it is desirable to provide each chapter with the independence necessary for its correct understanding. Thus, the present thesis is structured as follows:

Chapter 1: Introduction

This chapter addresses the genesis of an industrial waste known as phosphogypsum, as well as the problems associated with the release of highly acidic and polluted leakages from an uncontrolled deposit or stack of this waste on estuarine marsh soils in the city of Huelva. In addition, this section lists the objectives to be achieved with the development of this thesis, highlighting the gaps in knowledge that the present doctoral dissertation attempts to bridge.

Chapter 2: Phosphogypsum weathering and implications for pollutant discharge into an estuary.

The second chapter evaluates the hydrological response of the Huelva phosphogypsum stack to the weathering agents and studies the seasonal and spatial hydrochemical variability of the leachates released from this stack. The results obtained in this section have important implications for the correct design of effective remediation strategies for phosphogypsum leachates.

Chapter 3: Assessment of metals mobility during the alkaline treatment of highly acid phosphogypsum leachates.

This chapter describes an alkaline titration experiment in the laboratory, which simulates the active treatment of highly acid and polluted phosphogypsum leachates by alkaline addition of a $Ca(OH)_2$ solution. This study focuses mainly on the mobility of pollutants during the acid neutralization as a preliminary step to the design of a passive treatment. The newly-formed solids during the treatment were also characterized according to the standard leaching tests proposed by EU and US regulations in order to conduct a potential risk and environmental management assessment.

Chapter 4: Design and optimization of sustainable passive treatment systems for phosphogypsum leachates in an orphan disposal site

The fourth chapter focuses on evaluating the potential application of passive DAS technology to highly acidic and contaminated phosphogypsum leachates and selecting the most suitable reagent for their effective treatment. For this purpose, phosphogypsum leachates were flowed through columns filled with a mixture of a fine-grained alkaline reagent dispersed in an inert matrix. Different reactive materials were used in the column experiments (i.e., limestone, barium carbonate, biomass ash, fly ash, MgO, $Mg(OH)_2$ and $Ca(OH)_2$).

Chapter 5: Environmental management and potential valorization of wastes generated in passive treatments of fertilizer industry effluents.

This chapter confirms the efficiency of the $Ca(OH)_2$-DAS and MgO-DAS systems for the treatment of acidic leachates from the fertilizer industry. The metal-rich solid wastes generated by the passive treatment of highly polluted phosphogypsum leachates were also subjected to the international leaching tests proposed by the current environmental regulations of the EU and the US, in order to study the mobility of pollutants contained in the solid wastes under different weathering scenarios. These leaching tests classify solids according to their hazardousness in order to properly manage them. In addition, the potential valorization of solid wastes from DAS treatment systems as a secondary source of critical raw materials is considered.

Chapter 6: Combined procedure of metal removal and recovery of technology elements from fertilizer industry effluents.

The sixth chapter proposes an environmentally and friendly solution for the fertilizer industry effluents, removing selectively impurities and target elements and producing a promising exploitable metal concentrate. In the laboratory, treatment of phosphogypsum leachates was simulated using batch experiments and alkaline titrations. The potential recovery of the valuable elements (e.g., rare earth elements (REE), Y, Sc, Be, V, Ga or

U) contained in the newly-formed solids during the experimental run could help to cover the costs related to the passive treatment of these leachates.

Chapter 7: General conclusions

This last chapter summarizes the most relevant results obtained during the development of the thesis.

CHAPTER 2. PHOSPHOGYPSUM WEATHERING AND IMPLICATIONS FOR POLLUTANT DISCHARGE INTO AN ESTUARY

BASED ON:

Millán-Becerro, R., Pérez-López, R., Cánovas, C.R, Macías, F., León, R., Phosphogypsum weathering and implications for pollutant discharge into an estuary. Submitted to Journal of Hydrology.

ABSTRACT

Approximately 100 million tons of phosphogypsum were stockpiled onto marsh soils of the Tinto River estuary (Huelva, SW Spain). This study focuses on the hydraulic response of the phosphogypsum stack to the different weathering agents, as well as on the hydrochemical behavior of highly acidic and polluted effluents from its leaching during different hydrological conditions. To address these issues, a CTD-Diver was installed in a bore-hole within a phosphogypsum stack profile, which recorded the variations in the water-table of the stack, and edge outflows samples were collected around the perimeter of the stack during four sampling periods in different seasons. During dry periods, the water-table of the stack remains almost static and is controlled only by the tide oscillations. However, during rainy events this water-level rapidly increases up to 20 cm and subsequently decreases, defining peaks that coincide with the rainfalls. Having a hydraulic connection to the sea and groundwater flow in conduits, the phosphogypsum stack behaves as an anthropogenic karstic-coastal aquifer. Regarding the hydrochemical behavior of the edge outflows, the concentrations of most pollutants (e.g., PO_4, Al, As, Cd or U) suffered a slight decrease from the dry-warm to the rainy period. These leachates releases high concentrations of contaminants to the estuary, e.g., PO_4, As and U (average values of 5000, 6.9 and 3.0 tons/yr, respectively). The results obtained in this study could contribute to the development of effective treatment systems for leachates from phosphogypsum stacks worldwide to minimize their impact on the surrounding environment.

2.1. INTRODUCTION

The growing industrial activity during the last five decades, to satisfy the needs of an increasingly developed and globalized world population, has resulted in a significant growth of industrialized zones around the world. In this sense, the increasing industrialization of estuaries around major shipping routes promotes environmental concerns due to these areas are particularly sensitive to metal pollution. The Ría de Huelva estuary, formed by the confluence of the Odiel and Tinto Rivers (SW Spain), is a clear example of extensive development and industrialization. In this case, part of the industrial activity has been focused on the manufacture of phosphoric acid (H_3PO_4) for the production of phosphate fertilizers. As a result, an unwanted by-product, commonly known as phosphogypsum (mainly gypsum, $CaSO_4 \cdot 2H_2O$), is generated by the chemical digestion of phosphate rock (i.e., fluorapatite, $Ca_5(PO_4)_3F$) with sulfuric acid (H_2SO_4).

Phosphogypsum frequently contains impurities such as metal(loid)s (e.g., As and Cd) and radionuclides from the decay series of ^{238}U (i.e., U, Ra and Rn) (Macías et al., 2017a; Rutherford et al., 1994). Consequently, these toxic impurities limit the commercial usage of phosphogypsum. In fact, only around 15% of the phosphogypsum produced worldwide is recycled, mainly for the production of buildings materials (Cánovas et al., 2018a). With respect to the remaining 85%, it is transported as an aqueous slurry along with a residual fraction of the reagents (i.e., sulfuric acid) and products (i.e., phosphoric and hydrofluoric acids) from the manufacturing process and then stored in stacks, without any type of previous treatment, on large flat areas close to the phosphate fertilizer industries (Tayibi et al., 2009). Most of the phosphogypsum piles are located in coastal areas, where these wastes are usually exposed to strong weathering processes (e.g., El Samad et al., 2014; El Zrelli et al., 2016; Pérez-López et al., 2016; Sanders et al., 2013).

The phosphate fertilizer industry located in the Ría de Huelva estuary has been generating and dumping phosphogypsum for almost 40 years over a huge stack (approx. 100 million tons of wastes stockpiled on around 12 km^2 of surface) near the city of Huelva. The waste was deposited directly onto the marsh soils of the Tinto River estuary with no barrier or liner to avoid infiltration. The presence of acidic solutions trapped in the pores of the phosphogypsum makes the stack to behave similarly to an unconfined aquifer with highly-polluting groundwater (Pérez-López et al., 2011a).

When groundwater reaches the below-waste filled marsh level, these solutions flow laterally until emerging at the edges of the pile and forming superficial leakages known as edge outflows (Pérez-López et al., 2015; 2016). As a result, the phosphogypsum stack is a continuous source of pollution into the estuary due to the release of large volumes of acid effluents, i.e., around 335,000 m^3/yr, with high concentrations of dissolved pollutants, such as PO_4, F, Fe, Al, Zn, Cr, Cu, As, Sb and U, among others (Pérez-López et al., 2016).

Previous studies reported that the edge outflows have a geochemical fingerprint that indicates a predominantly estuarine origin (Papaslioti et al., 2018a; Pérez-López et al., 2016). The findings proposed that the intertidal estuarine water accesses to the phosphogypsum stack, possibly through the secondary tidal channels that are currently covered by the pile, washing the waste in depth and returning to the estuary in the form of edge outflows. Although geochemical connection between the estuary and the phosphogypsum stack has been previously shown, the hydraulic response of the stack to estuarine fluctuations, as well as the influence of other possible weathering agents such as rainwater, remains unclear. To bridge this gap in knowledge, the main objectives of this work are to assess (1) the temporal hydrological response of the water-table at the waste pile against possible weathering agents, as well as (2) the possible seasonal influence on the hydrochemistry of the edge outflows and therefore on the discharge of pollutants to the estuary. To our knowledge, the studies carried out so far to characterize the pollution from edge outflows are based on single sampling campaigns (Papaslioti et al., 2018a; Pérez-López et al., 2016), while the present study has analyzed the hydrochemistry of the leachates that emerge from the phosphogypsum stack during several sampling campaigns under different hydrological conditions. The information obtained in this study could be useful for the optimization of future remediation systems for acid and contaminated discharges from phosphogypsum stacks, mainly in coastal areas worldwide.

2.2. MATERIALS AND METHODS

2.2.1. Study site

The Huelva phosphogypsum stack is located in the tidal prism of the Ría de Huelva estuary, which ranges between 37 and 82 Mm^3 along a tidal half-cycle (6 h) (Grande et al., 2000). Since 1968 -when the industrial activity began- until its cessation in 2010, approximately 3 million tons of phosphogypsum were produced each year. From 1968 to 1997, the phosphogypsum was transported and deposited on four disposal areas using seawater, which was later discharged after waste decantation to the estuary without any type of treatment. However, in 1997 a legislative change forced the fertilizer company to present a new waste management project to avoid any direct discharge into the estuary (OSPAR, 2002; 2007). According to the new management policy, from 1997 to 2010, the waste was stored in a large pyramidal pile on a single zone already used previously. In addition, the transport and decantation of the phosphogypsum was carried out through a closed-loop system of freshwater, known as process water, instead of the old open-circuit system of seawater used until then. The process water was stored in shallow ponds on the stack in order to promote evaporation as a measure to reduce its volume.

At present, the phosphogypsum stack is comprised of four different disposal modules; while zones 1 and 4 are already considered as restored, zones 2 and 3 are currently pending restoration in the near future. The previous restoration consisted in covering the bare phosphogypsum with a soil cover. Zone 1 (4.5 km^2 of extension and 2-3 m of average thickness) is covered by a 25 cm thick layer of natural soil with vegetation; while zone 4 (3.0 km^2 and 8 m) has a more complex cover that consists of several layers: 1 m of construction debris, 2 m of inert industrial wastes and 30-50 cm of vegetable soil (in ascending order). On the other hand, in the unrestored zones 2 (2.7 km^2 and up to 30 m in height) and 3 (1.8 km^2 and 8-12 m), the phosphogypsum is directly exposed to weathering conditions. Both zones still contain surface ponds with process water characterized by extreme acidity and contaminant load, due to its continuous use in the closed-circuit system and to the evaporation to which it is subjected. Despite restoration measures, the four disposal modules currently show numerous edge outflows along their perimeters that continuously discharge pollutants to the Ría de Huelva estuary (Pérez-López et al., 2016).

2.2.2. Sampling

The perimeter of the four zones of the phosphogypsum stack was inspected in order to collect edge outflow waters during four sampling campaigns in different seasons (Fig. 2.1a): May-June 2014 and 2015 (warm-dry periods), November 2014 (rainy period) and June 2016 (beginning of warm-dry period after rainy events). Unfortunately, no samples were taken just after rainy events, leaving a gap of at least 10 days for safety issues. The pH, redox potential (ORP) and electrical conductivity (EC) were measured in the field using a portable Multiparametric Crison MM 40+ equipment. Measured ORP was referenced to the standard hydrogen electrode (Eh), as proposed by Nordstrom and Wilde (1998). Rainfall and temperature data from a meteorological station (at 1 km from phosphogypsum stack) were provided by the Regional Environmental Authorities and the Spanish Meteorological Service.

For the continuous control of the water-table variations in the stack, a CTD-Diver was installed in a bore-hole of 4.5 m of depth within a phosphogypsum profile in the zone 3 (around 8 m of waste thickness), and a BaroDiver was used to compensate measurements with atmospheric pressure. The installed sensors were manufactured by Schlumberger (accuracy for pressure: ±0.1%). In the moment of installation, the water-table was found at 2.67 m beneath the surface and the CTD-Diver was submerged about 18 cm. So, results will be also corrected with respect to the immersion depth. The measurement period comprised from February 22nd to June 28th 2016, with a sampling frequency of 10 min. Sea level variation measurements during the same period were also obtained from a buoy (at 500 m from phosphogypsum stack) belonging to the Spanish Wave Coastal Network. For a better understanding of the study area, localization of all sampling points can be seen in Figure AP1.1.

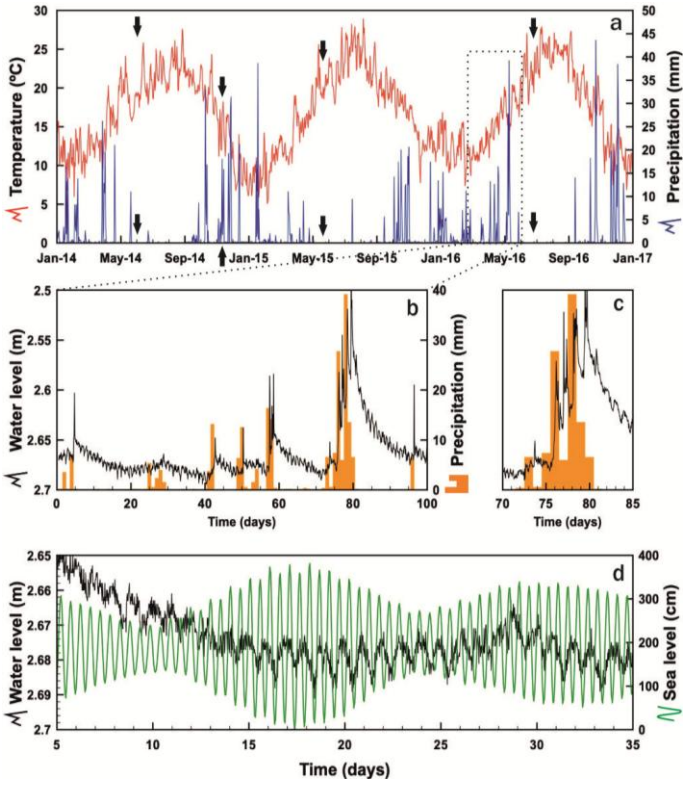

Figure 2.1. a) Daily evolution of rainfall and temperature during the study period. The arrows indicate the date on which the different sampling campaigns were carried out, b) response of the water-table of the phosphogypsum stack during rainy events, c) zoom of the relationship between certain rainy episodes and the water-level in the stack and d) relationship between the water-table level of the pile and the tidal fluctuations.

2.2.3. Chemical analyses

Edge outflow samples were filtered through 0.45 µm membrane filters and divided into two aliquots; one unacidified for anion and ammonia determination and another acidified with HNO_3 to pH < 1 for major and trace element analysis. As long as possible, the float method was used to estimate the flow rate at the sampling points of edge outflows.

Concentrations of anions (Br, Cl and F) and ammonia in all the unacidified samples were determined by high performance liquid chromatography (HPLC) using a Metrohm 883 basic ion chromatograph (IC) equipped with Metrosep columns. The acidified samples were analyzed using Inductively Coupled Plasma-Atomic Emission Spectroscopy (ICP-AES; Jobin Yvon Ultima 2) for determination of major elements (Al, Ca, Fe, K, Mg, Mn, Na, P and S) and Inductively Coupled Plasma-Mass Spectroscopy (ICP-MS; Agilent 7700) for trace elements (As, Cd, Co, Cr, Cu, Ni, Pb, Sb, U and Zn). Detection limits were: 0.2 mg/L for S; 0.1 mg/L for Na; 0.05 mg/L for

Fe, K and Mg; 0.02 mg/L for Al, Ca, Mn and P; and 0.1 μg/L for trace elements. All analyzes were performed in the laboratories of the University of Huelva. Three laboratory standards, prepared with concentrations within the range of the samples, were analyzed with every 10 samples to check for accuracy. Furthermore, dilutions were performed to ensure that the concentration of the samples was within the concentration range of the standards. Blank solutions with the same acid matrix as the samples were also analyzed. The average measurement error was less than 5%. A statistical analysis was performed using the statistical package. A Principal Component Analysis (PCA) of the results was performed to analyze the relationships among the different variables and seasonal patterns of edge outflows chemical composition. The PCA is based on a reduction in the number of variables in a multivariate dataset, conserving as much variance as possible in the dataset. The Spearman's correlation matrix was used because some variables did not show a normal distribution (Davis, 2002).

2.3. RESULTS AND DISCUSSION

2.3.1. Hydrological response to weathering

The daily evolution of rainfall and temperature in the study area from 2014 to 2016 (Fig. 2.1a) shows a cyclic pattern characteristic of semi-arid Mediterranean climate, with a rainy season in winter and a dry-warm season in summer. The annual average rainfall during this time series was 510 mm, and most rain events were short but intense downpours between October and April. During the hydraulic monitoring period, the accumulated rainfall was 220 mm and the events had a direct response in the water-table of the phosphogypsum stack (Fig. 2.1b). The water-table was quite stable during the study period but increased up to 20 cm during the rainy events. Figure 2.1c shows in detail the relation between some rainy episodes and water-table level in the stacks, indicating that the response of the system is immediate; i.e., without delay between the rainfall and water-table increases. Just after rain episodes, around half the height increased by the water-table is immediately recovered, defining peaks that coincide with the rainfalls. The water-table recovers more slowly its original state during a period of 5 to 15 days depending on the intensity of the rains.

In periods with absence of rains, the water-table shows low variability during most of the time (± 2 cm). However, when zooming in, small cyclical oscillations can be observed within these stability periods. These piezometric oscillations seem to be influenced by the tidal fluctuations, as observed from the data recorded by the buoy belonging to the Spanish Wave Coastal Network (Fig. 2.1d). The data of the buoy provided clear information on the semidiurnal character of the tidal oscillations, i.e., two high tides and two low tides are recorded alternately each day, which is consistent with the tidal regime of the study area (Borrego et al., 1995). The piezometric oscillations show maximum and minimum amplitudes that match the tidal cycles with a certain delay. Nevertheless, the second daily low tide often appears to be masked in the water-table variation, which could be due to its lower amplitude in relation to the first one. Moreover, the monitoring was carried out in a rainy period where there may be a higher contribution of fluvial flood events that also masks the piezometric tidal oscillations.

2.3.2. Hydrochemical characterization

During the four sampling campaigns (i.e., May-June 2014, November 2014, May-June 2015 and June 2016), a total of ninety-five edge outflow points were identified around the whole perimeter of the phosphogypsum stack (Fig. AP1.1). Zone 2 was by far the phosphogypsum disposal area where more discharging points were found, i.e., 51 edge leachates (samples 2-1 to 2-51), followed by zone 3 with 28 (samples 3-1 to 3-28) and zone 4 with 15 (samples 4-1 to 4-15). However, a large part of the perimeter of zone 4 could not be sampled since a fence restricts the access. Therefore, the total number of edge outflows emerging from the supposedly restored zone 4 could be even higher than that described in this manuscript. Finally, only one acid leachate was identified in zone 1. However, this acidic water sample is the result of the interaction of outcropping phosphogypsum and seawater during rising tide in a tidal channel and is therefore not strictly considered an edge outflow (Pérez-López et al., 2016). The number of edge outflows found in each zone of the phosphogypsum stack could be directly related to the thickness of waste piled up and/or the extent of marsh soils covered by the zone. On the one hand, the higher the height of the waste pile, the greater the thickness of the saturated zone and, therefore, the greater the potential for storing acidic and contaminated interstitial water. In this sense, the absence of edge outflows in zone 1 is

likely due to the low thickness of phosphogypsum, which determines that the whole profile of weathering corresponds to unsaturated zone; i.e., there is not a large stock of water in the deep pores that can subsequently emerge at the edges of the stack (Pérez-López et al., 2016). On the other hand, the larger the disposal area, the greater the number of secondary tidal channels covered by the stockpiled waste (Fig. 2.2), and therefore, the greater the hydraulic connection between the estuary and the zone, which could explain a greater number of edge outflows. The average flow found during the warm-dry periods was 0.2 L/s, with rates commonly comprised between 0.1 and 1.5 L/s. These values were only slightly higher during the rainy period (0.1 to 2.0 L/s, average of 0.4 L/s).

Figure 2.2. Overlay of aerial images of the marshes occupied by the phosphogypsum stack. Before starting the waste deposition (1956) and after finishing the deposition of phosphogypsum (2010).

Phosphogypsum edge outflows are characterized by high acidity and EC values, as well as by containing high concentrations of potentially toxic metal(loid)s (Tables AP1.1-AP1.4). With respect to zone 1, the sample resulting of the interaction of phosphogypsum and seawater displayed a lower acidity and pollutant concentration than the edge outflows released from the other disposal areas of the stack, with values oscillating between samplings depending clearly on the degree of tidal influence (Table AP1.1). The edge outflows of zone 2 showed the highest acidity and pollutant concentrations, irrespective of the sampling period. Thus, these acid leachates displayed high concentrations of pollutants, such as PO_4, F, Al, Zn and As (average values of the

four sampling ranging between 16,444 and 32,633 mg/L, 696-943 mg/L, 75-120 mg/L, 33-44 mg/L and 16-20 mg/L, respectively) and to a lesser extent of Cu, Cd, Cr, Ni, Sb and U (Figs. 2.3 and 2.4). On the other hand, the edge outflows emerging from zone 3 showed both slightly lower pH values and higher pollutant concentrations than those found in the zone 4, reaching values up to 2 to 3 times higher for PO_4 and metal(loid)s such as Al, Cu, Cr, Ni, Cd, As and U (Tables AP1.3 and AP1.4). On the contrary, the leachates of zone 4 showed average concentrations of SO_4 and Fe higher than the rest of the edge leachates (Fig. 2.3).

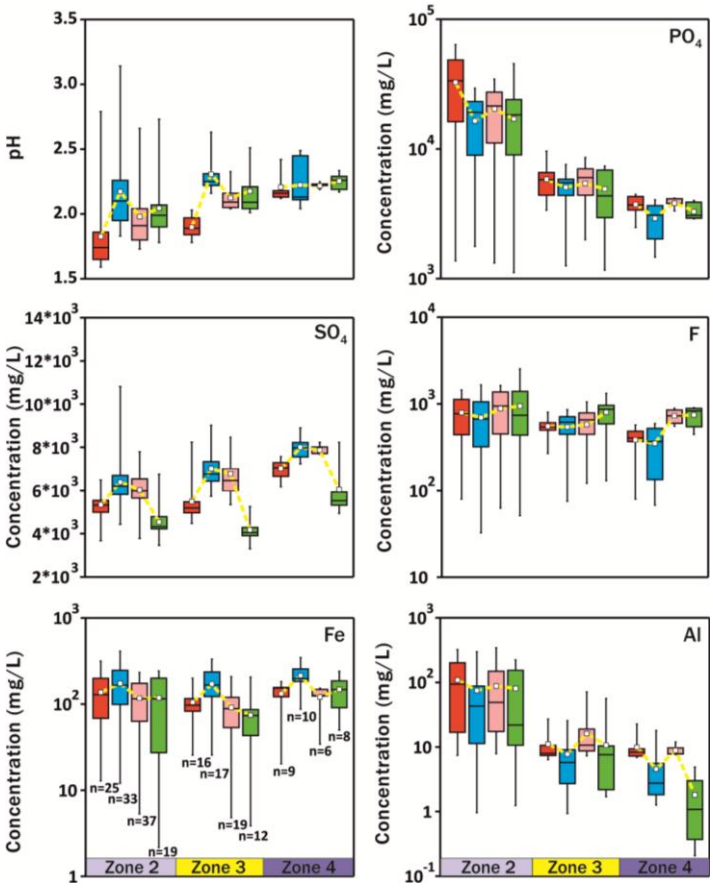

Figure 2.3. Box and whisker plots of pH and anions and major cations concentrations in the different sampling campaigns (orange: May-June 2014 (warm-dry period), blue: November 2014 (rainy period), pink: May-June 2015 (warm-dry period) and green: June 2016 (beginning of warm-dry period after rainy events)). Boxes represent 25th and 75th percentile range, while the horizontal lines at the whiskers ends depict the maximum and minimum values. The median and mean are represented by a horizontal line and a square, respectively, inside the boxes.

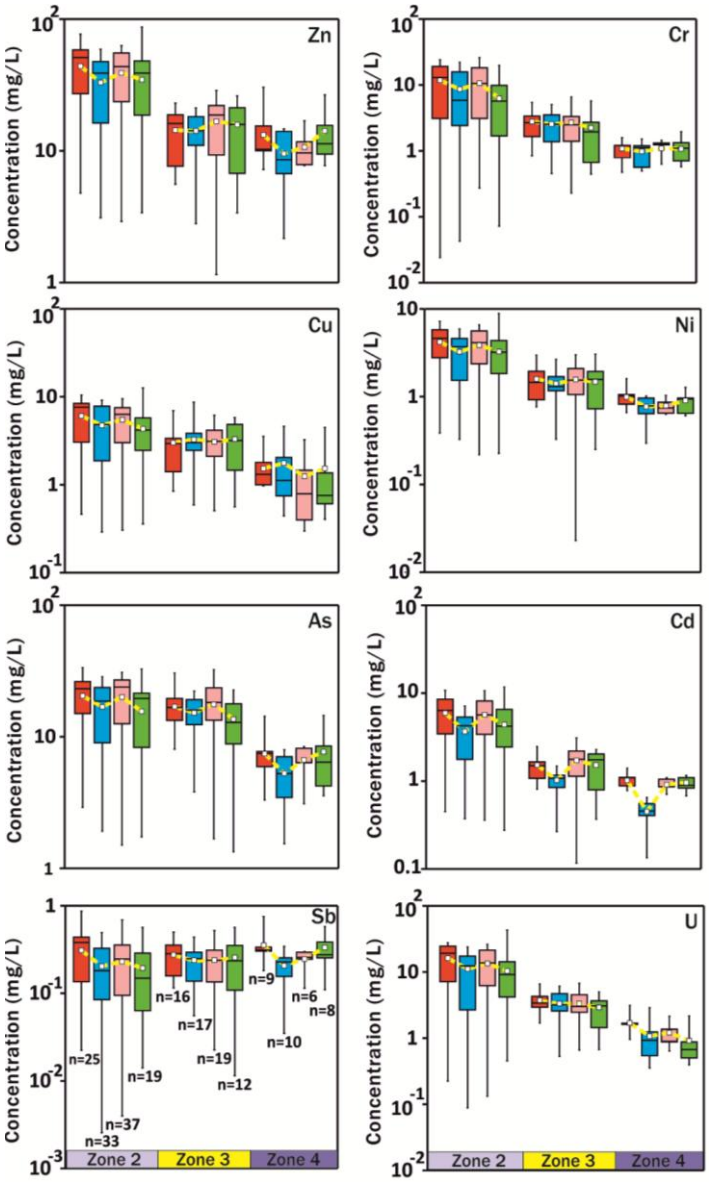

Figure 2.4. Box and whisker plots of minor cations concentrations in the different sampling campaigns (orange: May-June 2014 (warm-dry period), blue: November 2014 (rainy period), pink: May-June 2015 (warm-dry period) and green: June 2016 (beginning of warm-dry period after rainy events)). Boxes represent 25th and 75th percentile range, while the horizontal lines at the whiskers ends depict the maximum and minimum values. The median and mean are represented by a horizontal line and a square, respectively, inside the boxes.

The dissimilarities observed in the concentration of pollutants of the edge leachates between the different zones of the stack could be due to a combination of several factors such as the dumping history of phosphogypsum in each of the disposal areas, the morphodynamic domain of the estuary in which each zone is located and the preliminary restoration actions to which some zones have been subjected (Papaslioti et al., 2018a; Pérez-López et al., 2016; 2018). Thus, the higher concentrations of

pollutants observed in leachates from zone 2 than those from zones 3 and 4 would be closely related to the dumping history in this zone, since zone 2 is the only disposal area in which phosphogypsum was deposited using the recirculated and evaporated process water with the closed-loop system installed after 1997 (see Section 2.2.1). On the other hand, the vegetation cover spread in zone 4 as a restoration measure could explain the lower concentrations of most pollutants in this zone than in the unrestored zones. This is because the topsoil layer could be favoring sulfate-reduction processes and therefore the precipitation of metal sulfides, which would cause the removal of part of the pollution contained in the pore-solutions (Castillo et al., 2012; Pérez-López et al., 2018). This hypothesis becomes more relevant when comparing zones 3 and 4, since the phosphogypsum was deposited in a similar way in both zones using an open circuit system with seawater but zone 4 has undergone further restoration. Moreover, the zone 3 is currently naked and exposed to weathering with a large surface pond storing process water. The contribution of the process water infiltration to the composition of the edge leachates that emerge in this zone of the stack, although minimal (around 9% calculated using stable isotopes; Papaslioti et al., 2018a), could also explain the slightly higher concentrations observed in the leachates collected in zone 3 with respect to zone 4. On the other hand, a higher fluvial influence in the edge leachates of zone 4 could explain the highest average concentrations of SO_4 and Fe measured compared to those found in the other zones. According to Papaslioti et al. (2018a), zone 4 of the phosphogypsum stack is closer to the fluvial domain and hence is more influenced by the Tinto River, which is highly affected by acid mine drainage (AMD), i.e., acidic and sulfate- and iron-rich waters from the leaching of abandoned mining wastes mainly from the Riotinto mines (Cánovas et al., 2021; Nieto et al., 2013).

The influence of the different end-members on the hydrochemistry of edge outflows can be seen in Figure 2.5, where the results of the PCA for variables and samples are shown. Both factors (i.e., F1 and F2) explain 68% of variance and seem to be related to the different origin of pollutants in the outflows. As can be seen, three different groups of elements can be identified; i) those related to seawater, including Na, Cl, Mg, K, Br or SO_4, ii) those related to the acidic waters of the Tinto River, such as Fe, Sb, Pb, Cu, Zn or As, and iii) those related to phosphogypsum wastewaters such as F, Cr, U, PO_4, NH_4 and other trace metals. However, It is not surprising that some elements (e.g., As or Zn) are common between the different groups, taking into account that the edge

outflows originate from the leaching of the phosphogypsum stack with water of estuarine origin. Thus, the closeness of each sample to the different end-members (i.e., seawater, process water and Tinto river water) would define the level of influence of each end-member in these samples.

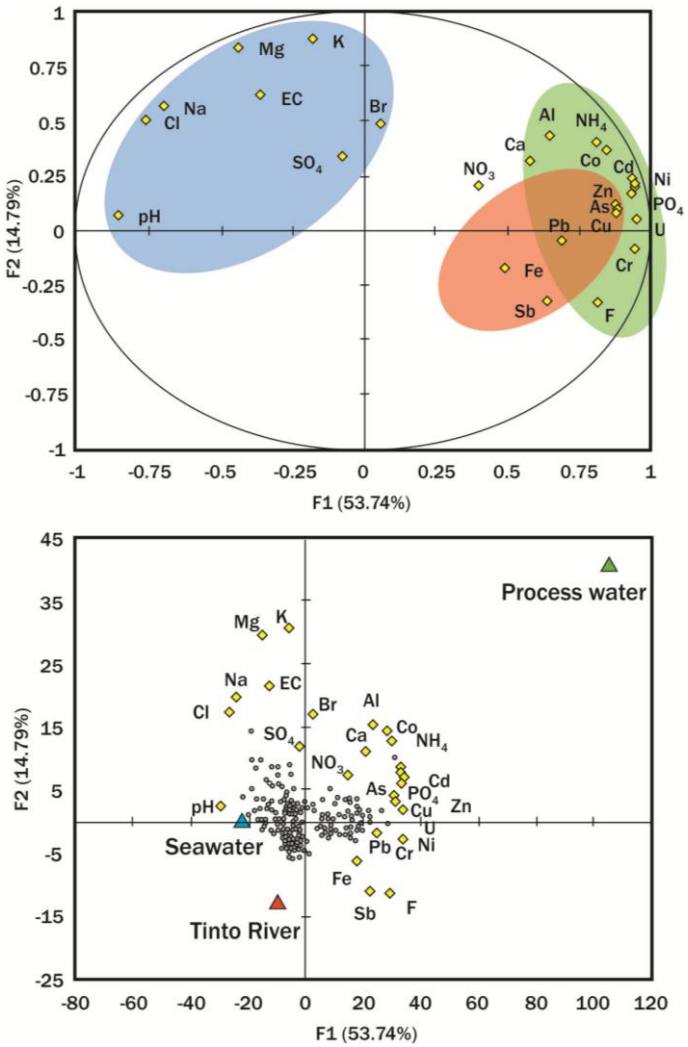

Figure 2.5. Principal component analysis (PCA) on samples and variables, including the main end-members (red: Tinto River, green: process water, and blue: seawater) responsible of hydrochemical variability of edge outflows.

2.3.3. Seasonal variability of the edge outflows hydrochemistry

As mentioned above, the Huelva phosphogypsum stack behaves as an anthropic aquifer with numerous springs releasing large amounts of pollutants to the Ría de Huelva estuary. These edge outflows showed low hydrochemical variability under the different hydrological conditions studied, i.e., warm-dry period, rainy period and beginning of warm-dry period after rainy events (Figs. 2.3 and 2.4). However, small fluctuations can be observed during the different scenarios. Thus, the lowest pH values

measured in the leachates from zones 2 and 3 occurred in the warm-dry periods (i.e., May-June 2014 and 2015) (average of 1.83-1.98 and 1.90-2.12, respectively), while the highest values were measured in the rainy period (average pH values of 2.17 and 2.31, respectively) and beginning of warm-dry period after rainy events (average pH values of 2.04 and 2.18, respectively). On the other hand, the pH values of the leachates from zone 4 remained almost constant during the different seasons, with average values between 2.21 and 2.27. The restoration measures implemented in this area likely minimize the infiltration of rainwater.

Regarding the seasonal variability in the concentrations of pollutants, these can be broadly classified into two groups according to their behavior during the different hydrological conditions. On the one hand, a group that includes most contaminants (e.g., PO_4, F, Al, Zn, Cr, Ni, As, Cd, Sb or U) whose dissolved concentrations decrease during the rainy period (i.e., November 2014) as a result of a dilution effect due to the recharge of rainwater (Figs. 2.3 and 2.4). On the other hand, a group that comprises pollutants such as SO_4 and Fe, which suffered an increase in the concentrations measured during the rainy period compared to the values analyzed in the leachates collected during the previous warm-dry period (i.e., May-June 2014) (Fig. 2.3). This increase in concentration of SO_4 and Fe observed during the rainy season is due to the increasing concentration of these dissolved pollutants in the Tinto River as a consequence of the washout of sulfate evaporitic salts, which are formed along the riverbanks and mine sites, mainly during the summer months and between rainfall events during warm-dry springs (Cánovas et al., 2021; Olías et al., 2006). The dissolution of these minerals together with the sweeping of sulfide oxidation products from mine sites lead to increasing metal concentrations in river waters entering the estuary. As mentioned above, there is a hydraulic connection between the estuary and the stack, and therefore it seems reasonable to think that certain variations in the hydrochemistry of the estuarine water could be reflected in the chemical composition of the discharges from the phosphogypsum stack.

In order to study the significance of seasonal hydrochemical variations of edge outflows, a statistical test was performed on samples collected during the rainy and dry seasons. As variables did not exhibit a normal distribution, the non-parametric test of Wilcoxon was selected, applying both the signed test and the Wilcoxon signed-rank

test. The signed test compares the number of exceeding cases between populations without considering the magnitude of these differences, while the Wilcoxon signed-rank test considers this magnitude. As a result, a spatial pattern was observed considering the seasonal differences noticed between the dry and rainy periods; the closer to the river the higher statistical differences in variables were recorded. For instance, the zone 4, the closer to the Tinto River, exhibited significant statistical differences for As, Ni, Co, U, Sb, Cd, Fe, SO_4, Zn, Al, Ca, and PO_4, between both periods. Only some metals such as Cr, Pb and Cu, together with F, Cl and pH showed similar distributions in both periods. In the case of zone 3, located downstream to the ocean, statistically significant differences were only observed for pH, Fe, SO_4, Sb, Al and Ca, while PO_4 showed only significant differences in the signed test. The zone 2, the farther area from the river (excluding zone 1, with only one sample), exhibited the lower number of variables displaying statistically significant differences for pH, Al, Ca, SO_4 and Fe, although in the latter two variables these differences were only observed in the signed test. These results supports previous findings about the control exerted on the hydrochemical spatial variations of edge outflows by the closeness to the Tinto River and its variability along the year.

2.3.4. Environmental implications

According to the hydrological response of the phosphogypsum stack, it can be considered as an anthropogenic aquifer with a similar hydrogeological behavior than coastal karstic aquifers. In fact, karstic features are widely recognized in phosphogypsum stacks worldwide (Lottermoser, 2010). Arfib and Charlier (2016) proposed a hydrological conceptual model for coastal karst aquifers divided into three reservoirs (deep, slow and fast), which could be adjusted to the results observed in the current study (see Figure 2.1). The deep reservoir would be characterized by brackish water, with low variations of discharge. This reservoir would represent the storage function of the aquifer, with a long residence time, strongly affected by saline intrusion. Under these circumstances, the water-level shows a low variability most of the time only controlled by tidal oscillations. In these prevailing conditions, waters may move by diffuse slow flow through the primary porous matrix which could supply the spring during low-flow period. On the other hand, both the slow and the fast reservoirs would

be characterized by freshwater input. The slow reservoir would represent the storage and the recession after rainfall events, whereas the fast reservoir would be characterized by a rapid infiltration and transfer through the aquifer during rainy events. Under these circumstances, the water quickly enters and emerges from the stack likely through large karst channels caused by gypsum dissolution.

Regarding the hydrochemical behavior of leachates from the phophogypsum stack, it is worth highlighting the low variability (although statistically significant in some cases) showed by these highly acidic and polluted waters under different hydrological conditions. However, it is of critical importance to sample in safe conditions the stack immediately after intense rainfall events, when a rapid discharge is observed and sharper hydrochemical differences would be expected. Thus, the results reported in this study have positive implications in the design of potential effective remediation treatments, since notable fluctuations in flow rates and pollutant load can cause operational problems in the treatment systems.

The findings obtained allow calculating the pollutant load that finally reaches the Ría de Huelva estuary with some reliability given the observed chemically homogeneous response throughout the system. Thus, an overall approach has been performed to calculate the metal loads released by the stack in each sampling period. To obtain the values in each sampling, the average concentrations of all the sampling points and the bulk discharge have been used. Considering all the edge outflows located around the perimeter of the phosphogypsum stack, a bulk discharge of acid leachates of around 500,000 m^3/yr has been estimated. However, these results may be underestimated due to the existence of diffuse edge outflows that are difficult to measure. These leachates release enormous amounts of pollutants to the estuary, e.g., PO_4, F, Fe, Zn, As, U, Cu, Cd and Ni (average values of 5000 tons/yr, 300 tons/yr, 76 tons/yr, 11 tons/yr, 6.9 tons/yr, 3.0 tons/yr, 1.7 tons/yr, 1.1 tons/yr and 1.0 ton/yr, respectively) (Table 2.1). Nevertheless, this estuarine environment is also affected by the Odiel and Tinto Rivers and their acidic and metal-rich waters due to AMD discharges from abandoned mining districts in the Iberian Pyrite Belt (IPB) (Nieto et al., 2013). In this sense, Table 2.1 also shows the average pollutant loads contributed by both rivers in the periods 1995-2003 (Olías et al., 2006) and 2004-2006 (Nieto et al., 2013). The results reported by these authors indicate a high variability in the average

pollutant load transported by the Odiel and Tinto Rivers, associated to hydrological variations between periods. Comparing both sources of contamination, i.e., phosphogypsum leachates and AMD-affected Tinto and Odiel Rivers, the phosphogypsum stack would be responsible for an average contribution of 16-85% of As, 9-27% of Cd, 3-16% of Ni, 1-4% of Fe and 0.3-2% of Zn of the total discharge reaching the estuary. In addition, as mentioned above, an important industrial complex is located in the Ría de Huelva estuary. Different industrial activities developed in this complex can also discharge metal-rich effluents directly into the estuary (Pérez-López et al., 2011c). In this sense, these authors calculated the average pollutant load from the Huelva industrial complex between 2003 and 2006 (no current data available). This value was much lower than that contributed by the Tinto and Odiel Rivers, exhibiting values of one to two orders of magnitude lower for most of the pollutants (Table 2.1). However, Pérez-López et al. (2011c) did not contemplate in the study the contribution of pollutants to the estuary from the phosphogypsum stack as a pollution source also of industrial origin. The capacity of contamination of the phosphogypsum pile is more significant taking into account that its extension is three orders of magnitude lower than the area of the fluvial basins (i.e., around 3979 km^2). In addition, some of the pollutants (e.g., PO_4, F and U) discharged into the estuary from the phosphogypsum stack are negligible in the mine waters. For these reasons, the treatment of effluents from the phosphogypsum stack is essential to minimize the pollution that reaches the Ría de Huelva estuary. In this sense, the application of passive dispersed alkaline substrate (DAS) technology for highly acidic and contaminated phosphogypsum leachates has shown to be highly effective in reducing the pollutant load and acidity (Millán-Becerro et al., 2020; 2022).

Table 2.1. Comparison of the average pollutant loads released by the phosphogypsum stack into the Ría de Huelva estuary with the discharges from the mining activity in the IPB during the period 1995-2003 (Olías et al., 2006)[a] and during the period 2004-2006 (Nieto et al., 2013)[b], plus the effluents poured by the factories of the Huelva industrial complex between 2003 and 2006 (Pérez-López et al., 2011)[c]. In addition, this table shows the contribution (%) of the pollutant load from the stack that reaches the estuary with respect to the total.

	Phosphogypsum stack (tons/yr)	AMD[a] (tons/yr)	AMD[b] (tons/yr)	Industrial estate[c] (tons/yr)	Phosphogypsum stack contribution (%)
PO_4	5000	-	-	-	-
F	300	-	-	-	-
Fe	76.3	7922	1719	10.7	0.95-4.21
Zn	10.5	3475	649	3.39	0.32-1.66
As	6.86	35.5	1	0.23	16.2-84.9
U	2.96	-	-	-	-
Cr	2.27	-	-	0.04	-
Cu	1.67	1721	412	-	-
Cd	1.13	11.0	3	0.03	9.07-26.6
Ni	1.00	36.2	5	0.20	2.67-16.1

2.4. CONCLUSIONS

This work is focused on studying of seasonal and spatial hydrochemical variability of highly acidic and contaminated leachates from a phosphogypsum stack dumped into estuarine marsh soils in SW Spain and evaluating its hydrological response under potential weathering agents.

The results obtained in this study clearly indicate that the phosphogypsum stockpiled behaves as an anthropic aquifer with karstic features. This aquifer shows two feeding ways; a continuous recharge of estuarine water in the deep zone of the stack, where phosphogypsum and marsh soil are directly in contact, and a punctual recharge by rainwater that infiltrates through the surface of the phosphogypsum stack and circulates through dissolution conduits. Thus, the water-table of this aquifer is controlled mainly by tidal fluctuations, remaining almost constant most of the time (± 2 cm). However, the water-table of the stack rapidly increased up to 20 cm during the rainy events studied. Later, almost half of the height increased by the water-table during the rain episode is immediately recovered when rainfalls cease, while pre-rainfalls conditions are reached within a period between 5 and 15 days depending on rainfall intensity.

During the development of this study, ninety-five edge outflows were identified around the perimeter of the stack, through which extremely acidic and polluted waters

continually emerge and subsequently reach the estuary. These leachates showed, as general rule, a low hydrochemical variability under different hydrological conditions. However, small variations in pollutant concentrations have been observed during the different periods. In this sense, two different processes have been proposed as possible mechanisms responsible for such variability: (1) dilution by rainwater recharge during the rainy period, which cause a slight decrease in concentration of most dissolved contaminants (e.g., PO_4, F, Al, Zn, Cr, Ni, As, Cd, Sb or U) observed in the edge outflows; and (2) the dissolution of the sulfate evaporitic salts precipitated during the summer along the banks of the Tinto River and mine sites, which cause an increase in the dissolved concentration of SO_4 and Fe in the river water and subsequently in the leachates released from the phosphogypsum stack during the rainy season.

The low variability hydrochemical shown in the current work has positive implications in the design and optimization of sustainable passive treatment systems for phosphogypsum leachates before their release to the Ría de Huelva estuary. According to the results obtained in this study, the stack releases high concentrations of pollutants such as PO_4, F and U (average values of 5000 tons/yr, 300 tons/yr and 3.0 tons/yr, respectively), which are only found in phosphogypsum leachates. In addition, between 16-85% and 9-27% of the total content of As and Cd, respectively, that reach the Ría de Huelva estuary come from the phosphogypsum stack. Therefore, the implementation of the aforementioned restoration measures in the phosphogypsum stack should be carried out urgently in order to minimize the pollutant load that reaches the estuary.

CHAPTER 3. ASSESSMENT OF METALS MOBILITY DURING THE ALKALINE TREATMENT OF HIGHLY ACID PHOSPHOGYPSUM LEACHATES

BASED ON:

Millán-Becerro, R., Pérez-López, R., Macías, F., Cánovas, C.R., Papaslioti, E.M., Basallote, M.D., 2019. Assessment of metals mobility during the alkaline treatment of highly acid phosphogypsum leachates. Science of the Total Environment, 660, 395–405.

ABSTRACT

This research evaluates the feasibility of an alkaline treatment system for highly acid leachates from a phosphogypsum stack located in an estuarine environment degraded by such pollution. The presented methodology consists of the addition of a $Ca(OH)_2$ solution to the different types of phosphogypsum-related acidic leachates with the aim to increase their pH and subsequently, to provoke the precipitation and immobilization of the dissolved contaminants. In fact, PO_4 and F reached removal of 100% and 90%, respectively. As regards metals, removal values close to 100% were reached for Fe, Al, Cr, Cd, U and Zn, whereas it did not seem to be totally effective for other elements such as As (removal of 57–82%) and Sb (4–36%). The decrease of contaminant concentrations was caused probably by co-precipitation and/or adsorption to phosphate phases, together with by fluoride precipitation. The solid phases formed during the treatment were subjected to two standard leaching tests (EN 12457-2 from the European Union and TCLP from the United States) in order to conduct a risk and management assessment. In this context, some of the precipitates formed during the treatment would be classified as hazardous wastes, due to the high concentration of As leached. Moreover, the potential economic costs of a convectional active treatment system were also explored. This study sets the basis for a new research line with the aim to minimize the impact of the phosphogypsum stacks worldwide to their adjacent environment.

CHAPTER 4. DESIGN AND OPTIMIZATION OF SUSTAINABLE PASSIVE TREATMENT SYSTEMS FOR PHOSPHOGYPSUM LEACHATES IN AN ORPHAN DISPOSAL SITE.

BASED ON:

Millán-Becerro, R., Pérez-López, R., Macías, F., Cánovas, C.R., 2020. Design and optimization of sustainable passive treatment systems for phosphogypsum leachates in an orphan disposal site. Journal of Environmental Management, 275, 111251.

ABSTRACT

The optimization of the dispersed alkaline substrate (DAS) technology was investigated to achieve the treatment of highly acidic and polluted effluents from a phosphogypsum pile in an orphan site of SW Spain. This phosphogypsum disposal area is located on the Tinto River marsh soils, where it acts as a source of pollution for the estuarine environment, releasing high concentrations of metal(loid)s and radionuclides, which degrade the surrounding waters. The methodology consists of flowing the leachates through columns loaded with a combination of a fine-grained alkaline reagent scattered in a non-reactive matrix to raise the water pH while decreasing the solubility of dissolved contaminants. Seven columns were built, one for each of the alkaline reagent used: limestone, barium carbonate, biomass ash, fly ash, MgO, $Mg(OH)_2$, and $Ca(OH)_2$. The $Ca(OH)_2$-DAS and MgO-DAS treatment systems showed the highest effectiveness, reaching near-total removal for PO_4, F, Fe, Zn, Cu, Al, Cr, and U with initial reagent mass:treated volume ratios of 36.3 g/L and 7.57 g/L, respectively. Total As removal was only achieved in the $Ca(OH)_2$-DAS treatment. Phosphate precipitation was the main mechanism responsible for pollutants removal. Geochemical modeling using PHREEQC code and mineralogical evidence confirmed the precipitation of these minerals. This study forms the basis of an effective and environmentally sustainable treatment system for phosphogypsum leachates to reduce the impact of the fertilizer industry worldwide.

CHAPTER 5. ENVIRONMENTAL MANAGEMENT AND POTENTIAL VALORIZATION OF WASTES GENERATED IN PASSIVE TREATMENTS OF FERTILIZER INDUSTRY EFFLUENTS.

BASED ON:

Millán-Becerro, R., Macías, F., Cánovas, C.R., Pérez-López, R., Fuentes-López, J.M., 2022. Environmental management and potential valorization of wastes generated in passive treatments of fertilizer industry effluents. Chemosphere, 295, 133876.

ABSTRACT

A phosphogypsum stack located in SW Spain releases highly acidic and contaminated leachates to the surrounding estuarine environment. Column experiments, based on a mixture of an alkaline reagent (i.e., MgO or $Ca(OH)_2$) dispersed in an inert matrix (dispersed alkaline substrate (DAS) technology), have shown high effectiveness for the treatment of phosphogypsum leachates. MgO-DAS and $Ca(OH)_2$-DAS treatment systems achieved near total removal of PO_4, F, Fe, Zn, Al, Cr, Cd, U, and As, with initial reactive mass:volume of leachate treated ratios of 3.98 g/L and 6.35 g/L, respectively. The precipitation of phosphate (i.e., brushite, cattiite, fluorapatite, struvite and $Mn_3Zn(PO_4)_2 \cdot 2H_2O$) and sulfate (i.e., despujolsite and gypsum) minerals could control the solubility of contaminants during the treatments. Therefore, the hazardousness of these wastes must be accurately assessed in order to be properly managed, avoiding potential environmental impacts. For this purpose, two standardized leaching tests (EN-12457-2 from the European Union and TCLP from the United States) were performed. According to European Union (EN-12457-2) regulation, some wastes recovered from DAS treatments should be classified as hazardous wastes because of the high concentrations of SO_4 or Sb that are leached. However, according to United States (US EPA-TCLP) legislation, all DAS wastes are designated as non-hazardous wastes. Moreover, the solids generated in the DAS systems could constitute a promising secondary source of calcite and/or P. This research could contribute to worldwide suitable waste management for the fertilizer industry.

5.1. INTRODUCTION

Phosphoric acid is the main raw material employed in the manufacture of phosphate fertilizers, which are essential to maintain current levels of agricultural production worldwide. Phosphoric acid is commonly obtained through the wet chemical digestion of phosphate rocks with sulfuric acid. However, during this industrial process, an unwanted waste known as phosphogypsum is generated (Cánovas et al., 2018a).

The phosphogypsum (mainly gypsum, $CaSO_4 \cdot 2H_2O$) contains a high amount of toxic elements (e.g., As or Cd) and radionuclides from the U^{238} decay series (Macías et al., 2017a; Rutherford et al., 1994). These impurities are contained in the raw materials used (i.e., phosphate rock and sulfuric acid) and subsequently transferred to the final products. The solid phosphogypsum interstitial space is filled with highly-polluting residual acids (i.e., phosphoric–sulfuric–hydrofluoric acids rich in metal(loid)s), which are part of the reagents and products that cannot be recovered during the manufacturing process (Lottermoser, 2010). However, despite its environmental concern, these highly acidic wastes are usually disposed in stacks close to coastal areas where they are exposed to strong weathering processes (Tayibi et al., 2009). Furthermore, some of these stacks are not covered by any type of material and/or are dumped directly over soils without any type of insulating barrier (Kuzmanović et al., 2020; Macías et al., 2017a; Vásconez-Maza et al., 2019), therefore favoring its weathering as well as the generation of dust with high amounts of ultrafine particles and nanominerals (Lütke et al., 2020). Consequently, phosphogypsum stacks usually constitute a significant source of contamination to the surrounding environment due to the existence of polluted acid effluents from their leaching (Pérez-López et al., 2016). These leakages that commonly emerge at the edges of the stacks, known as edge outflows, are characterized by very low pH values and extremely high concentrations of SO_4, PO_4, F, and metal(loid)s such as Fe, Al, Zn, Cu, As, U, and Cd, among others (Lysandrou and Pashalidis, 2008; Pérez-López et al., 2016). Additionally, other acid effluents related to the fertilizer industry are produced during the washing of acid gases from the industrial process, which must be treated prior to their release into the environment (Affonso et al., 2020).

Recently, for the first time, Millán-Becerro et al. (2020) demonstrated the use of passive dispersed alkaline substrate (DAS) technology to successfully remove the acidity and pollutants from phosphogypsum-related leachates. This passive technology

was initially designed for the treatment of acid leachates rich in SO_4 and metal(loid)s from sulfide mining wastes, the so-called acid mine drainage (AMD). This alkaline treatment is particularly interesting at orphan sites due to economic and environmental criteria (Ayora et al., 2013; Martinez et al., 2019; Pérez-López et al., 2011b) and because it is considered the best sustainable upcycling solution for AMD pollution (Orden et al., 2021). The DAS system consists of a mixture of a fine-grained alkaline material with high neutralization potential and an inert matrix to provide high porosity, avoiding passivation and clogging problems associated with mineral precipitation (Ayora et al., 2016; Macías et al., 2012c). Different types of alkaline materials were tested by Millán-Becerro et al. (2020) in the design and optimization of DAS technology for phosphogypsum leachates; from conventional alkaline reagents (limestone, barium carbonate, MgO, $Mg(OH)_2$, and $Ca(OH)_2$) to waste materials (fly or biomass ashes). In that study, it was concluded that MgO and $Ca(OH)_2$ are the most effective alkaline reagents to abate the pollution from these leachates, which could be applied in other phosphogypsum waste facilities worldwide. However, these previous works highlighted the need to optimize both the operational hydraulic parameters and the alkaline reagent:acid leachate ratio to significantly increase the performance in MgO-DAS and $Ca(OH)_2$-DAS systems. On the other hand, this treatment generated significant amounts of pollutant-rich solids (Millán-Becerro et al., 2020), which may require proper and long-term management. In this sense, the mineralogical and geochemical characterization, and the potential environmental risks of these solids, must be assessed in order to minimize the environmental impacts during their management. To the best of our knowledge, this research has not been previously reported in the literature.

Thus, the main objectives of this research were to optimize the DAS-based treatment of these leachates and to assess the stability and the potential environmental risks of these wastes while establishing the management bases for their secure disposal. In this sense, the metal-rich wastes generated during the DAS treatment of phosphogypsum leachates have been subjected to two standardized leaching tests (EN 12457-2, 2002 and US EPA TCLP, 1992) proposed by current European Union (EU) and United States (US) environmental regulations, respectively. These leaching tests were used to assess the waste hazardousness according to the regulated limits of several released pollutants. Additionally, these tests allow for the evaluation of DAS waste

weathering upon different environmental scenarios (i.e., weathering by rainfalls and weathering under reducing conditions). In addition, a detailed mineralogical and geochemical study has been done to adequately characterize the wastes and to estimate metal mobility. To our knowledge, this is the first time that this methodology has been applied to this type of waste, and it should, therefore, be considered when managing similar wastes generated during the passive treatment of fertilizer industry effluents worldwide. This work fills a gap in the knowledge of the sustainable management of wastes from the fertilizer industry, contributing to the circular economy objectives in this industrial sector.

5.2. MATERIALS AND METHODS

5.2.1. Study area

The site investigated is a controversial phosphogypsum stack located directly above salt-marshes of the Tinto River estuary (Huelva, SW Spain). The manufacture of phosphoric acid in the Huelva phosphate fertilizer industry took place for more than forty years (from 1968 to 2010). During this period, around 100 million tons of phosphogypsum were generated. This waste, classified as a hazardous material according to EU legislation (Macías et al., 2017a), was dumped in stacks (12 km^2 of surface) located directly on the marsh soil, less than 100 meters from the Huelva city. The stack is divided into four disposal modules; zones 1 and 4 are partially restored, while in zones 2 and 3 no restoration measures have been carried out yet. However, all disposal areas show edge outflows in their perimeters due to the hydraulic and chemical connection of the stack with the estuarine tidal channels and the lack of insulating materials in the stack (Pérez-López et al., 2016). The zone 4 of the stack raises a special concern since previous restoration measures were not effective and continues to release hazardous substances that poses serious threats to human health or the environment. In fact, zone 4 can be classed as an orphan site since the parties responsible for the contamination are unknown, unable or unwilling - to pay for needed remedial actions (Millán-Becerro et al., 2020). A broader description of the study area can be found in Pérez-López et al. (2016).

5.2.2. Column setup

Four columns made of polymethyl methacrylate (40 cm in height and 6 cm inner diameter) were built and provided with a drain pipe and a 3 cm layer of glass pearls (3 mm diameter) at the bottom to favor water drainage. Two columns were filled with MgO-DAS and the other two with $Ca(OH)_2$-DAS reactive material (20 cm of filling material each), consisting of a mixture of reagent (75.7 g of magnesia and 127 g of calcium hydroxide, respectively) with wood chips at a 1:4 ratio in volume. Each column was connected to a decantation vessel of 445 cm^3. One of the systems filled with each type of DAS reagent material (i.e., MgO-DAS and $Ca(OH)_2$-DAS) was used to study the hydrochemical evolution during the experiments, while the other DAS systems were used to obtain the solid precipitates originated during the alkaline treatment.

Magnesia (70% periclase (MgO)) was supplied by Magnesitas de Navarra S.A, while high purity calcium hydroxide (> 95% portlandite ($Ca(OH)_2$)) was provided by Fisher Chemical. The mineralogical composition and bulk chemistry of both alkaline reagents can be seen in Table AP4.1 of Appendix. Leachates from zone 4 were collected to feed the columns due to its status as an orphan site. The chemical composition and physico-chemical parameters of the input solution are shown in Table AP4.2. During the treatment, the input water was conducted by a peristaltic pump, with a constant flow rate of 0.3 mL/min, to the top of the DAS columns, and then flowed downward through the reactive materials and out of the drain pipe into the decantation vessels.

5.2.3. Water sampling and analysis

Water samples were daily collected from the different treatment components; input and outputs of DAS columns and decantation vessels. Different physico-chemical parameters such as pH, electrical conductivity (EC), oxidation-reduction potential (ORP) and temperature were measured in situ with a CRISON multi-parameter portable equipment MM 40+, previously calibrated with buffer solutions of 4.01, 7.00, and 9.21 for pH and with standard solutions of 147 µS/cm, 1413 µS/cm, and 12.88 mS/cm for CE. Furthermore, the accuracy of the ORP measurements was checked using buffer solutions of 220 and 470 mV. Values of ORP were corrected according to Nordstrom and Wilde (1998) to obtain Eh values, referenced to the standard hydrogen electrode.

Sampled solutions were filtered and divided into two aliquots, one non-acidified for anions and NH_4 analysis by high performance liquid chromatography (HPLC); and the other acidified with ultrapure HNO_3 (2%) at pH <1 for cations. Major element (Fe, Zn, Al, S and P) concentrations were determined by atomic emission spectroscopy with inductively coupled plasma (ICP-AES, Jobin Yvon Ultima 2) while those of trace elements (Cu, As, Cr, U, Cd, Ni, Co and Sb) were analyzed by mass spectrometry with inductively coupled plasma (ICP-MS; Agilent 7700). All analyzes were carried out in the Laboratories of the University of Huelva. The detection limits were: 0.2 mg/L for S; 0.05 mg/L for Fe; 0.02 mg/L for Al, Zn and P; and 0.1 μg/L for trace elements. In the laboratory, home-made standards with concentrations within the range of the samples were prepared from certified materials and included in each analysis sequence to verify the analytical accuracy. In this same sense, blank solutions made with the same acid matrix as the samples were also analyzed. Furthermore, dilutions were carried out to guarantee that sample concentrations were within the concentration range of the standards. The average measurement error was better than 5% in all samples.

5.2.4. Solid samples characterization

The columns aimed to collect solid samples were stopped during the maximum effectiveness period of pollutant removal, in order to avoid possible re-dissolution processes of newly-formed precipitates after this period, which has been reported in previous studies (Millán-Becerro et al., 2020). This period of maximum effectiveness ends once the alkaline reagent is consumed or coated by these precipitated solids and, consequently, there is a sharp decrease in the pH of the leachates treated and an increase in metal concentrations.

Once the experiments were stopped, the columns were disassembled, split into 5 cm-thick slice and dried at room temperature. The solids precipitated in the decantation vessels were also collected. The main mineral phases contained in these solids were identified by X-ray diffraction (XRD) using a Bruker D8 Advance X-ray diffractometer with Cu Kα monochromatic radiation, and examined by an Electron Probe Micro-Analyzer (EPMA), via a JEOL JXA-8200 SuperProbe using a fitted Wavelength-Dispersive Spectrometer (WDS) equipment.

The pseudo-total chemical composition of the solid samples was obtained by standardized aqua regia digestion as follows: 5 mL of aqua regia (12 mol/L HCl and 15.8 mol/L HNO_3 in a 3:1 ratio) were added to 0.5 g of sample in Teflon reactors and reacted for 24 h at room temperature in a fume cupboard, and then, on a heating plate for 2 h at 130 ºC.

5.2.5. Leaching protocols for the hazardousness classification and environmental assessment

The hazardousness of the solids collected from the DAS treatments was evaluated according to the international leaching test proposed by the EU and US EPA (US Environmental Protection Agency) regulations (EN 12457-2, 2002 and US EPA TCLP, 1992, respectively). The EN 12457-2 leaching test is employed to assess the suitability of disposing a waste in European landfills (landfills for inert, non-hazardous and hazardous wastes; EC Decision 2003/33/EC), based on the leached concentration of certain contaminants (i.e., SO_4, Ba, Zn, Cu, As, Cr, Mo, Pb, Ni, Se and Sb). This standardized leaching test is based on the interaction of the wastes with distilled water in a solid:liquid ratio of 1:10, followed by agitation on a shaker for 24 h. The supernatants were filtered and then analyzed to determine the dissolved contaminant concentrations.

The TCLP leaching test has traditionally been used to simulate co-disposal of materials with municipal wastes, although, its application has been extended to the management of other types of wastes (US EPA, 1998). Additionally, the concentrations of metals (As, Ba, Cd, Cr, Ni, Pb, V, Zn, Se, Sb, Be and Tl) leached during the TCLP test can also be used as a limit value to determine if a waste should be subjected to a universal treatment standard (UTS) in order to comply with land disposal restrictions (LDR, EPA 530-R-01-007) (US EPA, 2020a). This leaching test was performed based on method 1311 of the US EPA (US EPA, 1992). First, the extraction liquid was chosen based on the pH of the waste. For solids with pH<5, a solution of CH_3COOH buffered at pH 4.93 must be employed as extractant. On the contrary, if the residues have pH>5, a solution of CH_3COOH buffered at pH 2.88 must be used as extractant fluid. The MgO-DAS and $Ca(OH)_2$-DAS wastes collected at 0-15 and 0-10 cm depth, respectively,

had a pH close to 2. On the other hand, the MgO-DAS wastes taken at 15-20 cm depth and $Ca(OH)_2$-DAS solids collected at depths deeper than 10 cm, presented pHs of 6 and 10 respectively. Following this EPA method, the suspensions were centrifuged and the supernatants were filtered and stored for their subsequent chemical analysis.

Additionally, the results obtained from these tests can also be used to study the weathering of these materials in different environment conditions. Thus, the contact of these solids with water during the EN 12457-2 test would reproduce weathering by rainfall events, while the interaction with organics acids during TCLP protocol would mimic weathering upon reducing conditions. Both leaching tests have been previously employed for the classification, management and environmental assessment of wastes generated during alkaline treatments of acidic and metal-rich waters from mining with DAS technology (Macías et al., 2012a).

5.2.6. Geochemical modeling

The saturation indices (SI) of solutions with respect to certain mineral phases that could be controlling the solubility of contaminants during the DAS treatments were calculated with the code PHREEQC 3.0 (Parkhurst and Appelo, 2005) using the MINTEQ.V4 thermodynamic database (Allison et al., 1991). This database was slightly amended to include thermodynamic data of fluorapatite from Lawrence Livermore National Laboratory (llnl.dat) database.

An equilibrium-based geochemical modeling was performed to estimate the amount of calcite ($CaCO_3$) precipitated in the decantation vessel during the treatment of leachates with $Ca(OH)_2$-DAS technology. For the building of this geochemical model the "EQUILIBRIUM PHASES" data block was used, which was employed to impose the precipitation of this mineral phase if oversaturation in water were observed.

5.3. RESULTS AND DISCUSSION

5.3.1. Chemical evolution during DAS treatments

The acid leachates used in this study displayed extremely low pH values (average of 2.24) and high net acidity (of 6240 mg/L as $CaCO_3$ equivalents according to the definition of Kirby and Cravotta (2005a) and modified by Millán-Becerro et al. (2020)), as well as high dissolved concentrations of pollutants, i.e., 2513 mg/L of PO_4, 5321 mg/L of SO_4, 1328 mg/L of F, 160 mg/L of NH_4, 102 mg/L of Fe, 16 mg/L of Zn, 5.5 mg/L of Cu, 3.0 mg/L of As, 2.8 mg/L of Al, 2.8 mg/L of Cr, 1.8 mg/L of U, and 0.7 mg/L of Cd, among others (Table AP4.2).

MgO-DAS was run under optimal conditions for 43 days, successfully treating 19 L of leachates. The increase in pH values up to around 9.6 (Fig. 5.1a) promoted the total removal of F, Fe, Zn, Al, Cr, U, and Cd (around 98% of PO_4 and close to 77% for Cu) (Fig. 5.1a,b,c). Regarding As, the alkaline treatment showed removal percentages close to 100% for the first 32 days, reducing the removal rate to around 76% for the rest of the effective experimental runtime. Other pollutants, such as SO_4 and NH_4, showed more conservative behavior, reaching average removal rates of 15–43% (Fig. 5.1a,b). The sharp decrease in PO_4 and F may be due to the intense precipitation of Ca-Mg-Fe phosphates and Ca fluorides (i.e., hydroxylapatite ($Ca_5(PO_4)_3(OH)$), fluorapatite ($Ca_5(PO_4)_3F$), cattiite ($Mg_3(PO_4)_2{\cdot}22H_2O$), strengite ($FePO_4{\cdot}2H_2O$), and fluorite ($CaF_2$)) (Table AP4.3). These minerals could also control the solubility of other contaminants, such as NH_4, Zn, Cu, As, Al, Cr, U, and Cd, by co-precipitation and/or adsorption processes. In addition, the precipitation of oxyhydroxides (e.g., goethite (FeO(OH)), lepidocrocite (FeO(OH)), $Fe(OH)_{2.7}Cl_{0.3}$, spertiniite ($Cu(OH)_2$), and diaspore (AlO(OH))) oversaturated in the outflows, according to PHREEQC (Table AP4.3), cannot be ruled out. The slight decrease in SO_4 concentration could be attributed to gypsum ($CaSO_4{\cdot}2H_2O$) precipitation, which was close to equilibrium according to PHREEQC, and/or associated with co-precipitation processes onto the phosphate phases (Park et al., 2008). On the other hand, the precipitation of brucite ($Mg(OH)_2$) could also take place during the alkaline treatment since equilibrium with this mineral phase was predicted by PHREEQC.

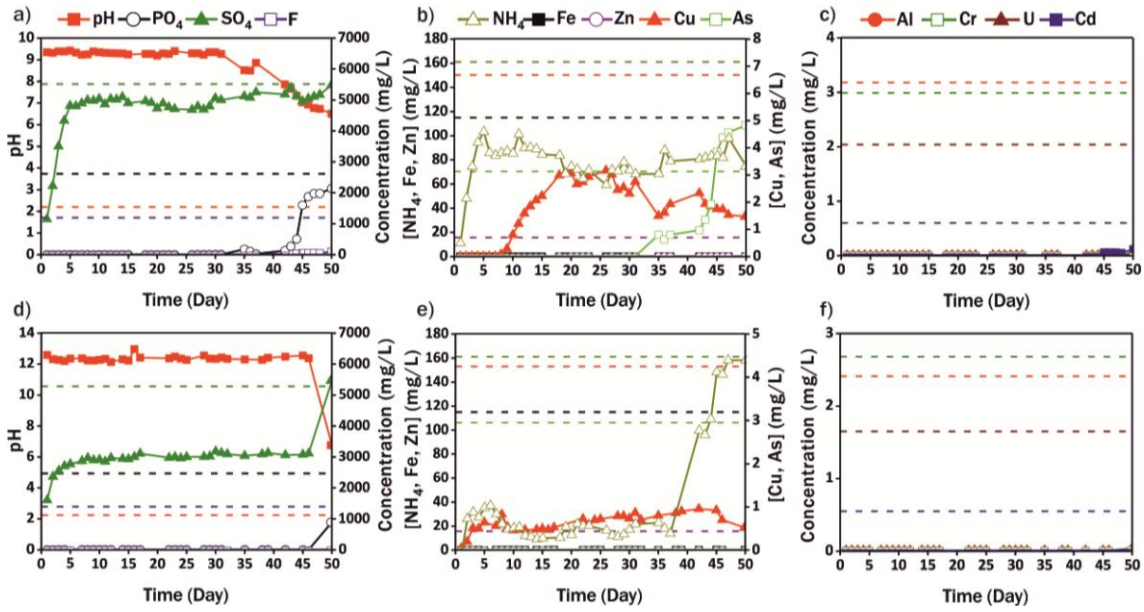

Figure 5.1. Evolution in the pH and output concentration of anions and cations dissolved in the phosphogypsum leachates during the neutralization experiments with both treatment systems; i.e., MgO-DAS (a,b,c) and $Ca(OH)_2$-DAS (d,e,f). The dashed lines indicate the initial concentration of the different pollutants.

The $Ca(OH)_2$-DAS column effectively treated 20 L of acid leachates during 46 days of the experimental run. The $Ca(OH)_2$ dissolution raised the pH up to average values of 12 (Fig. 5.1d), allowing the total elimination of PO_4, F, Fe, Zn, As, Al, Cr, U, and Cd (Fig. 5.1d,e,f). In addition, around 71–73% of NH_4 and Cu was removed. The average removal of SO_4 reached 45%, which is three times greater than that achieved in the MgO-DAS system. According to PHREEQC calculations, the $Ca(OH)_2$-DAS treated waters showed oversaturation with respect to calcium phosphates and fluoride (i.e., hydroxylapatite, fluorapatite, and fluorite) (Table AP4.4). These minerals could play a key role in the elimination of toxic pollutants, such as F, NH_4, Fe, Zn, Cu, As, Al, Cr, U, and Cd, according to the removal rates observed in Fig. 5.1. However, as in the case of MgO-DAS, the precipitation of oxyhydroxide minerals (i.e., goethite, lepidocrocite, $Fe(OH)_{2.7}Cl_{0.3}$, and spertiniite) is predicted to occur with this treatment. Gypsum was oversaturated in treated waters (Table AP4.4), which could explain the higher removal percentages with respect to the MgO-DAS system, where this mineral phase was found to be undersaturated. Finally, the solutions from the $Ca(OH)_2$-DAS system showed oversaturation with respect to brucite and calcite ($CaCO_3$).

The results described above indicate that $Ca(OH)_2$-DAS technology is the most effective remediation strategy for phosphogypsum leachates, achieving an initial reactive mass:volume of leachate treated ratio of 6.35 g/L. The MgO-DAS treatment system also showed high effectiveness at removing pollutants, with a mass:volume ratio of 3.98 g/L. These data represent an improvement in the volume of leachate treated per mass of reagents used with respect to those reported by Millán-Becerro et al. (2020) (i.e., 36.3 g/L for $Ca(OH)_2$-DAS and 7.57 g/L for MgO-DAS). This improvement involves obtaining ratios that are 6 and 2 times lower, respectively, than the reported rates by these authors.

5.3.2. Mineralogical characterization

In the MgO-DAS treatment system, periclase (MgO), dolomite ($CaMg(CO_3)_2$) and magnesite ($MgCO_3$) (inherited from the original reactive material; Table AP4.1) were identified by XRD along the depth profile of the reactive column (Fig. 5.2a). Brushite ($CaHPO_4{\cdot}2H_2O$), despujolsite ($Ca_3Mn(SO_4)_2(OH)_6{\cdot}3H_2O$), and brucite were the predominant newly-formed minerals at shallower depths (<10 cm), while at deeper depths (>10 cm) several phosphate minerals were identified (i.e., fluorapatite, cattiite, struvite ($NH_4MgPO_4{\cdot}6H_2O$), struvite-(K) ($KMgPO_4{\cdot}6H_2O$), and $Mn_3Zn(PO_4)_2{\cdot}2H_2O$) together with the aforementioned sulfate phase (i.e., despujolsite). On the other hand, the minerals precipitated in the decantation vessel correspond to evaporitic salts (halite (NaCl) and hexahydrite ($MgSO_4{\cdot}6H_2O$); Fig. 5.2a). The EPMA analyses of some selected solid samples (taken at 0–5 and 10–15 cm depths; Fig. 5.3a and b, respectively) showed the existence of sub-micrometer granular aggregates chemically constituted mainly of P, Ca, and Mg, which is indicative of brushite and cattiite. Other pollutants (Fe, Zn, Mn, K, and S) were detected in the same aggregates, suggesting the precipitation of strengite, $Mn_3Zn(PO_4)_2{\cdot}2H_2O$, struvite-(K), and despujolsite, or the co-precipitation and/or adsorption of these elements on these phosphate minerals (i.e., brushite and cattiite). It should be noted that the identification of individual phases was not possible due to the cryptocrystalline size of the solids. The evaporitic salts of the decantation vessel appeared as pure phases, with no presence of pollutants, which would confirm the efficiency of the treatments.

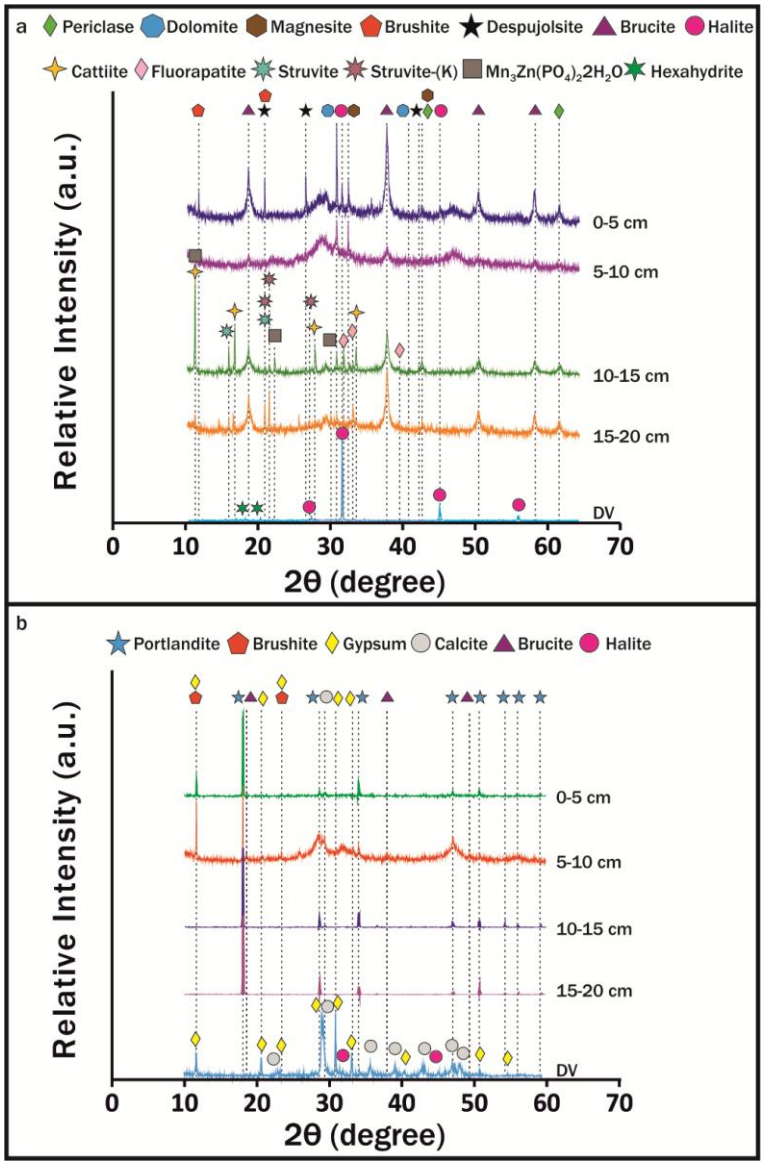

Figure 5.2. XRD spectra of the solid precipitates collected from the MgO-DAS system (a) and the $Ca(OH)_2$-DAS system (b).

The solids collected in the $Ca(OH)_2$-DAS column were identified as unreacted portlandite ($Ca(OH)_2$) (Fig. 5.2b) and a variety of newly-formed solids including phosphate (brushite), sulfate (gypsum), hydroxide (brucite), and carbonate (calcite) minerals (Fig. 5.2b). The high concentration of OH^- groups and Mg from the reagent dissolution and the phosphogypsum leachates, respectively, may favor brucite precipitation. In the case of calcite, this mineral may have precipitated after the dissolution of atmospheric CO_2 in the high pH and Ca-rich solutions. The newly-formed precipitates in the decantation vessel were identified by XRD as calcite, gypsum, and halite (Fig. 5.2b). The EPMA analysis performed on the newly-formed solids collected at a depth of 5–10 cm showed aggregates composed mainly of P, Ca, Mg, and S (Fig.

5.3c), which might suggest the precipitation of brushite, brucite, and gypsum. The solid precipitated inside the decantation vessel showed sub-rounded granular aggregates constituted mainly of Ca (Fig. 5.3d), indicative of calcite, and monoclinic aggregates of gypsum, confirming the results obtained by XRD. As in the case of MgO-DAS, the presence of pollutants was not detected in the phases precipitating in the decantation vessel, which is in agreement with the hydrochemical results.

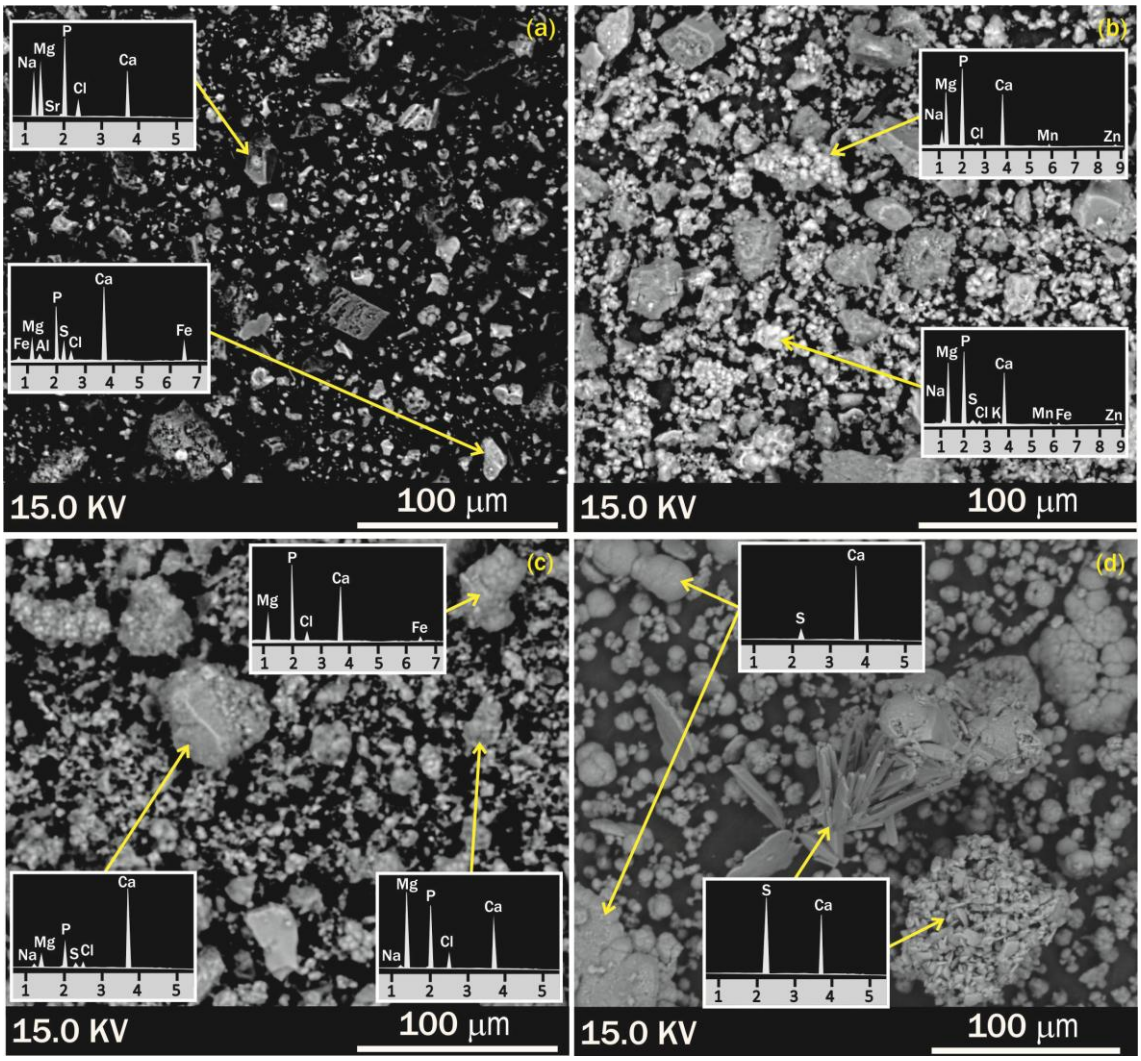

Figure 5.3. EMPA images and WDS spectra of the solid precipitates recovered from the MgO-DAS system (a,b) and the $Ca(OH)_2$-DAS system (c,d).

According to the mineralogical information, the newly-formed solids in the $Ca(OH)_2$-DAS treatment could be considered a resource of raw materials due to the presence of calcite and brucite, which are alkaline reagents commonly used for the treatment of AMD waters, i.e., limestone and magnesium hydroxide (Ayora et al., 2013; Masindi et al., 2017). To quantify the presence of these minerals within the precipitated

solids, a semi-quantitative mineralogical analysis of the crystalline phases was performed. This analysis estimated a percentage (in weight) of calcite and brucite in the precipitated solids of less than 11% and 7%, respectively, while the remaining 82% are mainly sulfate and phosphate phases rich in metallic impurities. On the other hand, the mineralogical composition of the precipitates in the decantation vessel was close to 54% of gypsum and 44% of calcite, with minor proportions of halite.

5.3.3. Risk assessment and management of solids generated in DAS treatment

The efficient treatment of the pollutant leachates led to the generation of metal-rich solid wastes. To assess their hazardousness for safe disposal, avoiding potential environmental impacts, these solids were subjected to different standardized leaching tests. This characterization was only performed on solids collected inside the columns due to the following: 1) more than 95% of total solids were generated in the columns and 2) the absence of toxic elements accumulated in the decantation vessels.

The hazardousness of solids generated in MgO-DAS treatment is depth-dependent (Table 5.1). The shallowest solids (<5 cm) should be classified as hazardous wastes due to the high concentration of SO_4 leached (21,126 mg/kg), exceeding the limit for disposal in non-hazardous waste landfills. The solids collected at a depth of 5–10 cm should be classified as non-hazardous wastes since the concentration of SO_4 and Sb released (8324 and 0.52 mg/kg, respectively) exceeded the threshold values for inert wastes. At depths deeper than 10 cm, the waste material should also be classified as hazardous waste considering the high concentration of Sb leached (0.81 mg/kg).

A decreasing hazardousness pattern with depth of solids from the $Ca(OH)_2$-DAS treatment was observed according to EU legislation (Table 5.1). At depths lower than 5 cm, the solids should be considered hazardous wastes due to the high release of SO_4 (24,508 mg/kg). Regarding solids recovered at a depth of 5–10 cm, they should be deposited in landfills for non-hazardous wastes since the SO_4 and Sb leached (11,050 and 0.12 mg/kg, respectively) exceed the limit for their disposal as inert wastes. Finally, the solids collected at depths deeper than 10 cm should be classified as inert wastes since they did not exceed any threshold value.

Table 5.1. Results of the EN 12457-2 leaching test applied to the solids collected from the DAS treatment systems, and comparison with the regulatory limits for waste acceptance at landfills in EU. Data in mg/kg.

	As	Ba	Cd	Cr	Cu	Mo	Ni	Pb	Sb	Se	Zn	SO_4^-
Inert wastes	0.5	20	0.04	0.5	2	0.5	0.4	0.5	0.06	0.1	4	6000
Non-hazardous wastes	2	100	1	10	50	10	10	10	0.7	0.5	50	20,000
Hazardous wastes	25	300	5	70	100	30	40	50	5	7	200	50,000
Solids derived from DAS columns												
MgO-DAS												
0-5 cm	0.17	<l.d.[a]	<l.d.	0.03	0.33	0.84	0.02	<l.d.	0.49	0.03	<l.d.	21,126
5-10 cm	0.14	<l.d.	<l.d.	0.04	0.15	0.21	0.02	<l.d.	0.52	<l.d.	<l.d.	8324
10-15 cm	0.24	<l.d.	<l.d.	0.03	0.15	0.06	<l.d.	<l.d.	0.81	<l.d.	<l.d.	4501
15-20 cm	0.15	<l.d.	<l.d.	<l.d.	0.44	0.04	<l.d.	<l.d.	0.81	<l.d.	<l.d.	7360
$Ca(OH)_2$-DAS												
0-5 cm	0.02	0.02	<l.d.	0.16	0.47	0.44	0.08	<l.d.	0.04	<l.d.	<l.d.	24,508
5-10 cm	0.04	<l.d.	<l.d.	0.21	0.46	0.18	0.11	<l.d.	0.12	<l.d.	<l.d.	11,050
10-15 cm	<l.d.	0.06	<l.d.	0.05	0.23	0.02	0.07	<l.d.	<l.d.	<l.d.	<l.d.	1024
15-20 cm	<l.d.	0.10	<l.d.	<l.d.	0.73	<l.d.	0.06	<l.d.	0.02	<l.d.	<l.d.	2600

[a]<l.d.: below detection limit

Table 5.2. Results of the TCLP leaching test (method 1311 of US EPA) applied to the solids collected from the DAS treatment systems, and comparison with the regulatory limits established by the Land Disposal Restrictions (LDR, EPA 530-R-01-007). Data in mg/L.

	As	Ba	Cd	Cr	Ni	Pb	V	Zn	Se	Sb	Be	Tl
TCLP	5	100	1	5	n.r.l[b]	5	n.r.l	n.r.l	1.00	n.r.l	n.r.l	n.r.l
UTS	5	21	0.11	0.6	11	0.75	1.6	4.3	5.7	1.15	1.22	0.2
Solids derived from DAS columns												
MgO-DAS												
0-5 cm	0.026	<l.d.[a]	<l.d.	<l.d.	0.006	<l.d.	0.233	<l.d.	0.002	0.040	<l.d.	<l.d.
5-10 cm	0.043	<l.d.	<l.d.	0.002	0.010	<l.d.	0.273	<l.d.	<l.d.	0.054	<l.d.	<l.d.
10-15 cm	0.036	<l.d.	<l.d.	<l.d.	0.004	<l.d.	0.067	<l.d.	<l.d.	0.064	<l.d.	<l.d.
15-20 cm	0.023	<l.d.	<l.d.	<l.d.	0.004	<l.d.	0.031	<l.d.	<l.d.	0.090	<l.d.	<l.d.
$Ca(OH)_2$-DAS												
0-5 cm	<l.d.	<l.d.	<l.d.	0.011	<l.d.	<l.d.	0.019	<l.d.	<l.d.	0.004	<l.d.	<l.d.
5-10 cm	0.003	<l.d.	<l.d.	0.009	0.003	<l.d.	0.032	<l.d.	<l.d.	0.012	<l.d.	<l.d.
10-15 cm	<l.d.	0.010	<l.d.	0.004	0.004	<l.d.	<l.d.	<l.d.	<l.d.	<l.d.	<l.d.	<l.d.
15-20 cm	<l.d.	0.010	<l.d.	<l.d.	0.003	<l.d.	<l.d.	<l.d.	<l.d.	0.002	<l.d.	0.003

[a]<l.d.: below detection limit

[b]n.r.l: no referenced limit

According to the US regulation, all the solids sampled should be classified as non-hazardous wastes since the TCLP limits were not exceeded (Table 5.2). Furthermore, these solids did not exceed the UTS limits; thus, they could be directly disposed of in a non-hazardous waste landfill, without additional treatments.

These discrepancies between both regulations have already been previously reported by Millán-Becerro et al. (2019) during the hazardousness classification of solids from the active treatment of phosphogypsum leachates. In addition, these discrepancies have been observed during the classification of other wastes, such as those from passive and active treatments of AMDs (Macías et al., 2012a; 2017b) or solid phosphogypsum (Macías et al., 2017a). The lack of agreement between both environmental legislations comes from the use of different extracting solutions and the differences between the restrictive levels established by each legislation, i.e., the organic solutions used in the TCLP leaching tests have a higher leaching capacity (Tables AP4.5 and AP4.6). Nevertheless, their threshold values are less restrictive. Hence, it would be highly advisable to use additional assessment protocols to achieve a more accurate hazardousness evaluation for these wastes. Among these complementary protocols, the study of possible adverse effects on aquatic life will be approached. For this purpose, the results obtained during the different leaching tests mimicking weathering after rainfalls (i.e., EN 12457-2) and reducing conditions (i.e., TCLP) were compared with the threshold values of the Criterion Continuous Concentration (CCC) issued by the aquatic life criteria of the US EPA (US EPA, 2020b). The CCC is the limit value of concentration above which a certain pollutant present in water poses an unacceptable effect to aquatic organisms upon chronic exposure. As seen in Fig. 5.4a, CCC limits were not exceeded after the interaction of MgO-DAS and $Ca(OH)_2$-DAS wastes with rainwater, highlighting their chemical stability upon rainwater weathering. On the other hand, most metal concentrations remained below the CCC limits after interaction of treatment wastes with organic acids, except for Al in the $Ca(OH)_2$-DAS profile, which exceeded the limits below 10 cm (Fig. 5.4b). Therefore, these wastes should not be co-disposed with municipal wastes or covered with vegetation or organic-rich amendments to avoid weathering under reducing conditions.

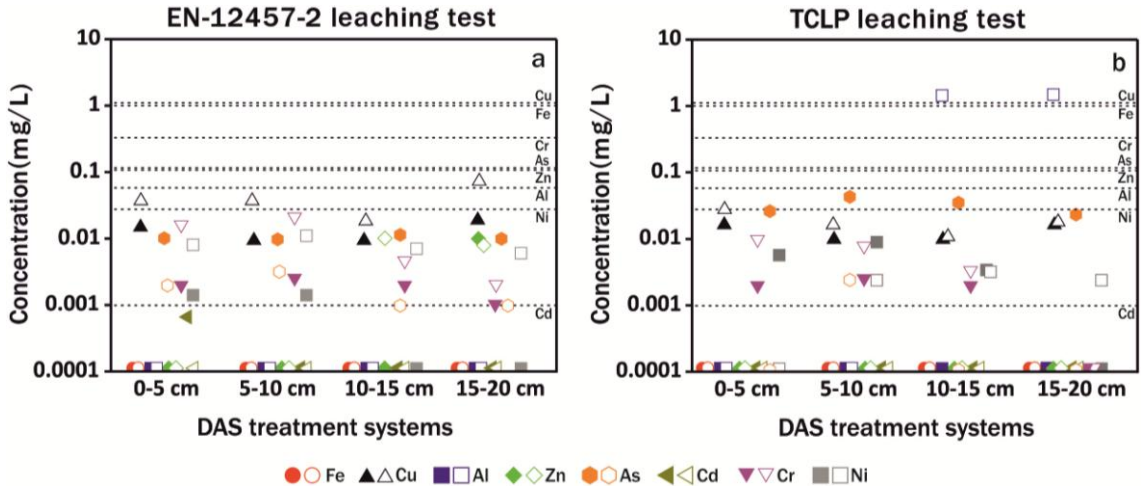

Figure 5.4. Metal(loid)s concentrations released after EN 12457-2 test (a) and TCLP test (b). Continuous Concentration Criteria (CCC) limits for those pollutants are included (horizontal dashed lines). The solid markers indicate that the leached element comes from the MgO-DAS waste whereas the hollow markers indicate that the contaminant comes from the $Ca(OH)_2$-DAS solid.

A rough estimation of the contaminants released from the treatment wastes after rainfall weathering and reducing conditions can be made (Tables AP4.5 and AP4.6). In this sense, the low mobility of metal(loids) contained in DAS wastes is striking, with values below 2%, except for Al in the deeper layers of the $Ca(OH)_2$-DAS profile, where release rates close to 70% were observed (Table AP4.6). On the other hand, the high release of SO_4 from both wastes is remarkable (58–70% in MgO-DAS wastes, Table AP4.5; 5–46% in the $Ca(OH)_2$-DAS profile), being slightly higher upon reducing conditions. By comparing these results with those obtained after applying the same leaching schemes to solid phosphogypsum (Macías et al., 2017a), the low mobility of Cd and As from the treatment wastes compared with the latter waste is especially noticeable. This implies that DAS treatment must be considered an efficient stabilization method for these highly toxic metalloids.

5.3.4. Environmental and economic implications

Acidic leachates arising from the Huelva phosphogypsum stack constitute an important source of contamination to the Ría de Huelva estuary (Pérez-López et al., 2016). In this context, DAS technology is an effective and environmentally sustainable solution for the treatment of these acid leachates. Considering the total annual volume

of edge outflows that emerges from the phosphogypsum stack, i.e., approximately 335,000 m^3 (Pérez-López et al., 2016), treatment using DAS technology could avoid the release of significant amounts of pollutants to the estuary; around 842 tons/yr of PO_4, 445 tons/yr of F, 48 tons/yr of NH_4, 42 tons/yr of Fe, 12 tons/yr of Zn and Al, 6.7 tons/yr of As, 4.2 tons/yr of U, 3.5 tons/yr of Cr, 1.6 tons/yr of Cd, 1.3 tons/yr of Cu, and 0.9 tons/yr of Al. To achieve effective treatment of the total volume of phosphogypsum leachate, around 1335 tons of magnesia or 2127 tons of calcium hydroxide would be necessary. Although the $Ca(OH)_2$-DAS system requires almost twice the reactive mass of the MgO-DAS system per volume of leachate treated, the cost of calcium hydroxide is 7–10 times lesser than magnesia (INAP, 2021). Thus, considering a market price for calcium hydroxide of 60–100 USD/ton (INAP, 2021), the annual cost related to the purchase of this may vary between 128,000 and 213,000 USD. On the other hand, if the alkaline reagent selected was magnesia, this would imply an economic cost associated with its purchase that could reach values around 0.56 and 1.34 MUSD. Therefore, the selection of $Ca(OH)_2$ as an alkaline reagent for the treatment of phosphogypsum leachates would imply an annual economic cost that is 4 to 6 times lower.

During $Ca(OH)_2$-DAS treatment, calcite and brucite are generated, which have several environmental applications (e.g., passive treatment of acid mine waters). However, such practice could be limited for the precipitated solids inside the DAS column due to the low amounts of these mineral phases (11% calcite, 7% brucite) and the high content (around 82%) of sulfate and phosphate phases rich in metallic impurities. Therefore, the potential valorization of solids collected only in the decantation vessel appears to be more suitable. These solid are mainly composed of gypsum (54 wt%) and calcite (44 wt%), with no metal(loid)s impurities. In addition, the simple distilled water washing of these solids allows for an increased concentration of calcite of up to 80% due to the high solubility of gypsum (Fig. AP4.1). The precipitation of calcite is generated by the natural sequestering of CO_2, which is one of the main greenhouse gases (Morales-Flórez et al., 2011). According to the PHREEQC calculations, around 0.5 g of calcite precipitates in the decantation vessel after the treatment of 1 L of leachates, which would equate to a rough generation of 173 tons/yr of calcite and a CO_2 sequestration of around 34 tons/yr of atmospheric CO_2 if all leachates (i.e., 335,000 m^3/yr) were treated with $Ca(OH)_2$-DAS.

The calcite generated is an alkaline reagent is currently used for the treatment of extremely acidic and polluted mine waters (Martinez et al., 2019; Orden et al., 2021). Thus, the generation of this raw material during phosphogypsum leachate treatment could be used as a reagent in AMD treatment by DAS technology. According to Orden et al. (2021), 57 tons of calcite were used to successfully treat highly polluted AMD from Mina Esperanza (SW Spain) over the course of 840 days (close to 25 tons/yr of calcite used). In this sense, the potential treatment of the whole volume of phosphogypsum leachates by $Ca(OH)_2$-DAS treatment would generate the calcite needed (173 tons/yr) for around 7 DAS plants of AMD waters.

On the other hand, the solid wastes generated during DAS treatments may constitute a secondary source of P, taking into account the abundance of phosphate minerals. Thus, phosphate rock, a marketable resource, would be replaced by waste for the production of phosphoric acid so that a circular economy could be achieved. Phosphorous is considered a critical raw material (European Commission, 2020), with a worldwide production of phosphate rock in 2013 of around 210 million tons (Sverdrup and Ragnarsdottir, 2014). Although, this value is expected to increase until reaching an annual production of around 520 million tons in 2050 (Nedelciu et al., 2020). Therefore, the search for secondary sources of phosphorus is of paramount importance, especially in countries with the absence of primary deposits. In this sense, a potential source of phosphorus could be wastewater (Cordell and White, 2014; Shaddel et al., 2020). Currently, the main methods for the recovery of phosphorus from wastewater are biological treatment, electrochemical processes, and chemical precipitation (Cichy et al., 2019; Deng et al., 2020; Lei et al., 2019; Li et al., 2018; Martin et al., 2020). In this same sense, the treatment of the leachates released using DAS technology could generate around 842 tons/yr of PO_4 by passive chemical precipitation, which would be otherwise released into the estuary. The recovery of phosphorous from these newly-formed phosphate phases (e.g., brushite, cattiite, and fluorapatite, among others) could help to achieve the principles of a circular economy in the fertilizer industry as well as to contribute to the mitigation of the supply risk worldwide. The high amount of impurities contained in these phosphates could be a barrier for the recovery of P in a marketable product. However, the development of innovative recovery schemes in the last year opens the door to the recycling of P from the generated wastes. For example, the improved hard process is an innovative phosphorus recovery technology, where a

reduction reaction releases P at around 1250ºC, eliminating the impurities and achieving highly pure P (Worrell et al., 2017). These phosphates may contain not only a high concentration of impurities but also of valuable metals. For example, Millán-Becerro et al. (2021) reported concentrations of up to 4092 mg/kg of rare earth elements (REE), 2974 mg/kg of V, and 164 mg/kg of Sc in solids precipitated during the neutralization of these leachates with $Ca(OH)_2$. The selective recovery of these valuable metals could improve the environmental and cost-effectiveness performance of the proposed water treatment.

5.4. CONCLUSIONS

Different techniques for chemical and mineralogical characterization and standardized leaching protocols have been applied to optimize a sustainable treatment of fertilizer industry leachates and to assess the stability and the potential environmental impact of this treatment wastes. This study confirms the efficiency of dispersed alkaline substrate technology in the passive treatment of acidic leachates generated in phosphogypsum waste piles from the fertilizer industry. The findings revealed that $Ca(OH)_2$ is by far the most suitable alkaline chemical for the treatment based on effectiveness and economic criteria. During treatment, metals pass from the soluble forms to an insoluble solid waste mineralogically composed of phosphate (i.e., brushite, cattiite, fluorapatite, struvite, and $Mn_3Zn(PO_4)_2{\cdot}2H_2O$) and sulfate (i.e., despujolsite and gypsum) phases. Calcite precipitation also occurs due to atmospheric CO_2 dissolution in the treated leachates. The hazardousness of these solid wastes was assessed for proper management using EU and US regulations based on leaching tests. According to current EU legislation, the high mobility of sulfate and Sb confers these metal-rich solids the classification of hazardous waste in some zones of the treatment. However, according to US regulation, these same solids can be considered non-hazardous wastes. The discrepancies observed between both international legislations justify the need of complimentary tools to evaluate the hazardousness of these wastes. In this sense, the comparison between leaching tests and limit values established by the EPA Continuous Concentration Criterion (CCC) revealed the stability of the wastes upon rainfall weathering but a noticeable environmental risk when interacting with organic acids, which recommends avoiding their co-disposal with municipal wastes or the use of

organic amendment-based covers. On the other hand, solid wastes can be injected back into the economy as secondary raw materials as a source of calcite, brucite, gypsum, phosphate minerals, or even valuable metals (e.g., REE, Sc, or V), improving the environmental and cost-effectiveness performance of the treatment. Thus, the results obtained in this research work could also contribute to achieve the principles of sustainability and the circular economy in the fertilizer industry.

CHAPTER 6. COMBINED PROCEDURE OF METAL REMOVAL AND RECOVERY OF TECHNOLOGY ELEMENTS FROM FERTILIZER INDUSTRY EFFLUENTS.

BASED ON:

Millán-Becerro, R., Cánovas, C.R., Pérez-López, R., Macías, F., León, R., 2021. Combined procedure of metal removal and recovery of technology elements from fertilizer industry effluents. Journal of Geochemical Exploration, 221, 106698.

ABSTRACT

This study focuses on the search for a sustainable treatment and metal recovery system for acid discharges from a fertilizer industry in SW Spain. The methodology proposed involves the addition of two types of alkaline materials (an industrial waste and a commercial reagent) to neutralize the acidity and remove dissolved elements. In the first case, the treatment consisted on batch reactions between biomass ashes and phosphogypsum leachates at different solid-liquid ratios (i.e., 1:2.5, 1:5, and 1:10). On the other hand, a 0.01 M solution of $Ca(OH)_2$ was used. The experiment with biomass ashes at a solid:liquid ratio of 1:2.5 showed a high effectiveness, reaching removal percentages close to 100% for F, Fe, Zn, Al, Cr, U, Cu and Cd. The depletion of contaminants from solutions during the alkaline treatments occurred mainly by co-precipitation and/or adsorption onto phosphate phases, in addition to precipitation of fluorides. Moreover, the solids precipitated during the alkaline treatments contain elements of high economic interest such as rare earth elements plus Y (353–3992 mg/kg), Sc (21–164 mg/kg), Be (5.0–7.0 mg/kg), V (1036–2974 mg/kg), Ga (16–40 mg/kg) or U (721–2963 mg/kg). These values could make this by-product a promising source of technology metals. This study proposes an environmentally-friendly solution for these industrial leachates, removing selectively impurities and target elements and producing a promising exploitable metal concentrate. This research could lay the foundations for an effective and sustainable treatment system for acid leachates from phosphogypsum stacks. Furthermore, the costs related with the treatments could be covered by recovering the valuable elements contained in the newly-formed precipitates during the treatments.

CHAPTER 7. GENERAL CONCLUSIONS

The phosphoric acid production in the Huelva phosphate fertilizer industry for four decades (from 1968 to 2010), originated around 100 million tons of phosphogypsum. The wastes were deposited in a stack located on salt-marsh soils of the Tinto River. Currently, the Huelva phosphogypsum stack is divided into four disposal areas; zones 1 and 4 are considered already restored, while zones 2 and 3 are currently pending to be restored in the near future. Nevertheless, the four disposal areas show numerous superficial leakages in their perimeters. These acidic and polluted effluents that emerge from the edges of the stack, known as edge outflows, continuously release large amounts of contaminants into the Ría de Huelva estuary. In addition, the unrestored areas have surface ponds with extremely acidic and contaminated process water, which was used for the transport and decantation of the phosphogypsum. This doctoral thesis has focused on the development of an efficient and sustainable treatment system for acid leachates from phosphogypsum stacks. To achieve this goal, the following objectives were proposed: (i) to geochemically characterize all the acid leachates that emerge from the Huelva phosphogypsum stack and clarify the weathering model explaining the origin of these leakages, (ii) to study the behavior of acidity and the main anions and cations dissolved in phosphogypsum-related leachates during the treatment with a conventional alkaline reactive ($Ca(OH)_2$), (iii) to assess the feasibility of dispersed alkaline substrate (DAS) technology for the passive treatment of effluents from the phosphate fertilizer industry, as well as to select the most effective reactive material (limestone, barium carbonate, magnesia, magnesium hydroxide, calcium hydroxide, biomass ash or fly ash), (iv) to evaluate the stability and hazardousness of solid wastes generated during the DAS treatment for a proper management, and (v) to study the behavior of elements of high economic interest dissolved in phosphogypsum leachates during the acid neutralization. From the development of this doctoral thesis, the following conclusions were obtained:

- The phosphogypsum stack behaves as an anthropic aquifer with coastal karstic features. This aquifer shows two feeding ways; a continuous recharge of estuarine water in the deep zone of the stack, where phosphogypsum and salt-marsh soils are directly in contact, and a punctual recharge by rainwater that infiltrates through the surface of the phosphogypsum stack and circulates through dissolution conduits.

- The water-table of the phosphogypsum stack is controlled mainly by tidal oscillations, showing low variability most of the time (± 2 cm). Nevertheless, the water-table level of the pile rapidly rises up to 20 cm during the rainy episodes studied. Just after rainfall events, around half of the height increased by the water-table is instantly recovered, while pre-rainfalls conditions are reached during a period of 5 to 15 days depending on the intensity of the rainfalls.

- Edge outflows sampled around the whole perimeter of the phosphogypsum pile show generally low hydrochemical variability under different hydrological conditions. Nevertheless, small variations are observed in the contaminant concentrations measured during the different periods. In this sense, two possible mechanisms responsible for such variability are proposed; on the one hand, a dilution by rainwater recharge during the rainy season, which causes a slight decrease in the concentration of most dissolved pollutants in the edge leachates (e.g., PO_4, F, Al, Zn, Cr, Ni, As, Cd, Sb or U), and on the other hand, the washing of the sulfate evaporitic salts accumulated during the summer along the margins of the Tinto River and mine sites, which causes an rise in the dissolved concentration of SO_4 and Fe in the river and estuarine waters and subsequently in the leachates released from the phosphogypsum stack during the rainy period.

- The phosphogypsum pile releases high concentrations of pollutants to the Ría de Huelva estuary such as PO_4, F and U (average values of 5000 tons/yr, 300 tons/yr and 3.0 tons/yr, respectively). These pollutants are not discharged, at least in appreciable proportions, by the other sources of pollution that affect this estuarine system; i.e., mine waters from Iberian Pyrite Belt and effluents from Huelva industrial complex. In addition, between 16-85% and 9-27% of the total content of As and Cd, respectively, that reaches the estuary comes from the phosphogypsum stack.

- The results of the weathering model seem to predict that the treatment of edge leachate is one of the few options available to minimize the discharge of pollutants to the Ría de Huelva estuary. The first step towards an alkaline treatment of phosphogypsum-related acid leachates consisted in a titration with a

$Ca(OH)_2$ solution in which it is observed the total removal of PO_4, F, Fe, Zn, Al, Cr, Cu, Cd and U from solution. However, the treatment is not totally effective for As, reaching removal values of up to 82%.

- Mineralogical evidences point to the precipitation of phosphate phases (i.e., strengite, brushite, hydroxylapatite) as the main solubility control of pollutants during the acid neutralization of phosphogypsum leachates, hosting high metal concentrations.

- According to the current legislations of the European Union (EN-12457-2 leaching test) and United States (US EPA-TCLP test), the solids precipitated during the alkaline treatment of the edge outflows from the unrestored zones of the phosphogypsum stack exceeds the As leaching limits for hazardous wastes. However, the solids from the treatment of the edge outflows from the restored zones comply with criteria for non-hazardous wastes. The treatment of process water generates solids whose hazardousness classification is discrepant based on the applied international legislation.

- Everything seems to indicate that it is not reasonably practicable to undertake active remediation at the phosphopgypsum stack, where remediation goals and end-points have not been achieved and an actual harm still remains even in supposedly restored zones. Therefore, it is likely to be necessary to consider passive remediation options for the edge outflows. The second step towards an alkaline treatment of phosphogypsum leachates consisted of using the passive DAS technology. Such DAS technology achieves a significant improvement in the chemical water quality, regardless of the alkaline reagent used (i.e., limestone, barium carbonate, biomass ash, fly ash, MgO, $Mg(OH)_2$ and $Ca(OH)_2$). Moreover, the treatments do not show clogging problems, which implies that the DAS system is also hydraulically efficient for this type of acid leachates.

- The MgO-DAS and $Ca(OH)_2$-DAS treatment systems achieve the total removal of PO_4, F, Fe, Zn, Al, Cr, U and Cd with initial reactive mass:volume of leachate

treated ratios of 3.98 g/L and 6.35 g/L, respectively. Nevertheless, the total elimination of As is only reached with the $Ca(OH)_2$-DAS treatment. The findings reveal that $Ca(OH)_2$ is by far the most suitable alkaline chemical for the treatment based on effectiveness and economic criteria.

- The mineralogical characterization of the newly-formed solids in the MgO-DAS and $Ca(OH)_2$-DAS systems, indicates that the precipitation of phosphate (i.e., brushite, cattiite, fluorapatite, struvite, and $Mn_3Zn(PO_4)_2 \cdot 2H_2O$) and sulfate (i.e., despujolsite and gypsum) phases could be controlling the solubility of dissolved contaminants in phosphogypsum leachates during the passive treatments. In addition, calcite is identified, which probably originates from the atmospheric CO_2 dissolution in the treated leachates.

- According to current European Union (EN 12457-2 test) legislation, the high mobility of SO_4 and Sb confers these metal-rich DAS solids the classification of hazardous wastes in some zones of the treatment. However, according to United States (US EPA-TCLP test) regulation, these same solids can be considered non-hazardous wastes.

- A comparison of the concentrations released of certain contaminants during the leaching tests used according to the European Union and United States legislations with the limit values established for these contaminants by the EPA Continuous Concentration Criterion (CCC), evidences a high stability of the wastes upon rainfall weathering. However, the contact of $Ca(OH)_2$-DAS wastes with organic acids should be prevented to avoid the pollution of aquatic systems.

- Finally, the third step towards an alkaline treatment of phosphogypsum leachates consisted in the search for economic profitability. The solid wastes generated in the DAS systems could be considered as secondary sources of calcite, brucite, gypsum, phosphate minerals, or even valuable metals (e.g., rare earth elements (REE), Sc, or V), improving the environmental and cost-effectiveness performance of the treatment. Thus, this research could also contribute to

achieve the principles of sustainability and the circular economy in the fertilizer industry.

- The newly-formed solids during the treatments of the process water with biomass ash and $Ca(OH)_2$ contain high amounts of elements of high economic value such as V (1036 and 2974 mg/kg, respectively), U (721-2963 mg/kg), Sc (21-164 mg/kg), light rare earth elements (LREEs; La-Sm) (sum of values of 190 and 1935 mg/kg) and heavy rare earth elements (HREEs; Tb-Lu, plus Y) (163-2057 mg/kg), among others. In addition, an economic estimate of the metal reserves contained in both solids suggests a total valuation of 2314 and 1539 MUSD for the precipitates generated during treatments with biomass ash and with $Ca(OH)_2$, respectively.

- The newly-formed precipitates derived from the treatments could be considered as a promising secondary source of REE, Y, V, U, Sc, Ga and Be, whose recovery could help to offset the costs associated with the treatments.

The results achieved during the development of this doctoral thesis allow us to open new lines of research, such as:

- To recover the calcite-rich solids generated during the treatment of phosphogypsum leachates with passive DAS technology. Some XRD mineralogical studies show that the newly-formed solids in decantation vessel during the treatment of leachates with $Ca(OH)_2$-DAS technology are mainly composed of gypsum (54% wt) and calcite (44% wt), and do not contain metallic impurities. This calcite generated is an alkaline reagent that could be currently used for the treatment of highly acidic and contaminated mine waters.

- To study the potential valorization of the solid wastes generated during the DAS treatments as a secondary source of P, since the DAS wastes are mainly composed of phosphate phases (e.g., brushite, cattiite and fluorapatite, among others). Phosphorous is currently considered a critical raw material, so the

search for secondary sources of P is an important parameter, especially in countries with no primary deposits.

- To assess the potential recovery of elements of high economic interest (e.g., REE, Y, Sc, Be, V, Ga and U) contained in the solids generated during the alkaline treatment of phosphogypsum-related acidic leachates.

CAPÍTULO 7. CONCLUSIONES GENERALES

La producción de ácido fosfórico en la industria de fertilizantes fosfatados de Huelva durante cuatro décadas (1968-2010), originó alrededor de 100 millones de toneladas de fosfoyesos. Los residuos fueron depositados en una balsa localizada sobre suelos de marismas saladas del Río Tinto. Actualmente, la balsa de fosfoyesos de Huelva está dividida en cuatro áreas de depósito; las zonas 1 y 4 se consideran ya restauradas, mientras que las zonas 2 y 3 están actualmente pendientes de ser restauradas en un futuro próximo. Sin embargo, las cuatro áreas de depósito muestran numerosas fugas superficiales en sus perímetros. Estos efluentes ácidos y contaminados que emergen de los bordes de la balsa, conocidos como salidas de borde, liberan continuamente grandes cantidades de contaminantes al estuario Ría de Huelva. Además, las áreas no restauradas tienen estanques superficiales con agua de proceso extremadamente ácida y contaminada, la cual fue empleada para transportar y decantar el fosfoyeso. Esta tesis doctoral se ha centrado en el desarrollo de un sistema de tratamiento eficiente y sostenible para los lixiviados ácidos procedentes de balsas de fosfoyesos. Para lograr este fin, se propusieron los siguientes objetivos: (i) Caracterizar geoquímicamente todos los lixiviados ácidos que emergen de la balsa de fosfoyesos de Huelva y esclarecer el modelo de meteorización explicando el origen de estos lixiviados, (ii) estudiar el comportamiento de la acidez y de los principales aniones y cationes disueltos en los lixiviados relacionados con los fosfoyesos durante el tratamiento con un reactivo alcalino convencional ($Ca(OH)_2$), (iii) evaluar la viabilidad de la tecnología DAS para el tratamiento pasivo de efluentes de la industria de fertilizantes fosfatados, así como seleccionar el reactivo más efectivo (caliza, carbonato de bario, magnesia, hidróxido de magnesio, hidróxido de calcio, cenizas de biomasa o cenizas volantes), (iv) evaluar la estabilidad y peligrosidad de los residuos sólidos generados durante el tratamiento DAS para una adecuada gestión, (v) estudiar el comportamiento de los elementos de alto interés económico disuelto en los lixiviados de fosfoyeso durante la neutralización de la acidez. Del desarrollo de esta tesis doctoral se han obtenido las siguientes conclusiones:

- La balsa de fosfoyesos se comporta como un acuífero antrópico con características kársticas costeras. Este acuífero presenta dos vías de alimentación; una recarga continua de agua estuarina en la zona profunda de la balsa, donde el fosfoyeso y los suelos de marismas saladas están en contacto directo, y una recarga puntual por agua de lluvia que se infiltra a través de la superficie de la balsa de fosfoyesos y circula por conductos de disolución.

- El nivel freático de la balsa de fosfoyesos está controlado principalmente por las oscilaciones mareales, mostrando baja variabilidad la mayor parte del tiempo (± 2 cm). Sin embargo, el nivel freático de la pila sube rápidamente hasta 20 cm durante los episodios de lluvia estudiados. Justo después de los eventos de lluvia, se recupera instantáneamente alrededor de la mitad de la altura aumentada por el nivel freático, mientras que las condiciones previas a las lluvias se alcanzan en un período de 5 a 15 días, dependiendo de la intensidad de las lluvias.

- Las salidas de borde muestreadas alrededor de todo el perímetro de la pila de fosfoyesos muestran generalmente baja variabilidad hidroquímica bajo diferentes condiciones hidrológicas. Sin embargo, se han observado pequeñas variaciones en las concentraciones de los contaminantes medidas durante los diferentes períodos. En este sentido, se han propuesto dos posibles mecanismos responsables de dicha variabilidad; por un lado, una dilución por recarga de agua de lluvia durante el periodo lluvioso, la cual provoca una ligera disminución en la concentración de la mayoría de los contaminantes disueltos en los lixiviados de borde (e.g., PO_4, F, Al, Zn, Cr, Ni, As, Cd, Sb o U), y por otra parte, el lavado de las sales evaporíticas sulfatadas acumuladas durante el verano en los márgenes del Río Tinto y en los distritos mineros, que provocan un aumento de la concentración disuelta de SO_4 y Fe en el agua del río y consecuentemente en los lixiviados procedentes de la balsa de fosfoyesos durante el período lluvioso.

- La pila de fosfoyesos libera altas concentraciones de contaminantes al estuario Ría de Huelva tales como PO_4, F y U (valores medios de 5000 toneladas/año, 300 toneladas/año y 3.0 toneladas/año, respectivamente). Estos contaminantes no son descargados, al menos en proporciones apreciables, por las otras fuentes de contaminación que afectan a este sistema estuarino; i.e., aguas de mina procedentes de la Faja Pirítica Ibérica (FPI) y efluentes procedentes del complejo industrial de Huelva. Además, entre el 16-85% y el 9-27% del contenido total de As y Cd, respectivamente, que llegan al estuario provienen de la balsa de fosfoyesos.

- Los resultados del modelo de meteorización parecen predecir que el tratamiento de los lixiviados de borde es una de las pocas opciones disponibles para minimizar la descarga de contaminantes al estuario Ría de Huelva. El primer paso hacia un tratamiento alcalino de los lixiviados ácidos relacionados con los fosfoyesos consistió en una valoración con una solución de $Ca(OH)_2$, en la que se observa la retirada total de PO_4, F, Fe, Zn, Al, Cr, Cu, Cd y U de la solución. Sin embargo, el tratamiento no es totalmente efectivo para el As, alcanzando valores de eliminación de hasta el 82%.

- Las evidencias mineralógicas apuntan a la precipitación de fases fosfatadas (i.e., strengita, brushita, hidroxiapatito) como el principal control de solubilidad de los contaminantes durante la neutralización de la acidez de los lixiviados de fosfoyesos, los cuales albergan altas concentraciones de metales.

- De acuerdo con las legislaciones vigentes en la Unión Europea (test de lixiviación EN-12457-2) y Estados Unidos (test TCLP de la US EPA), los sólidos precipitados durante el tratamiento alcalino de los lixiviados de borde de las zonas no restauradas de la balsa de fosfoyesos deberían ser depositados en un vertedero para residuos peligrosos como consecuencia de las concentraciones de As lixiviadas. Sin embargo, los sólidos resultantes del tratamiento de las salidas de borde de las zonas restauradas, cumplen con los criterios de residuos no peligrosos. El tratamiento del agua de proceso genera sólidos cuya clasificación de peligrosidad crea discrepancias en base a la legislación internacional aplicada.

- Todo parece indicar que no es razonablemente viable llevar a cabo una remediación activa en la balsa de fosfoyesos, donde los objetivos de remediación no han sido logrados y aún persiste un daño real incluso en zonas supuestamente restauradas. Por lo tanto, probablemente sea necesario considerar opciones de remediación pasiva para las salidas del borde. El segundo paso hacia un tratamiento alcalino de los lixiviados de fosfoyesos consistió en utilizar la tecnología pasiva DAS. Dicha tecnología DAS logra una mejora en la calidad química del agua, independientemente del reactivo alcalino utilizado (i.e., caliza, carbonato de bario, cenizas de biomasa, cenizas volante, MgO, $Mg(OH)_2$ y

$Ca(OH)_2$). Además, los tratamientos no presentan problemas de atascos, lo que implica que el sistema DAS es hidráulicamente eficiente para este tipo de lixiviados ácidos.

- Los sistemas de tratamiento DAS-MgO y DAS-$Ca(OH)_2$ logran la eliminación total de PO_4, F, Fe, Zn, Al, Cr, U y Cd con relaciones masa de reactivo inicial:volumen de lixiviado tratado de 3.98 g/L y 6.35 g/L, respectivamente. Sin embargo, la retirada total de As sólo es alcanzado con el tratamiento DAS-$Ca(OH)_2$. Los resultados revelan que el $Ca(OH)_2$ es, con diferencia, el reactivo alcalino más adecuado para el tratamiento según criterios económicos y de eficacia.

- La caracterización mineralógica de los sólidos neoformados en los sistemas DAS-MgO y DAS-$Ca(OH)_2$, señala que la precipitación de fases fosfatadas (i.e., brushita, cattiita, fluorapatita, estruvita y $Mn_3Zn(PO_4)_2 \cdot 2H_2O$) y sulfadas (i.e., despujolsita y yeso) podría estar controlando la solubilidad de los contaminantes disueltos en los lixiviados de fosfoyesos durante los tratamientos pasivos. Además, se identifica calcita, la cual se origina probablemente a partir de la disolución del CO_2 atmosférico en los lixiviados tratados.

- Según la legislación vigente de la Unión Europea (test EN 12457-2), la alta movilidad del SO_4 y Sb confiere a estos sólidos DAS ricos en metales la clasificación de residuos peligrosos en algunas zonas del tratamiento. Sin embargo, de acuerdo con la regulación de los Estados Unidos (test TCLP de la US EPA), estos mismos sólidos pueden ser considerados residuos no peligrosos.

- Una comparación de las concentraciones liberadas de ciertos contaminantes durante la ejecución de los tests de lixiviación utilizados según las legislaciones de la Unión Europea y Estados Unidos con los valores límite establecidos para dichos contaminantes por el Criterio de Concentración Continua (CCC) de la EPA, evidencia una alta estabilidad de los residuos DAS frente a la meteorización por agua de lluvia. Sin embargo, debe evitarse la interacción de

los residuos DAS-$Ca(OH)_2$ con ácidos orgánicos para evitar la contaminación de los sistemas acuáticos.

- Finalmente, el tercer paso hacia un tratamiento alcalino de los lixiviados de fosfoyesos consistió en la búsqueda de la rentabilidad económica. Los residuos sólidos generados en los sistemas DAS podrían ser considerados como fuentes secundarias de calcita, brucita, yeso, minerales fosfatados o incluso metales valiosos (e.g., tierras raras (REE), Sc o V), reduciendo los costes económicos y ambientales del tratamiento. Así, esta investigación también podría contribuir a alcanzar los principios de sostenibilidad y economía circular en la industria de los fertilizantes.

- Los sólidos neoformados durante los tratamientos del agua de proceso con cenizas de biomasa y con $Ca(OH)_2$ contienen altas cantidades de elementos de alto valor económico tales como V (1036 y 2974 mg/kg, respectivamente), U (721-2963 mg/kg), Sc (21-164 mg/kg), tierras raras ligeras (LREEs; La-Sm) (sumatorio de 190-1935 mg/kg) y tierras raras pesadas (HREEs; Tb-Lu, más Y) (163-2057 mg/kg), entre otros. Además, una estimación económica de las reservas metálicas contenidas en ambos sólidos sugiere una valoración total de 2314 y 1539 MUSD para los precipitados generados durante los tratamientos con cenizas de biomasa y con $Ca(OH)_2$, respectivamente.

- Los precipitados neoformados derivados de los tratamientos podrían ser considerados como una prometedora fuente secundaria de REE, Y, V, U, Sc, Ga y Be, cuya recuperación podría ayudar a compensar los costes asociados con los tratamientos.

Los resultados logrados durante el desarrollo de esta tesis doctoral permiten abrir nuevas líneas de investigación, tales como:

- Recuperar los sólidos ricos en calcita generados durante el tratamiento de los lixiviados de los fosfoyesos con la tecnología pasiva DAS. Algunos estudios mineralógicos por DRX muestran que los sólidos neoformados en el vaso de

decantación durante el tratamiento de los lixiviados con la tecnología DAS-$Ca(OH)_2$ están compuestos principalmente por yeso (54% en peso) y calcita (44% en peso), y no contienen impurezas metálicas. La calcita generada es un reactivo alcalino que podría ser utilizado actualmente para el tratamiento de aguas de mina altamente ácidas y contaminadas.

- Estudiar la potencial valorización de los residuos sólidos generados durante los tratamientos DAS como una fuente secundaria de P, ya que los residuos DAS están compuestos principalmente por fases fosfatadas (e.g., brushita, cattiita y fluorapatito, entre otras). Actualmente, el P es considerado una materia prima crítica, por lo que la búsqueda de fuentes secundarias de P es un parámetro importante, especialmente en países sin depósitos primarios.

- Evaluar la potencial recuperación de elementos de alto interés económico (e.g., REE, Y, Sc, Be, V, Ga y U) contenidos en los sólidos generados durante el tratamiento alcalino de los lixiviados ácidos relacionados con los fosfoyesos.

BIBLIOGRAPHY

Affonso, L.N., Marques Jr, J.L., Lima, V.V.C., Gonçalves, J.O., Barbosa, S.C., Primel, E.G., Burgo, T.A.L., Dotto, G.L., Pinto, L.A.A., Cadaval Jr, T.R.S., 2020. Removal of fluoride from fertilizer industry effluent using carbon nanotubes stabilized in chitosan sponge. J. Hazard. Mater. 388, 122042.

Alemrajabi, M., Rasmuson, Å.C., Korkmaz, K., Forsberg, K., 2017. Recovery of rare earth elements from nitrophosphoric acid solutions. Hydrometallurgy 169, 253–262.

Alemrajabi, M., Rasmuson, Å.C., Korkmaz, K., Forsberg, K., 2019. Processing of a rare earth phosphate concentrate obtained in the nitrophosphate process of fertilizer production. Hydrometallurgy. 189, 105144.

Allison, J.D., Brown, D.S., Novo-Gradac, K.J., 1991. MINTEQA2/PRODEFA2, A geochemical assessment model for environmental systems. Version 3.0 User's Manual, EPA/600/3-911021. Environmental Research Laboratory, Office of Research and Development, US Environmental Protection Agency, Athens, Georgia.

Al-Masri, M.S., Amin, Y., Ibrahim, S., Al-Bich, F., 2004. Distribution of some trace metals in Syrian phosphogypsum. Appl. Geochem. 19, 747–753.

Arfib, B., Charlier, J.B., 2016. Insights into saline intrusion and freshwater resources in coastal karstic aquifers using a lumped Rainfall–Discharge–Salinity model (the Port-Miou brackish spring, SE France). J. Hydrol. 540, 148-161.

Asaoka, S., Takahashi, Y., Araki, Y., Tanimizu, M., 2012. Comparison of antimony and arsenic behavior in an Ichinokawa River water–sediment system. Chem. Geol. 334, 1–8.

Ayora, C., Caraballo, M.A., Macías, F., Rötting, T.S., Carrera, J., Nieto, J.M., 2013. Acid mine drainage in the Iberian Pyrite Belt: 2. Lessons learned from recent passive remediation experiences. Environ. Sci. Pollut. Res. 20 (11), 7837–7853.

Ayora, C., Macias, F., Torres, E., Lozano, A., Carrero, S., Nieto, J.M., Perez-Lopez, R., Fernandez-Martinez, A., Castillo-Michel, H., 2016. Recovery of rare earth elements and yttrium from passive-remediation systems of acid mine drainage. Environ. Sci. Technol. 50, 8255–8262.

Bibi, S., Kamran, M.A., Sultana, J., Farooqi, A., 2017. Occurrence and methods to remove arsenic and fluoride contamination in water. Environ. Chem. Lett. 15 (1), 125–149.

Bogush, A.A., Dabu, C., Tikhova, V.D., Kim, J.K., Campos, L.C., 2019. Biomass Ashes for Acid Mine Drainage Remediation. Waste Biomass Valori. 1-13, 467.

Bolívar, J.P., García-Tenorio, R., Más, J.L., Vaca, F., 2002. Radioactive impact in sediments from an estuarine system affected by industrial waste releases. Environ. Int. 27, 639-645.

Bolívar, J.P., Martin, J.E., García-Tenorio, R., Pérez-Moreno, J.P., Mas, J.L., 2009. Behaviour and fluxes of natural radionuclides in the production process of a phosphoric acid plant. Appl. Radiat. Isot. 67, 345–356.

Borges, R.C., Fávaro, D.I.T., Caldas, V.G., Lauria, D.C., Bernedo, A.V.B., 2016. Instrumental neutron activation analysis, gamma spectrometry and geographic information system techniques in the determination and mapping of rare earth element in phosphogypsum stacks. Environ. Earth Sci. 75, 705.

Borkiewicz, O., Rakovan, J., Cahill, C.L., 2010. Time-resolved in situ studies of apatite formation in aqueous solutions. Am. Mineral. 95, 1224–1236.

Borra, C.R., Pontikes, Y., Binnemans, K., Van Gerven, T., 2015. Leaching of rare earths from bauxite residue (red mud). Miner. Eng. 76, 20–27.

Borrego, J., Morales, J.A., Pendón, J.G., 1995. Holocene estuarine facies along the mesotidal coast of Huelva, south-western Spain. Tidal signatures in modern and ancient sediments, 24, 151-170.

Brundavanam, S., Poinern, G.E.J., Fawcett, D., 2014. Growth of flower-like Brushite structures on magnesium substrates and their subsequent low temperature transformation to hydroxyapatite. Am. J. Biomed. Eng. 4, 79–87.

Cánovas, C.R., Basallote, M.D., Macías, F., Olías, M., Pérez-López, R., Ayora, C., Nieto, J.M., 2021. Geochemical behaviour and transport of technology critical

metals (TCMs) by the Tinto River (SW Spain) to the Atlantic Ocean. Sci. Total Environ. 764, 143796.

Cánovas, C.R., Chapron, S., Arrachart, G., Pellet-Rostaing, S., 2019. Leaching of rare earth elements (REEs) and impurities from phosphogypsum: a preliminary insight for further recovery of critical raw materials. J. Clean. Prod. 219, 225–235.

Cánovas, C.R., Macías, F., Pérez-López, R., Basallote, M.D., Millán-Becerro, R., 2018a. Valorization of wastes from the fertilizer industry: Current status and future trends. J. Clean. Prod. 174, 678-690.

Cánovas, C.R., Macías, F., Pérez-López, R., Nieto, J.M., 2018b. Mobility of rare earth elements, yttrium and scandium from a phosphogypsum stack: environmental and economic implications. Sci. Total Environ. 618, 847–857.

Cánovas, C.R., Pérez-López, R., Macías, F., Chapron, S., Nieto, J.M., Pellet-Rostaing, S., 2017. Exploration of fertilizer industry wastes as potential source of critical raw materials. J. Clean. Prod. 143, 497–505.

Caraballo, M.A., Macías, F., Nieto, J.M., Ayora, C., 2016. Long term fluctuations of groundwater mine pollution in a sulfide mining district with dry Mediterranean climate: implications for water resources management and remediation. Sci. Total Environ. 539, 427–435.

Caraballo, M.A., Macías, F., Rötting, T.S., Nieto, J.M., Ayora, C., 2011. Long term remediation of highly polluted acid mine drainage: a sustainable approach to restore the environmental quality of the Odiel river basin. Environ. Pollut. 159 (12), 3613–3619.

Castillo, J., Pérez-López, R., Sarmiento, A.M., Nieto, J.M., 2012. Evaluation of organic substrates to enhance the sulfate-reducing activity in phosphogypsum. Sci. Total Environ. 439, 106-113.

Cichy, B., Kużdżał, E., Krztoń, H., 2019. Phosphorus recovery from acidic wastewater by hydroxyapatite precipitation. J. Environ. Manage. 232, 421-427.

Cordell, D., White, S., 2014. Life's bottleneck: sustaining the world's phosphorus for a food secure future. Annu. Rev. Environ. Resour. 39, pp. 161-188.

Davis, J.C., 2002. Statistics and Data Analysis in Geology. JohnWiley & Sons, USA.

Deng, S., Zhang, C., Dang, Y., Collins, R.N., Kinsela, A.S., Tian, J., Waite, T.D., 2020. Iron transformation and its role in phosphorus immobilization in a UCT-MBR with vivianite formation enhancement. Environ. Sci. Technol. 54(19), 12539-12549.

Deng, X.H., Chen, Y.J., Yao, J.M., Bagas, L., Tang, H.S., 2014. Fluorite REE-Y (REY) geochemistry of the ca. 850 Ma Tumen molybdenite–fluorite deposit, eastern Qinling, China: constraints on ore genesis. Ore Geol. Rev. 63, 532–543.

EC Decision, 2003. 33/CE, Council Decision of 19 December 2002 Establishing Criteria and Procedures for the Acceptance ofWaste at Landfills Pursuant toArticle16 of an Annex II to Directive 1999/31/EC, Off. J. L 011, 16/01/2003. pp. 0027–0049.

El-Didamony, H., Ali, M.M., Awwad, N.S., Fawzy, M.M., Attallah, M.F., 2012. Treatment of phosphogypsum waste using suitable organic extractants. J. Radioanalytical Nucl. Chem. 291 (3), 907-914.

El-Didamony, H., Gado, H., Awwad, N., Fawzy, M., Attallah, M., 2013. Treatment of phosphogypsum waste produced from phosphate ore processing. J.Hazard.Mater. 244, 596-602.

El Samad, O., Aoun, M., Nsouli, B., Khalaf, G., Hamze, M., 2014. Investigation of the radiological impact on the coastal environment surrounding a fertilizer plant. J. Environ. Radioact. 133, 69–74.

El Zrelli, R., Courjault-Radé, P., Rabaoui, L., Castet, S., Michel, S., Bejaoui, N., 2016. Heavy metal contamination and ecological risk assessment in the surface sediments of the coastal area surrounding the industrial complex of Gabes city, Gulf of Gabes. SE Tunisia. Mar Pollut Bull.

EN 12457-2, 2002. Characterization of Waste, Compliance Test for Leaching of Granular Wastes Materials and Sludges, Part 2: One Stage Batch Test at a Liquid to

Solid Ratio of 10 l/kg-1 for Materials with Particle Size Below 4 mm (without or with Size Reduction). European Committee of Standardization, p. 28 CEN/TC 292, 12/02.

Ericson, W.A., Patel, S.K., Marek, A.C., Brown, C.M., 1997. Proposed design for fertilizer gypsum stack and acid pond closure. In: Tailings and Mine Waste'97, pp. 69–77.

EU, 2013. Council Directive 2013/59/Euratom of 5 December 2013 Laying Down Basic Safety Standards for Protection against the Dangers Arising from Exposure to Ionising Radiation, and Repealing Directives 89/618/Euratom, 90/641/Euratom, 96/29/Euratom, 97/43/Euratom and 2003/122/Euratom.

European Commission, 2020. Study on the EU's List of Critical Raw Materials - Final Report, 525 Critical Raw Materials Factsheets. 10.2873/11619.

Ficklin, W.H., Plumlee, G.S., Smith, K.S., McHugh, J.B., 1992. Geochemical classification of mine drainages and natural drainages in mineralized areas. Proceedings of the 7th International Symposium on Water Rock Interaction, pp. 381–384. Park City, Utah.

Fuleihan, N.F., Werner, R.J., 2011. Evaluation of lime treatment sludge alternative disposal methodologies including utilization in closure of phosphogypsum stacks. Florida Industrial and Phosphate Research Institute (FIPR). http://fipr.state.fl.us/wp-content/ uploads/2014/12/03-143-247Final.pdf, Accessed date: 28 January 2020.

Grande, J.A., Borrego, J., Morales, J.A., 2000. A study of heavy metal pollution in the Tinto-Odiel estuary in southwestern Spain using factor analysis. Environ. Geol. 39, 1095–1101.

Heviánková, S., Špakovská, B., Klimko, T., Kyncl, M., Bílská, Z., Kučerová, L., 2014. Acid mine drainage treatment by ash from wooden chip combustion: study of mine water composition in dependence on the ash dose and duration of mutual interaction. Carpathian J. Earth Environ. Sci. 9(2), 159-170.

Huang, G., Liu, C., Zhang, Y., Chen, Z., 2020. Groundwater is important for the geochemical cycling of phosphorus in rapidly urbanized areas: a case study in the Pearl River Delta. Environ. Pollut. 260, 114079.

IAEA, 2003. Extent of Environmental Contamination by Naturally Occurring Radioactive Material (NORM) and Technological Options for Mitigation. Technical Reports Ser. No 419. IAEA.

INAP (The International Network for Acid Prevention), 2021. Drainage treatment. http://www. gardguide.com/index.php?title=Chapter_7, Accessed date: 11 February 2021.

Jin, S., Hu, Z., Huang, Y., Hu, Y., Pan, H., 2019. Evaluation of several phosphate amendments on rare earth element concentrations in rice plant and soil solution by X-ray diffraction. Chemosphere 236, 124322.

Johnson, D.B., Hallberg, K.B., 2005. Acid mine drainage remediation options: a review. Sci. Total Environ. 338 (1–2), 3–14.

Jones, S.N., Cetin, B., 2017. Evaluation of waste materials for acid mine drainage remediation. Fuel 188, 294–309.

Kirby, C.S., Cravotta, C.A., 2005a. Net alkalinity and net acidity 1: theoretical considerations. Appl. Geochem. 20, 1920–1940.

Kirby, C.S., Cravotta, C.A., 2005b. Net alkalinity and net acidity 2: practical considerations. Appl. Geochem. 20 (10), 1941–1964.

Kulczycka, J., Kowalski, Z., Smol, M., Wirth, H., 2016. Evaluation of the recovery of rare earth elements (REE) from phosphogypsum waste - case study of the WIZ_OW chemical plant (Poland). J. Clean. Prod. 113, 345–354.

Kuzmanović, P., Todorović, N., Forkapić, S., Petrović, L.F., Knežević, J., Nikolov, J., Miljević, B., 2020. Radiological characterization of phosphogypsum produced in Serbia. Radiat. Phys. Chem. 166, 108463.

Lei, Y., Narsing, S., Saakes, M., Van Der Weijden, R.D., Buisman, C.J., 2019. Calcium carbonate packed electrochemical precipitation column: new concept of phosphate removal and recovery. Environ. Sci. Technol. 53(18), 10774-10780.

Li, R.H., Cui, J.L., Li, X.D., Li, X.Y., 2018. Phosphorus removal and recovery from wastewater using Fe-dosing bioreactor and cofermentation: investigation by X-ray absorption near-edge structure spectroscopy. Environ. Sci. Technol, 52(24), 14119-14128.

LME, 2020. London metal exchange official prices for metal global market. https://lme.com/. (Accessed date: 28 April 2020).

Lottermoser, B.G., 2010. Mine Wastes: Characterization, Treatment and Environmental Impacts. Third ed. Springer-Verlag, Berlin, Heidelberg.

Lütke, S.F., Oliveira, M.L., Silva, L.F., Cadaval Jr, T.R., Dotto, G.L., 2020. Nanominerals assemblages and hazardous elements assessment in phosphogypsum from an abandoned phosphate fertilizer industry. Chemosphere, 256, 127138.

Lysandrou, M., Pashalidis, I., 2008. Uranium chemistry in stack solutions and leachates of phosphogypsum disposed at a coastal area in Cyprus. J. Environ. Radioact. 99(2), 359-366.

Macías, F., Cánovas, C.R., Cruz-Hernández, P., Carrero, S., Asta, M.P., Nieto, J.M., Pérez-López, R., 2017a. An anomalous metal-rich phosphogypsum: characterization and classification according to international regulations. J. Hazard. Mater. 331, 99–108.

Macías, F., Caraballo, M.A., Nieto, J.M., 2012a. Environmental assessment and management of metal-rich wastes generated in acid mine drainage passive remediation systems. J. Hazard. Mater. 229/230, 107–114.

Macías, F., Caraballo, M.A., Nieto, J.M., Rötting, T.S., Ayora, C., 2012b. Natural pretreatment and passive remediation of highly polluted acid mine drainage. J. Environ. Manag. 104, 93–100.

Macías, F., Caraballo, M.A., Rötting, T.S., Pérez-López, R., Nieto, J.M., Ayora, C., 2012c. From highly polluted Zn-rich acid mine drainage to non-metallic waters: implementation of a multi-step alkaline passive treatment system to remediate metal pollution. Sci. Total Environ. 433, 323–330.

Macías, F., Pérez-López, R., Caraballo, M.A., Cánovas, C.R., Nieto, J.M., 2017b. Management strategies and valorization for waste sludge from active treatment of extremely metal-polluted acid mine drainage: a contribution for sustainable mining. J. Clean. Prod. 141, 1057–1066.

Maeda, N., Katakura, T., Fukasawa, T., Huang, A.N., Kawano, T., Fukui, K., 2017. Morphology of woody biomass combustion ash and enrichment of potassium components by particle size classification. Fuel Process. Technol. 156, 1–8.

Manning, B.A., Goldberg, S., 1996. Modeling competitive adsorption of arsenate with phosphate and molybdate on oxide minerals. Soil Sci. Soc. Am. J. 60, 121–131.

Martínez-Aguirre, A., García-León, M., 1991. Natural radioactivity enhancement by human activities in rivers of southwest of Spain. J. Radioanal. Nucl. Chem. 155, 97–106.

Martínez-Aguirre, A., García-León, M., Gascó, C., Travesí, A., 1996. Anthropogenic emissions of ^{210}Po, ^{210}Pb and ^{226}Ra in an estuarine environment. J. Radioanal. Nucl. Chem. 207, 357-367.

Martínez-Aguirre, A., García-León, M., Ivanovich, M., 1994. The distribution of U, Th and ^{226}Ra derived from the phosphate fertilizer industries on an estuarine system in Southwest Spain. J. Environ. Radioact. 22(2), 155-177.

Martínez, N.M., Basallote, M.D., Meyer, A., Cánovas, C.R., Macías, F., Schneider, P., 2019. Life cycle assessment of a passive remediation system for acid mine drainage: towards more sustainable mining activity. J. Clean. Prod. 211, 1100–1111.

Martin, N., Ya, V., Leewiboonsilp, N., Choo, K.H., Noophan, P.L., Li, C.W., 2020. Electrochemical crystallization for phosphate recovery from an electronic industry wastewater effluent using sacrificial iron anodes. J. Clean Prod. 276, 124234.

Más, J.L., San Miguel, E.G., Bolívar, J.P., Vaca, F., Pérez-Moreno, J.P., 2006. An assay on the effect of preliminary restoration tasks applied to a large TENORM wastes disposal in the south-west of Spain. Sci. Total Environ. 364, 55-66.

Masindi, V., Akinwekomi, V., Maree, J.P., Muedi, K.L., 2017. Comparison of mine water neutralisation efficiencies of different alkaline generating agents. J. Environ. Chem. Eng. 5 (4), 3903–3913.

Millán-Becerro, R., Cánovas, C.R., Pérez-López, R., Macías, F., León, R., 2021. Combined procedure of metal removal and recovery of technology elements from fertilizer industry effluents. J Geochem Explor 221, 106698.

Millán-Becerro, R., Macías, F., Cánovas, C.R., Pérez-López, R., Fuentes-López, J.M. 2022. Environmental management and potential valorization of wastes generated in passive treatments of fertilizer industry effluents. Chemosphere, 133876.

Millán-Becerro, R., Pérez-López, R., Macías, F., Cánovas, C.R., Papaslioti, E.M., Basallote, M.D., 2019. Assessment of metals mobility during the alkaline treatment of highly acid phosphogypsum leachates. Sci. Total Environ. 660, 395–405.

Millán-Becerro, R., Pérez-López, R., Macías, F., Cánovas, C.R., 2020. Design and optimization of sustainable passive treatment systems for phosphogypsum leachates in an orphan disposal site. J. Environ. Manage. 275, 111251.

Morales-Flórez, V., Santos, A., Lemus, A., Esquivias, L., 2011. Artificial weathering pools of calcium-rich industrial waste for CO_2 sequestration. Chem. Eng. J. 166(1), 132-137.

Nedelciu, C.E., Ragnarsdottir, K.V., Schlyter, P., Stjernquist, I., 2020. Global phosphorus supply chain dynamics: Assessing regional impact to 2050. Glob. Food Secur. 26, 100426.

Nieto, J.M., Sarmiento, A.M., Canovas, C.R., Olias, M., Ayora, C., 2013. Acid mine drainage in the Iberian Pyrite Belt: 1. Hydrochemical characteristics and pollutant load of the Tinto and Odiel rivers. Environ. Sci. Pollut. Res. Int. 20 (11), 7509–7519.

Nordstrom, D.K., Wilde, F.D., 1998. Reduction-Oxidation Potential (Electrode Method). National FieldManual for the Collection ofWater Quality Data. U.S. Geological Survey Techniques of Water-Resources Investigations (Book 9, chapter 6.5).

Nordstrom, D.K., Blowes, D.W., Ptacek, C.J., 2015. Hydrogeochemistry and microbiology of mine drainage: an update. Appl. Geochem. 57, 3–16.

Olías, M., Cánovas, C.R., Nieto, J.M., Sarmiento, A.M., 2006. Evaluation of the dissolved contaminant load transported by the Tinto and Odiel rivers (South West Spain). Appl. Geochem. 21(10), 1733-1749.

Orden, S., Macías, F., Cánovas, C.R., Nieto, J.M., Pérez-López, R., Ayora, C., 2021. Eco-sustainable passive treatment for mine waters: Full-scale and long-term demonstration. J. Environ. Manage. 280, 111699.

OSPAR, 2002. Discharges of radioactive substances into the maritime area by non-nuclear industry. Radioactive Substances Series. Publication No. 161. OSPAR Commission, London, 60 p.

OSPAR, 2007. PARCOM Recommendation 91/4 on Radioactive Discharges: Spanish Implementation Report. Radioactive Substances Series. Publication No. 342. OSPAR Commission, London, 49 p.

Pan, J., Zhou, C., Liu, C., Tang, M., Cao, S., Hu, T., Ji, W., Luo, Y., Wen, M., Zhang, N., 2018. Modes of occurrence of rare earth elements in coal fly ash: a case study. Energy Fuel 32 (9), 9738–9743.

Papaslioti, E.M., Pérez-López, R., Parviainen, A., Macías, F., Delgado-Huertas, A., Garrido, C.J., Nieto, J.M., 2018a. Stable isotope insights into the weathering processes of a phosphogypsum disposal area. Water Res. 140, 344–353.

Papaslioti, E.M., Pérez-López, R., Parviainen, A., Sarmiento, A.M., Nieto, J.M., Marchesi, C., Garrido, C.J., 2018b. Effects of seawater mixing on the mobility of trace elements in acid phosphogypsum leachates. Mar. Pollut. Bull. 127, 695–703.

Papassiopi, N., Kontoyianni, A., Vaxevanidou, K., Xenidis, A., 2009. Assessment of chromium biostabilization in contaminated soils using standard leaching and sequential extraction techniques. Sci. Total Environ. 407, 925–936.

Parkhurst, D.L., Appelo, C.A.J., 2005. PHREEQC-2 version 2.12: a hydrochemical transport model. http://wwwbrr.cr.usgs.gov2005.

Park, J.Y., Byun, H.J., Choi, W.H., Kang, W.H., 2008. Cement paste column for simultaneous removal of fluoride, phosphate, and nitrate in acidic wastewater. Chemosphere 70 (8), 1429–1437.

Pérez-López, R., Carrero, S., Cruz-Hernández, P., Asta, M.P., Macías, F., Cánovas, C.R., Guglieri, C., Nieto, J.M., 2018. Sulfate reduction processes in salt marshes affected by phosphogypsum: geochemical influences on contaminant mobility. J. Hazard. Mater. 350, 154–161.

Pérez-López, R., Castillo, J., Sarmiento, A.M., Nieto, J.M., 2011a. Assessment of phosphogypsum impact on the salt-marshes of the Tinto river (SW Spain): Role of natural attenuation processes. Mar. Pollut. Bull. 62(12), 2787-2796.

Pérez-López, R., Macías, F., Cánovas, C.R., Sarmiento, A.M., Pérez-Moreno, S.M., 2016. Pollutant flows from a phosphogypsum disposal area to an estuarine environment: an insight from geochemical signatures. Sci. Total Environ. 553, 42–51.

Pérez-López, R., Macías, F., Caraballo, M.A., Nieto, J.M., Román-Ross, G., Tucoulou, R., Ayora, C., 2011b. Mineralogy and geochemistry of Zn-rich mine-drainage precipitates from an MgO passive treatment system by synchrotron-based X-ray analysis. Environ. Sci. Technol. 45(18), 7826-7833.

Pérez-López, R., Nieto, J.M., de la Rosa, J.D., Bolívar, J.P., 2015. Environmental tracers for elucidating the weathering process in a phosphogypsum disposal site: implications for restoration. J. Hydrol. 529, 1313–1323.

Pérez-López, R., Nieto, J.M., López-Cascajosa, M.J., Díaz-Blanco, M.J., Oliveira, V., Sánchez-Rodas, D., 2011c. Evaluation of heavy metals and arsenic speciation

discharged by the industrial activity on the Tinto-Odiel estuary, SW Spain. Mar. Pollut. Bull. 62 (2), 405–411.

Pérez-López, R., Nieto, J.M., López-Coto, I., Aguado, J.L., Bolívar, J.P., 2010. Dynamics of contaminants in phosphogypsum of the fertilizer industry of Huelva (SW Spain): from phosphate rock ore to the environment. Appl. Geochem. 25 (5), 705–715.

Pingitore, N., Clague, J., Gorski, D., 2014. Round Top Mountain rhyolite (Texas, USA), a massive, unique Y-bearing-fluorite-hosted heavy rare earth element (HREE) deposit. J. Rare Earths 32 (1), 90–96.

Qin, J., Hovmand, M.F., Ekelund, F., Rønn, R., Christensen, S., de Groot, G.A., Krogh, P.H., 2017. Wood ash application increases pH but does not harm the soil mesofauna. Environ. Pollut. 224, 581–589.

Qureshi, A., Jia, Y., Maurice, C., Öhlander, B., 2016. Potential of fly ash for neutralisation of acid mine drainage. Environ. Sci. Pollut. Res. 23 (17), 17083–17094.

Rabi, J.A., Mohamad, A.A., 2006. Parametric modelling and numerical simulation of natural-convective transport of radon-222 from a phosphogypsum stack into open air. Appl. Math. Model. 30, 1546-1560.

Ríos, C.A., Williams, C.D., Roberts, C.L., 2008. Removal of heavy metals from acid mine drainage (AMD) using coal fly ash, natural clinker and synthetic zeolites. J. Hazard Mater. 156, 23–35.

Rutherford, P.M., Dudas, M.J., Samek, R.A., 1994. Environmental impacts of phosphogypsum. Sci. Total Environ. 149, 1–38.

Sadri, F., Nazari, A.M., Ghahreman, A., 2017. A review on the cracking, baking and leaching processes of rare earth element concentrates. J. Rare Earths 35 (8), 739–752.

Sahoo, P.K., Tripathy, S., Equeenuddin, S.M., Panigrahi, M.K., 2012. Geochemical characteristics of coal mine discharge vis-`a-vis behavior of rare earth elements at Jaintia Hills coalfield, northeastern India. J. Geochem. Explor. 112, 235–243.

Sanders, L.M., Luiz-Silva, W., Machado, W., Sanders, C.J., Marotta, H., Enrich-Prast, A., Bosco-Santos, A., Boden, A., Silva, E.V., Santos, I.R., Patchineelam, S.R., 2013. Rare earth element and radionuclide distribution in surface sediments along an estuarine system affected by fertilizer industry contamination. Water Air Soil Pollut. 224, 1742–1749.

Shaddel, S., Grini, T., Ucar, S., Azrague, K., Andreassen, J.P., Østerhus, S.W., 2020. Struvite crystallization by using raw seawater: Improving economics and environmental footprint while maintaining phosphorus recovery and product quality. Water Res. 173, 115572.

Smith, K.L., Figueroa, L.A., Plumlee, G.S., 2013. Can treatment and disposal costs be reduced through metal recovery? In: Wolkersdorfer, Brown, Figueroa (Eds.), Proceedings of the Annual International Mine Water Association Conference-Reliable Mine Water Technology. Golden, Colorado (USA).

SMM, 2020. Shangai metals market. https://www.metal.com/. (Accessed date: 28 April 2020).

Sverdrup, H.U., Ragnarsdóttir, K.V., 2014. Natural resources in a planetary perspective. Geochemical perspectives, 3(2), 129-130.

Tayibi, H., Choura, M., López, F.A., Alguacil, F.J., López-Delgado, A., 2009. Environmental impact and management of phosphogypsum. J. Environ. Manag. 90, 2377–2386.

Torres, E., Lozano, A., Macías, F., Gomez-Arias, A., Castillo, J., Ayora, C., 2018. Passive elimination of sulfate and metals from acid mine drainage using combined limestone and barium carbonate systems. J. Clean. Prod. 182, 114–123.

US EPA (US Environmental Protection Agency), 1992. TCLP, Method 1311, Rev 0. InSW-846: Test Methods for Evaluating Solid Waste, Physical/Chemical Methods. Office of Solid Waste, Washington, DC.

US EPA (US Environmental Protection Agency), 1998. Applicability of the Toxicity Characteristic Leaching Procedure to Mineral Processing Wastes. United States Environmental Protection Agency, Washington, DC, p. 28.

US EPA. (US Environmental Protection Agency), 2020a. Land disposal restrictions, rules and regulations. http://www.epa.gov/osw/hazard/tsd/ldr/regs.htm. (Accessed date: 11 November 2020).

US EPA. (US Environmental Protection Agency), 2020b. National Recommended Water Quality Criteria (last Accessed. http://www2.epa.gov/wqc/national-recommended-water-quality-criteria. (Accessed date: 11 November 2020).

USGS, 2020. Mineral Commodity Summaries 2020. U.S. Geological Survey, 2020, Mineral Commodity Summaries 2020. U.S. Geological Survey (200 pp.).

Vásconez-Maza, M.D., Martínez-Segura, M.A., Bueso, M.C., Faz, Á., García-Nieto, M.C., Gabarrón, M., Acosta, J.A., 2019. Predicting spatial distribution of heavy metals in an abandoned phosphogypsum pond combining geochemistry, electrical resistivity tomography and statistical methods. J. Hazard. Mater. 374, 392-400.

Vassilev, S.V., Baxter, D., Andersen, L.K., Vassileva, C.G., 2013. An overview of the composition and application of biomass ash. Part 1. Phase–mineral and chemical composition and classification. Fuel 105, 40–76.

Vemic, M., Bordas, F., Guibaud, G., Joussein, E., Labanowski, J., Lens, P.N., Van Hullebusch, E.D., 2015. Mineralogy and metals speciation inMo richmineral sludges generated at a metal recycling plant. Waste Manag. 38, 303–311.

Walawalkar, M., Nichol, C.K., Azimi, G., 2016. Process investigation of the acid leaching of rare earth elements from phosphogypsum using HCl, HNO_3, and H_2SO_4. Hydrometallurgy 166, 195e204.

WHO, 2011. Guidelines for Drinking-Water Quality, fourth ed. World Health Organization http://www.who.int/water_sanitation_health/publications/2011/dwq_guidelines/en/index.html. (Accessed date: 27 January 2020).

Worrell, W.A., Vesilid, P.A., Ludwig, C., 2017. Solid waste engineering - A global perspective. Cengage Learning, pp 499.

Yang, L., Zhang, Y., Yan, Y., 2016. Utilization of original phosphogypsum as raw material for the preparation of self-leveling mortar. J. Clean. Prod., 127, 204-213.

Ziemkiewicz, P.F., Skousen, J.G., Simmons, J., 2003. Long-term performance of passive acid mine drainage treatment systems. Mine Water Environ. 22, 118–129.

APPENDIX

AP1. CHAPTER 2 SUPPLEMENTARY INFORMATION

Figure AP1.1. Location map of the phosphogypsum pile on the salt-marsh soils of the Tinto River estuary and sampling points of edge outflows.

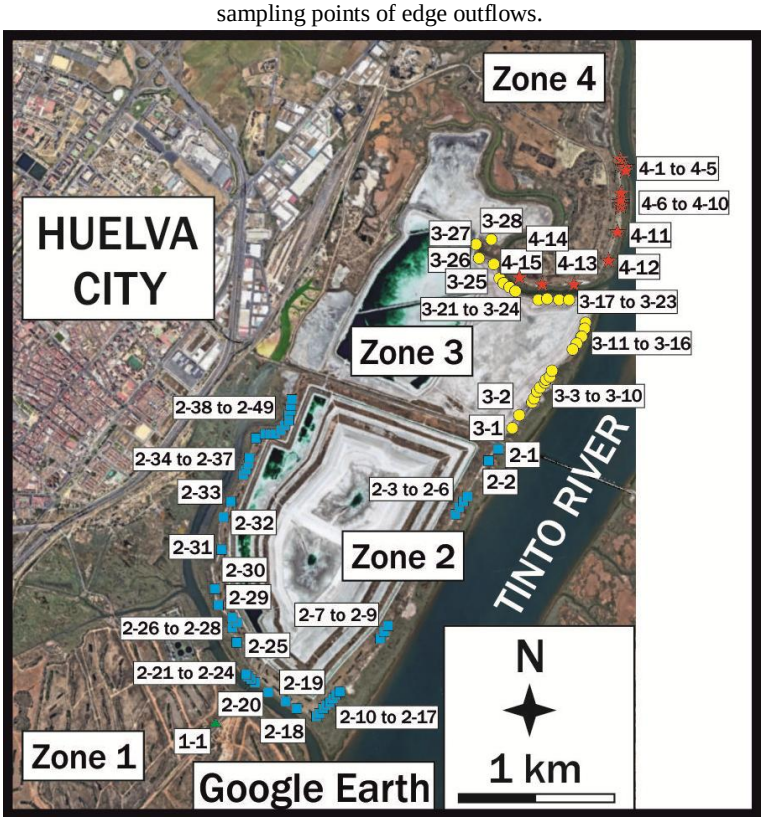

Table AP1.1. Compilation of the physicochemical parameters and concentration of pollutants of the acid leachate of zone 1 collected during the four sampling campaigns.

Sampling campaings	pH	EC mS/cm	Eh mV	PO_4 mg/L	SO_4 mg/L	F mg/L	Cl mg/L	Fe mg/L	Al mg/L	Zn mg/L	As mg/L	Cu µg/L	Cd µg/L	Sb µg/L	Cr µg/L	Ni µg/L	U µg/L
May-June 2014	3.19	92.5	342	578	9029	76.7	38,351	1.47	8.34	1.38	0.30	1.20	0.15	0.34	<.l.d	0.15	0.20
November 2014	2.26	33.8	246	1479	7070	269	15,028	42.6	1.00	1.86	0.25	1.49	0.26	0.02	0.54	0.27	0.53
May-June 2015	5.14	61.4	23.7	68.6	6478	23.1	21,714	1.00	7.30	0.17	0.09	<.l.d.	<.l.d.	<.l.d.	0.07	<.l.d.	<.l.d.
June 2016	4.75	56.0	284	72.8	3306	63.7	19,587	<.l.d.	<.l.d.	0.60	0.06	0.16	0.02	<.l.d.	<.l.d.	<.l.d.	<.l.d.

Table AP1.2. Compilation of the physicochemical parameters and concentration of pollutants of the edge outflows of zone 2 collected during the four sampling campaigns.

Sampling campaings May-June 2014 n=25	pH	EC	Eh	PO_4	SO_4	F	Cl	Fe	Al	Zn	As	Cu	Cd	Sb	Cr	Ni	U
		mS/cm	mV	mg/L	mg/L	mg/L	mg/L	mg/L	mg/L	mg/L	mg/L	µg/L	µg/L	µg/L	µg/L	µg/L	µg/L
Minimum	1.59	30.1	246	1371	3677	79.9	4530	12.9	7.43	4.78	2.90	462	449	22	24	385	224
Maximum	2.79	61.7	319	63,741	6485	1446	23,306	315	321	76.8	33.6	10,451	10,790	865	24,110	7218	27,715
Mean	1.83	38.8	290	32,633	5351	793	9944	137	108	43.9	20.4	6071	5945	309	11,721	4210	16,141
Median	1.74	33.8	293	33,605	5322	769	7480	129	94.0	51.1	23.2	7611	6368	381	12,937	4611	19,185
Percentile 25	1.65	32.3	276	16,221	4996	441	6220	68.5	16.9	27.2	15.0	3037	3445	135	3102	2775	7159
Percentile 75	1.86	45.7	300	48,554	5545	1126	12,707	199	201	58.4	26.3	8409	8540	438	19,126	5776	24,546
Standard Deviation	0.28	9.07	18.1	19,427	641	417	5134	87.4	99.7	21.0	8.81	3180	3177	210	8169	2025	9744

Sampling campaings November 2014 n=33	pH	EC	Eh	PO_4	SO_4	F	Cl	Fe	Al	Zn	As	Cu	Cd	Sb	Cr	Ni	U
		mS/cm	mV	mg/L	mg/L	mg/L	mg/L	mg/L	mg/L	mg/L	mg/L	µg/L	µg/L	µg/L	µg/L	µg/L	µg/L
Minimum	1.83	19.2	178	1771	4431	32.6	4308	12.0	0.97	3.11	1.92	290	372	2.55	42.6	326	88.2
Maximum	3.14	43.0	317	29,403	10,814	1651	22,888	411	298	59.0	28.6	9138	7148	493	22,019	5896	23,823
Mean	2.17	26.9	265	16,444	6388	696	11,202	174	74.7	32.9	16.9	4729	3655	204	8596	3241	11,081
Median	2.10	26.7	270	19,138	6200	668	9673	166	43.0	38.9	18.7	4820	4262	181	5852	3710	12,383
Percentile 25	1.95	21.5	253	8945	5830	320	7165	99.2	11.3	16.3	8.99	1876	1764	84.7	2424	1533	2679
Percentile 75	2.26	32.8	281	23,170	6698	1059	15,721	246	87.8	47.6	23.7	7799	5338	327	15,743	4602	17,397
Standard Deviation	0.32	7.88	26.5	8933	1168	482	5092	102	86.1	17.2	8.13	3001	2149	138	7366	1716	8433

Sampling campaings May-June 2015 n=37	pH	EC	Eh	PO_4	SO_4	F	Cl	Fe	Al	Zn	As	Cu	Cd	Sb	Cr	Ni	U
		mS/cm	mV	mg/L	mg/L	mg/L	mg/L	mg/L	mg/L	mg/L	mg/L	µg/L	µg/L	µg/L	µg/L	µg/L	µg/L
Minimum	1.73	31.9	279	1318	3780	63.0	5123	5.30	7.90	2.91	1.50	304	359	3.96	272	218	132
Maximum	2.66	73.7	343	34,509	7791	1625	27,081	234	344	62.8	30.9	9475	10,653	690	25,970	6587	26,184
Mean	1.98	43.1	311	20,362	6024	884	10,970	117	87.9	39.1	20.1	5411	5684	231	10,647	3871	13,500
Median	1.91	38.7	309	21,442	5993	944	8333	115	48.9	43.6	23.8	6301	5671	246	10,510	4121	13,691
Percentile 25	1.80	36.0	302	11,115	5651	451	6264	63.2	17.4	23.6	12.6	3009	3409	94.8	3103	2368	6204
Percentile 75	2.04	50.2	317	27,462	6539	1371	14,266	174	149	55.2	27.0	7508	8159	356	18,252	5617	21,448
Standard Deviation	0.26	9.61	15.6	9944	787	503	5777	66.7	86.7	19.2	9.02	2708	3071	161	8042	1949	8505

Sampling campaings June 2016 n=19	pH	EC	Eh	PO_4	SO_4	F	Cl	Fe	Al	Zn	As	Cu	Cd	Sb	Cr	Ni	U
		mS/cm	mV	mg/L	mg/L	mg/L	mg/L	mg/L	mg/L	mg/L	mg/L	µg/L	µg/L	µg/L	µg/L	µg/L	µg/L
Minimum	1.78	35.2	256	833	3466	51.2	6086	2.32	1.24	3.39	1.74	358	276	14.1	72.0	225	454
Maximum	2.73	63.6	377	45,384	6754	2541	22,435	255	222	86.9	32.7	12,604	11,762	564	19,815	8857	43,109
Mean	2.04	48.4	309	17,053	4550	946	13,195	102	81.1	34.6	15.6	4321	4396	194	6281	3261	10,310
Median	1.99	46.1	309	18,317	4325	740	11,104	124	22.0	38.9	19.5	4176	4221	149	5695	3204	9175
Percentile 25	1.91	39.3	293	9235	4229	442	8615	31.1	10.7	18.7	8.34	2774	2437	64.4	1700	1841	4708
Percentile 75	2.05	58.3	325	22,251	4777	1276	17,836	205	155	45.9	21.4	5504	5732	275	9520	4118	12,466
Standard Deviation	0.25	10.1	28	10,420	665	629	5824	93.5	88	20.4	8.12	2817	2819	152	5497	2002	9765

Table AP1.3. Compilation of the physicochemical parameters and concentration of pollutants of the edge outflows of zone 3 collected during the four sampling campaigns.

Sampling campaings May-June 2014 n=16	pH	EC	Eh	PO_4	SO_4	F	Cl	Fe	Al	Zn	As	Cu	Cd	Sb	Cr	Ni	U
		mS/cm	mV	mg/L	mg/L	mg/L	mg/L	mg/L	mg/L	mg/L	mg/L	µg/L	µg/L	µg/L	µg/L	µg/L	µg/L
Minimum	1.78	28.3	259	3373	4484	266	7934	25.5	6.36	5.83	8.04	844	810	115	843	756	1697
Maximum	2.03	74.8	306	9617	8239	733	21,448	200	26.9	24.1	30.5	6955	2466	501	5444	2931	6572
Mean	1.90	40.3	279	5827	5491	547	13,291	105	11.0	15.0	16.9	3011	1525	276	2794	1580	3734
Median	1.89	35.0	279	5794	5195	537	11,164	97.0	7.96	16.9	16.7	2939	1493	283	2679	1437	3391
Percentile 25	1.84	32.1	274	4403	4967	501	10,416	82.7	7.41	8.00	13.3	1408	1076	158	1653	911	2938
Percentile 75	1.97	39.7	282	6575	5479	611	15,424	116	10.6	19.6	19.6	3366	1652	355	3381	1924	4278
Standard Deviation	0.08	13.83	10.2	1790	1068	114	4544	44.3	6.10	5.43	5.93	1894	476	114	1318	577	1300

Sampling campaings November 2014 n=17	pH	EC	Eh	PO_4	SO_4	F	Cl	Fe	Al	Zn	As	Cu	Cd	Sb	Cr	Ni	U
		mS/cm	mV	mg/L	mg/L	mg/L	mg/L	mg/L	mg/L	mg/L	mg/L	µg/L	µg/L	µg/L	µg/L	µg/L	µg/L
Minimum	2.16	18.6	245	1257	5733	75.3	9000	25.5	0.93	2.80	3.81	589	266	55.5	453	328	530
Maximum	2.63	41.7	307	7585	9021	857	25,441	333	25.5	21.2	22.3	8684	1477	438	5043	2665	6093
Mean	2.31	25.3	264	5060	7010	542	14,224	171	7.77	14.2	15.2	3276	1022	239	2557	1417	3336
Median	2.25	22.3	264	5489	6766	613	13,431	166	5.75	14.2	15.9	3007	1075	248	2522	1305	3188
Percentile 25	2.22	20.8	255	4376	6435	445	11,365	123	2.72	11.0	12.4	2457	845	138	1378	1169	2579
Percentile 75	2.31	30.3	268	5845	7333	712	17,083	236	9.06	18.2	19.2	3843	1165	294	3524	1690	4705
Standard Deviation	0.15	6.55	14.1	1806	1005	245	4254	80.4	6.80	5.24	4.98	1807	298	114	1437	537	1703

Sampling campaings May-June 2016 n=19	pH	EC	Eh	PO_4	SO_4	F	Cl	Fe	Al	Zn	As	Cu	Cd	Sb	Cr	Ni	U
		mS/cm	mV	mg/L	mg/L	mg/L	mg/L	mg/L	mg/L	mg/L	mg/L	µg/L	µg/L	µg/L	µg/L	µg/L	µg/L
Minimum	2.04	30.9	277	1967	5347	122	8053	4.80	7.30	1.15	1.68	506	116	22.6	229	22.9	297
Maximum	2.33	85.9	345	8595	8480	1053	21474	208	70.9	28.8	32.4	6165	3085	521	6577	3003	6755
Mean	2.12	47.2	299	5693	6609	604	13403	91.5	16.1	16.8	17.6	3081	1716	240	2694	1570	3181
Median	2.11	44.0	294	6002	6422	656	12979	88.3	10.7	18.7	18.2	3171	1764	238	2483	1538	3014
Percentile 25	2.05	36.7	286	4500	5979	457	10400	61.2	8.75	12.2	13.7	2266	1298	149	1488	1140	2337
Percentile 75	2.16	53.9	305	6917	7001	786	16127	114	18.5	21.2	22.8	4082	2099	301	3153	2057	4226
Standard Deviation	0.08	14.8	19.4	1857	902	274	4040	50.8	14.2	7.04	7.13	1490	691	139	1747	699	1739

Sampling campaings June 2016 n=12	pH	EC	Eh	PO_4	SO_4	F	Cl	Fe	Al	Zn	As	Cu	Cd	Sb	Cr	Ni	U
		mS/cm	mV	mg/L	mg/L	mg/L	mg/L	mg/L	mg/L	mg/L	mg/L	µg/L	µg/L	µg/L	µg/L	µg/L	µg/L
Minimum	2.01	27.3	256	1037	3304	130	8688	3.85	1.71	3.38	1.33	561	369	11.4	443	251	671
Maximum	2.51	30.3	332	7367	5256	1324	18260	206	56.3	26.1	22.7	5790	2280	564	5708	3051	4995
Mean	2.18	28.8	287	4915	4180	802	12956	74.6	10.6	15.8	13.6	3306	1517	256	2243	1475	2905
Median	2.09	28.8	285	5104	4100	871	12243	74.3	7.60	18.1	14.2	3487	1775	241	2273	1577	3084
Percentile 25	2.06	28.1	279	3775	3919	719	11040	52.5	2.22	7.24	10.6	1516	1014	150	1135	851	2056
Percentile 75	2.25	29.6	290	6900	4357	984	14305	86.6	10.3	22.0	18.0	4886	2054	356	2717	1967	3717
Standard Deviation	0.17	11.2	18.3	2190	511	332	2921	50.0	15.2	8.35	6.28	1835	676	174	1561	807	1421

Table AP1.4. Compilation of the physicochemical parameters and concentration of pollutants of the edge outflows of zone 4 collected during the four sampling campaigns.

Sampling campaings May-June 2014 n=9	pH	EC	Eh	PO_4	SO_4	F	Cl	Fe	Al	Zn	As	Cu	Cd	Sb	Cr	Ni	U
		mS/cm	mV	mg/L	mg/L	mg/L	mg/L	mg/L	mg/L	mg/L	mg/L	µg/L	µg/L	µg/L	µg/L	µg/L	µg/L
Minimum	2.12	32.1	260	2481	6172	79.6	8744	20.2	6.89	7.22	3.30	972	780	182	475	659	960
Maximum	2.42	78.2	293	4465	7611	571	15,375	183	22.7	30.3	14.3	3541	1400	752	1562	1599	3117
Mean	2.21	47.4	270	3737	7051	384	12,875	133	9.90	13.2	7.43	1529	1018	354	1097	992	1698
Median	2.16	47.2	267	3695	7109	404	13,825	154	8.31	10.3	7.46	1309	1094	312	1190	1015	1649
Percentile 25	2.13	42.9	266	3385	6951	367	11,312	121	7.25	10.0	5.92	999	881	303	1077	822	1616
Percentile 75	2.18	48.6	272	4289	7322	485	14,545	156	9.36	15.4	7.71	1793	1102	336	1208	1057	1679
Standard Deviation	0.12	13.1	9.53	638	451	152	2378	46.9	4.97	7.01	3.00	825	199	158	331	272	592

Sampling campaings November 2014 n=10	pH	EC	Eh	PO_4	SO_4	F	Cl	Fe	Al	Zn	As	Cu	Cd	Sb	Cr	Ni	U
		mS/cm	mV	mg/L	mg/L	mg/L	mg/L	mg/L	mg/L	mg/L	mg/L	µg/L	µg/L	µg/L	µg/L	µg/L	µg/L
Minimum	2.04	30.4	230	1465	7230	67.9	9354	87.5	1.26	2.16	1.53	442	134	34.9	482	295	354
Maximum	2.49	46.8	251	4051	8897	592	16,310	347	18.0	14.7	7.95	4611	652	343	1491	1017	4192
Mean	2.22	37.3	242	2917	7998	350	12,624	215	4.56	9.53	5.28	1763	451	208	1003	769	1391
Median	2.13	36.0	242	3188	7998	394	12,119	201	2.77	8.99	5.26	1375	460	237	1133	826	1037
Percentile 25	2.11	32.9	238	2206	7637	151	10,939	186	1.92	6.77	3.74	823	416	168	714	658	623
Percentile 75	2.39	41.7	248	3588	8201	520	14,639	251	5.11	13.6	6.99	1965	533	254	1210	948	1291
Standard Deviation	0.18	6.07	6.60	896	520	205	2550	67.4	4.98	4.24	2.09	1364	140	91.1	364	233	1220

Sampling campaings May-June 2015 n=6	pH	EC mS/cm	Eh mV	PO_4 mg/L	SO_4 mg/L	F mg/L	Cl mg/L	Fe mg/L	Al mg/L	Zn mg/L	As mg/L	Cu µg/L	Cd µg/L	Sb µg/L	Cr µg/L	Ni µg/L	U µg/L
Minimum	2.19	35.0	237	3255	7680	552	9504	34.3	7.70	7.74	3.09	298	707	114.4	598	632	638
Maximum	2.23	73.2	298	4172	8230	890	16,575	153	11.9	16.9	8.40	3254	1093	299	1312	1032	2141
Mean	2.22	44.9	275	3804	7873	725	12,713	121	8.87	10.7	6.67	1248	914	247	1141	790	1211
Median	2.22	39.1	278	3745	7720	732	12,552	133	8.05	9.91	7.00	1040	886	263	1263	782	1119
Percentile 25	2.22	38.8	275	3721	7719	599	11,394	125	7.80	8.30	6.36	495	862	248	1238	671	882
Percentile 75	2.23	43.2	282	4127	8015	851	13,704	146	9.35	11.3	8.04	1417	1015	288	1296	854	1362
Standard Deviation	0.02	14.2	20.3	371	241	149	2466	43.9	1.66	3.40	1.96	1087	140	68.1	305	150	539

Sampling campaings June 2016 n=8	pH	EC mS/cm	Eh mV	PO_4 mg/L	SO_4 mg/L	F mg/L	Cl mg/L	Fe mg/L	Al mg/L	Zn mg/L	As mg/L	Cu µg/L	Cd µg/L	Sb µg/L	Cr µg/L	Ni µg/L	U µg/L
Minimum	2.17	40.5	253	2873	4938	446	8143	50.1	0.20	7.71	3.56	404	681	110	575	607	397
Maximum	2.33	75.5	286	3880	8236	900	16,259	239	4.87	26.6	14.5	4488	1156	579	1859	1274	2160
Mean	2.25	54.4	272	3203	6013	745	13,633	148	1.81	14.2	7.68	1537	958	334	1110	903	916
Median	2.26	50.1	272	3013	5600	836	14,107	149	1.08	13.2	7.33	781	961	310	1079	948	724
Percentile 25	2.23	47.3	260	2907	5446	645	13,526	111	0.61	10.5	5.56	695	875	262	830	785	571
Percentile 75	2.28	57.6	285	3420	6204	872	15,414	190	2.65	15.9	8.86	1807	1092	404	1297	974	992
Standard Deviation	0.06	12.6	13.7	444	1077	179	2910	61.6	1.69	5.93	3.51	1477	161	143	430	212	581

AP2. CHAPTER 3 SUPPLEMENTARY INFORMATION

Figure AP2.1. Results of aqueous speciation (in percentage) according to PHREEQC for P and As (anions) and some metals such as Cu and Zn (cations) for the entire pH range in the neutralization experiments of edge outflows of zones 3, 4 and process water.

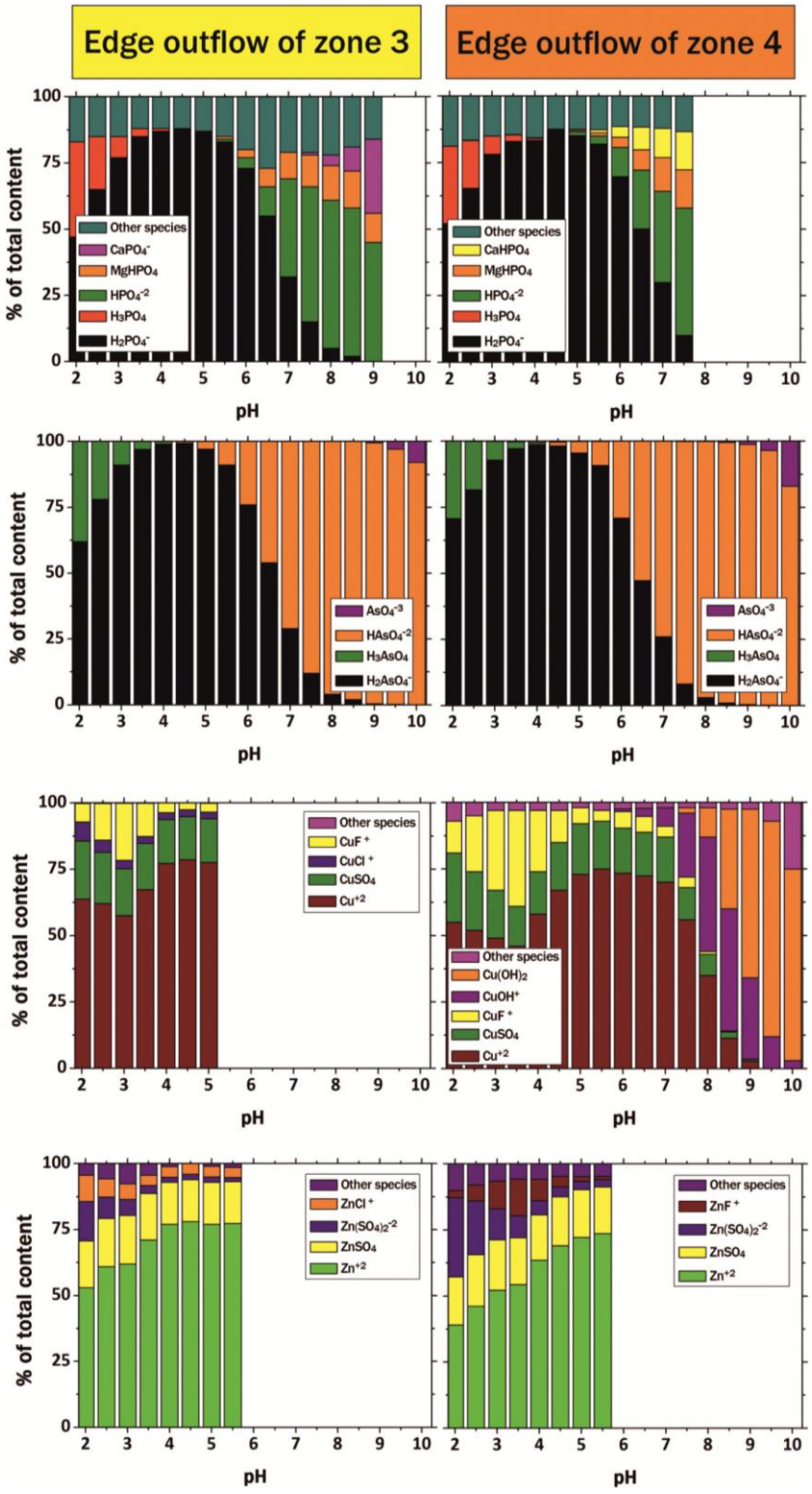

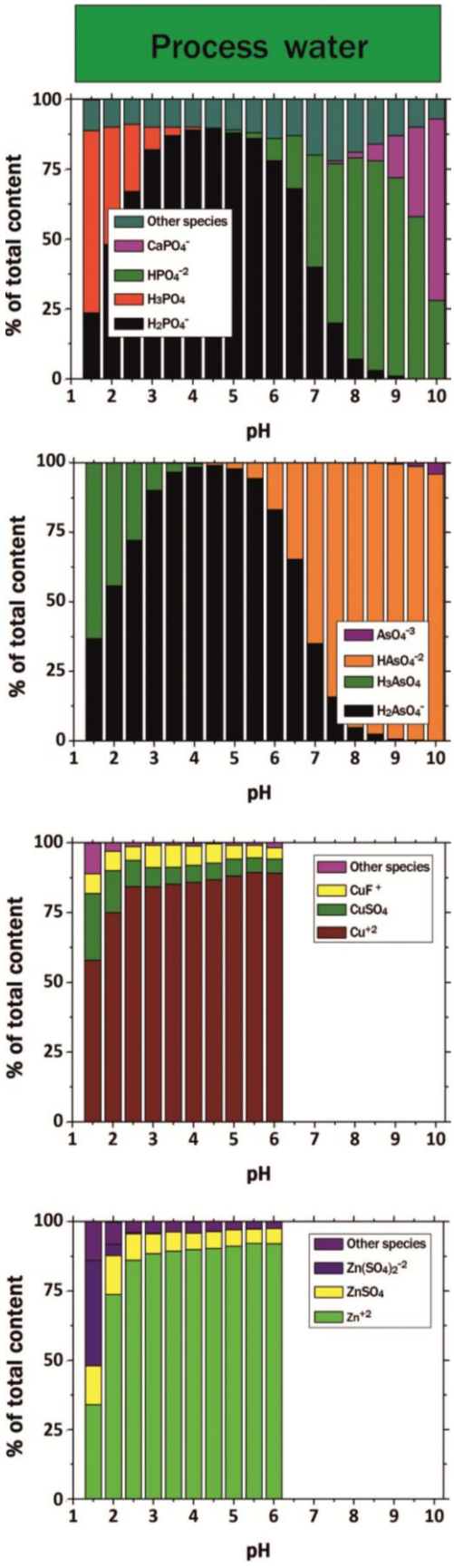
Process water
% of total content
pH
Other species
CaPO4-
HPO4-2
H3PO4
H2PO4-
AsO4-3
HAsO4-2
H3AsO4
H2AsO4-
CuF+
CuSO4
Cu+2
Zn(SO4)2-2
ZnSO4
Zn+2

Table AP2.1. Physicochemical parameters and contaminant concentrations of the solutions collected from the titration experiment of the edge outflow of zone 3.

	mL $Ca(OH)_2$ added to 50 mL	pH	CE (mS/cm)	Eh (mV)	mg/L			mg/L										
					Fluoride	Sulfate	Phosphate	Fe	As[a]	Zn	Al	Cr[a]	U	Cu	Cd	Ni	Co[b]	Sb[b]
M0-EO-Z3	0.00	2.09	32.8	486	974	4018	3998	90.8	15.1	13.2	4.61	3.57	3.38	3.36	1.34	1.25	184	37.1
M1-EO-Z3	41.0	2.50	22.6	459	990	2711	2429	62.9	9.87	9.06	3.28	2.47	2.31	2.34	0.93	0.89	128	24.6
M2-EO-Z3	111	3.00	14.4	417	790	2180	2169	40.9	7.09	6.45	2.58	1.51	1.42	1.60	0.59	0.58	83.6	15.6
M3-EO-Z3	149	3.52	13.2	380	234	1325	1166	8.01	4.41	4.27	<l.d.	0.72	0.42	0.97	0.38	0.40	53.3	9.64
M4-EO-Z3	152	4.04	8.39	350	50.0	964	752	8.08	3.67	3.19	<l.d.	0.58	0.04	0.84	0.33	0.36	49.0	8.50
M5-EO-Z3	155	4.50	8.21	343	30.8	917	833	0.81	3.48	2.51	<l.d.	0.44	<l.d.	0.57	0.31	0.32	45.8	8.05
M6-EO-Z3	167	5.00	8.08	374	39.4	915	719	<l.d.	3.34	1.70	<l.d.	0.37	<l.d.	0.33	0.29	0.32	45.1	7.99
M7-EO-Z3	173	5.50	7.94	375	47.0	887	625	<l.d.	3.16	0.90	<l.d.	0.25	<l.d.	0.16	0.24	0.29	40.5	7.23
M8-EO-Z3	188	6.03	7.48	372	32.8	780	636	<l.d.	2.94	<l.d.	<l.d.	0.12	<l.d.	0.04	0.13	0.27	35.2	7.13
M9-EO-Z3	206	6.48	6.92	369	24.7	706	352	<l.d.	2.67	<l.d.	<l.d.	0.06	<l.d.	<l.d.	0.05	0.21	25.3	6.03
M10-EO-Z3	256	6.99	5.74	354	16.4	596	138	<l.d.	2.19	<l.d.	<l.d.	0.02	<l.d.	<l.d.	<l.d.	0.12	7.20	4.87
M11-EO-Z3	276	7.49	5.38	340	38.2	600	86.1	<l.d.	1.70	<l.d.	<l.d.	<l.d.	<l.d.	<l.d.	<l.d.	0.06	2.24	4.37
M12-EO-Z3	304	8.00	4.91	324	26.9	448	16.1	<l.d.	1.33	<l.d.	<l.d.	<l.d.	<l.d.	<l.d.	<l.d.	0.04	1.44	3.92
M13-EO-Z3	345	8.47	4.46	299	9.18	476	13.4	<l.d.	1.28	<l.d.	<l.d.	<l.d.	<l.d.	<l.d.	<l.d.	0.03	0.70	3.66
M14-EO-Z3	367	9.04	4.23	283	8.48	430	3.23	<l.d.	1.03	<l.d.	<l.d.	<l.d.	<l.d.	<l.d.	<l.d.	0.02	0.36	3.27
M15-EO-Z3	420	9.47	4.10	274	20.4	424	n.d.	<l.d.	0.73	<l.d.	<l.d.	<l.d.	<l.d.	<l.d.	<l.d.	0.03	0.39	2.99
M16-EO-Z3	435	9.99	3.98	271	9.96	416	n.d.	<l.d.	0.66	<l.d.	<l.d.	<l.d.	<l.d.	<l.d.	<l.d.	0.02	0.20	2.86

n.d.: not detected

<l.d.: below detection limit

[a] Specific valences for these elements were As(V) and Cr(III) during the entire alkaline treatment according to the PHREEQC modelling

[b] concentration in µg/L

Table AP2.2. Physicochemical parameters and contaminant concentrations of the solutions collected from the titration experiment of the edge outflow of zone 4.

	mL $Ca(OH)_2$ added to 50 mL	pH	CE (mS/cm)	Eh (mV)	mg/L			mg/L										
					Fluoride	Sulfate	Phosphate	Fe	Zn	Cu	Cr[a]	Al	As[a]	U	Ni	Cd	Co[b]	Sb[b]
M0-EO-Z4	0.00	2.20	33.5	483	1639	5664	2601	183	11.5	5.81	3.05	2.49	2.29	2.18	0.86	0.76	298	256
M1-EO-Z4	20.0	2.52	23.8	473	1905	4352	1863	76.3	8.84	4.43	2.34	2.00	1.71	1.62	0.67	0.57	231	194
M2-EO-Z4	45.0	3.03	16.0	432	1370	3108	1353	54.6	7.18	3.28	1.63	1.61	1.33	1.11	0.49	0.42	170	151
M3-EO-Z4	60.0	3.51	14.8	382	1157	2561	1173	46.0	6.19	3.03	1.40	1.45	1.12	0.94	0.46	0.39	157	128
M4-EO-Z4	80.0	4.06	12.1	339	484	1998	972	37.9	5.38	2.55	1.01	1.28	1.00	0.67	0.38	0.33	132	117
M5-EO-Z4	135	4.58	8.73	305	189	1550	670	18.7	3.64	1.68	0.54	<l.d.	0.72	<l.d.	0.28	0.23	94.2	78.7
M6-EO-Z4	143	5.05	6.83	262	82.1	1393	582	7.73	2.19	1.50	0.40	<l.d.	0.67	<l.d.	0.26	0.21	89.8	81.8
M7-EO-Z4	155	5.46	6.91	235	57.0	1307	492	3.18	0.80	1.22	0.23	<l.d.	0.62	<l.d.	0.24	0.17	80.1	71.2
M8-EO-Z4	198	6.04	3.72	318	82.7	1128	419	<l.d.	0.14	0.17	0.13	<l.d.	0.53	<l.d.	0.20	0.10	65.2	60.3
M9-EO-Z4	205	6.53	3.26	302	80.2	1064	340	<l.d.	<l.d.	0.08	0.06	<l.d.	0.50	<l.d.	0.16	0.04	46.9	64.1
M10-EO-Z4	213	6.95	3.03	320	50.0	1038	274	<l.d.	<l.d.	0.04	0.04	<l.d.	0.47	<l.d.	0.14	<l.d.	28.6	54.3
M11-EO-Z4	258	7.55	2.84	355	63.4	837	32.1	<l.d.	<l.d.	0.04	<l.d.	<l.d.	0.30	<l.d.	0.08	<l.d.	11.8	46.5
M12-EO-Z4	260	8.05	2.45	376	16.2	834	40.4	<l.d.	<l.d.	0.04	<l.d.	<l.d.	0.33	<l.d.	0.05	<l.d.	5.83	51.5
M13-EO-Z4	275	8.55	2.37	365	20.9	787	<l.d.	<l.d.	<l.d.	0.05	<l.d.	<l.d.	0.25	<l.d.	0.05	<l.d.	3.33	42.6
M14-EO-Z4	286	8.97	2.06	344	50.2	755	<l.d.	<l.d.	<l.d.	0.06	<l.d.	<l.d.	0.13	<l.d.	0.05	<l.d.	4.24	41.8
M15-EO-Z4	288	9.46	2.02	322	46.2	756	<l.d.	<l.d.	<l.d.	0.06	<l.d.	<l.d.	0.08	<l.d.	0.05	<l.d.	2.68	39.7
M16-EO-Z4	335	10.0	1.90	300	14.3	644	<l.d.	<l.d.	<l.d.	0.02	<l.d.	<l.d.	0.05	<l.d.	0.03	<l.d.	0.40	32.7

<l.d.: below detection limit

[a] Specific valences for these elements were As(V) and Cr(III) during the entire alkaline treatment according to the PHREEQC modelling

[b] concentration in µg/L

Table AP2.3. Physicochemical parameters and contaminant concentrations of the solutions collected from the titration experiment of the process water.

	mL $Ca(OH)_2$ added to 5 mL	pH	CE (mS/cm)	Eh (mV)	mg/L			mg/L										
					Fluoride	Sulfate	Phosphate	Fe	Al	Zn	As[a]	Cr[a]	U	Cd	Cu	Ni	Co[b]	Sb[b]
M0-PW	0.00	1.49	57.0	655	4354	7240	70,464	171	126	121	59.5	51.9	49.1	19.4	18.7	12.9	1364	739
M1-PW	13.0	2.03	21.9	629	1200	1877	20,180	53.1	39.4	36.1	17.5	15.1	14.3	5.77	5.51	3.83	400	214
M2-PW	60.0	2.46	7.35	651	273	546	5208	14.9	10.7	10.1	4.18	4.58	4.20	1.65	1.68	1.04	110	60.7
M3-PW	105	3.04	4.58	590	169	312	3304	2.18	6.92	6.16	2.58	1.68	2.15	0.92	0.94	0.58	61.9	37.6
M4-PW	118	3.55	3.55	538	110	261	2772	0.65	5.69	5.11	2.30	1.18	1.93	0.92	0.89	0.57	60.7	32.4
M5-PW	125	3.97	3.35	506	92.9	243	2659	0.21	5.55	5.00	2.15	0.62	1.20	0.74	0.70	0.46	49.3	28.7
M6-PW	130	4.56	3.08	415	72.0	226	2516	<l.d.	4.05	4.12	1.95	0.27	0.39	0.58	0.42	0.38	40.0	27.0
M7-PW	145	4.96	3.04	397	55.2	213	2434	<l.d.	2.41	3.63	1.94	0.25	0.21	0.73	0.45	0.49	51.5	26.8
M8-PW	147	5.47	2.63	394	38.5	174	1963	<l.d.	0.15	0.87	1.72	0.11	<l.d.	0.54	0.15	0.45	45.7	23.0
M9-PW	163	5.98	2.26	424	31.5	165	1525	<l.d.	<l.d.	0.07	1.53	0.05	<l.d.	0.26	0.04	0.39	38.3	18.7
M10-PW	245	6.49	1.34	409	22.1	95.5	431	<l.d.	<l.d.	<l.d.	1.00	<l.d.	<l.d.	0.06	<l.d.	0.21	20.2	12.1
M11-PW	285	7.05	1.18	404	13.4	78.1	232	<l.d.	<l.d.	<l.d.	0.93	<l.d.	<l.d.	0.04	<l.d.	0.16	21.0	10.6
M12-PW	315	7.53	1.00	402	8.34	64.8	154	<l.d.	<l.d.	<l.d.	0.77	<l.d.	<l.d.	<l.d.	<l.d.	0.05	1.65	7.95
M13-PW	340	8.07	0.91	371	6.70	59.8	101	<l.d.	<l.d.	<l.d.	0.66	<l.d.	<l.d.	<l.d.	<l.d.	0.02	<l.d.	7.18
M14-PW	410	8.45	0.74	361	4.12	56.3	52.3	<l.d.	<l.d.	<l.d.	0.44	<l.d.	<l.d.	<l.d.	<l.d.	<l.d.	<l.d.	5.70
M15-PW	415	8.99	0.75	359	4.47	66.5	51.0	<l.d.	<l.d.	<l.d.	0.48	<l.d.	<l.d.	<l.d.	<l.d.	<l.d.	<l.d.	5.38
M16-PW	450	9.45	0.65	321	3.52	54.5	17.1	<l.d.	<l.d.	<l.d.	0.29	<l.d.	<l.d.	<l.d.	<l.d.	<l.d.	<l.d.	5.90
M17-PW	475	9.98	0.62	293	4.73	52.4	3.15	<l.d.	<l.d.	<l.d.	0.23	<l.d.	<l.d.	<l.d.	<l.d.	<l.d.	<l.d.	5.79

<l.d.: below detection limit

[a] Specific valences for these elements were As(V) and Cr(III) during the entire alkaline treatment according to the PHREEQC modelling

[b] concentration in µg/L

Table AP2.4. Theoretical reactions, equilibrium constants and saturation indices (SI) for treated edge outflows of zone 3 with respect to some minerals according to PHREEQC simulations using the MINTEQ database. Negative and positive SI values indicate undersaturation and oversaturation, respectively.

Mineral	Reaction	Saturation index																	
		pH / LogKeq	2.1	2.5	3.0	3.5	4.0	4.5	5.0	5.5	6.0	6.5	7.0	7.5	8.0	8.5	9.0	9.5	10
Brushite	$CaHPO_4{\cdot}2H_2O \leftrightarrow Ca^{+2}+H^{+}+PO_4^{-3}+2H_2O$	-19.0	-2.6	-2.3	-1.9	-1.7	-1.3	-0.9	-0.4	0.1	0.5	0.7	0.6	0.2	-0.4	-0.6	-1.3	-1.9	-2.4
Cryolite	$Na_3AlF_6 \leftrightarrow 3Na^{+}+Al^{+3}+6F^{-}$	-33.8	3.2	3.2	3.2	0.3	-1.3	-1.8	-1.5	-1.4	-1.9	-2.4	-3.0	-2.2	-3.6	-8.3	-11	-10	-14
$Fe(OH)_{2.7}Cl_{0.3}$	$Fe(OH)_{2.7}Cl_{0.3}+2.7H^{+} \leftrightarrow Fe^{+3}+2.7H_2O+0.3Cl^{-}$	-3.04	-1.8	-1.8	-1.4	0.8	3.6	4.6	4.1	4.8	5.3	5.6	5.9	6.2	6.4	6.4	6.1	5.6	5.0
Fluorite	$CaF_2 \leftrightarrow Ca^{+2}+2F^{-}$	-10.5	3.2	3.8	4.3	3.5	2.3	1.9	2.1	2.3	2.0	1.8	1.3	2.0	1.7	0.6	0.5	1.4	0.8
Goethite	$FeOOH+3H^{+} \leftrightarrow Fe^{+3}+2H_2O$	0.49	-4.6	-4.5	-3.9	-1.5	1.6	2.7	2.4	3.1	3.8	4.3	4.8	5.2	5.6	5.8	5.6	5.3	4.8
Hydroxylapatite	$Ca_5(PO_4)_3OH+H^{+} \leftrightarrow 5Ca^{+2}+3PO_4^{-3}+H_2O$	-44.3	-17	-15	-11	-9.0	-5.9	-2.6	0.7	4.2	7.4	10	11	12	12	13	14	14	14
Lepidocrocite	$FeOOH+3H^{+} \leftrightarrow Fe^{+3}+2H_2O$	1.37	-5.3	-5.2	-4.6	-2.2	0.8	1.9	1.6	2.4	3.1	3.6	4.1	4.5	4.9	5.1	4.9	4.6	4.1
MgF_2	$MgF_2 \leftrightarrow Mg^{+2}+2F^{-}$	-8.13	0.8	1.3	1.6	0.9	-0.3	-0.7	-0.4	-0.3	-0.6	-0.9	-1.3	-0.6	-0.9	-1.8	-1.9	-1.2	-1.8
Strengite	$FePO_4{\cdot}2H_2O \leftrightarrow Fe^{+3}+PO_4^{-3}+2H_2O$	-26.4	-1.1	-1.4	-1.4	0.3	2.8	3.4	2.5	2.8	2.8	2.7	2.2	1.3	0.1	-0.8	-2.7	-4.7	-6.7

Table AP2.5. Theoretical reactions, equilibrium constants and saturation indices (SI) for treated edge outflows of zone 4 with respect to some minerals according to PHREEQC simulations using the MINTEQ database. Negative and positive SI values indicate undersaturation and oversaturation, respectively.

Mineral	Reaction	Saturation index																	
		pH / LogKeq	2.2	2.5	3.0	3.5	4.1	4.6	5.1	5.5	6.0	6.5	7.0	7.6	8.1	8.6	9.0	9.5	10
Brushite	$CaHPO_4 \cdot 2H_2O \leftrightarrow Ca^{+2} + H^+ + PO_4^{-3} + 2H_2O$	-19.0	-2.6	-2.4	-2.0	-1.6	-1.1	-0.9	-0.5	-0.2	0.3	0.5	0.5	-0.3	-0.2	-0.8	-1.4	-2.0	-2.8
Cryolite	$Na_3AlF_6 \leftrightarrow 3Na^+ + Al^{+3} + 6F^-$	-33.8	4.0	4.2	4.1	4.1	3.3	0.8	-0.2	-0.6	-0.3	-0.5	-1.0	-0.8	-4.1	-5.5	-4.9	-7.0	-14
$Fe(OH)_{2.7}Cl_{0.3}$	$Fe(OH)_{2.7}Cl_{0.3} + 2.7H^+ \leftrightarrow Fe^{+3} + 2.7H_2O + 0.3Cl^-$	-3.04	-2.7	-3.2	-2.6	-1.7	0.6	2.6	4.3	4.5	5.3	5.6	5.9	6.3	6.5	6.5	6.2	5.7	4.9
Fluorite	$CaF_2 \leftrightarrow Ca^{+2} + 2F^-$	-10.5	3.8	4.4	4.7	5.0	4.4	3.5	2.7	2.5	2.8	2.8	2.3	2.5	1.2	1.5	2.3	2.3	0.7
Goethite	$FeOOH + 3H^+ \leftrightarrow Fe^{+3} + 2H_2O$	0.49	-5.7	-6.0	-5.2	-4.2	-1.7	0.6	2.4	2.8	3.8	4.2	4.7	5.2	5.6	5.7	5.6	5.2	4.7
Hydroxylapatite	$Ca_5(PO_4)_3OH + H^+ \leftrightarrow 5Ca^{+2} + 3PO_4^{-3} + H_2O$	-44.3	-17	-15	-12	-8.6	-4.9	-2.7	0.6	3.1	7.1	9.5	11	11	13	13	13	14	13
Lepidocrocite	$FeOOH + 3H^+ \leftrightarrow Fe^{+3} + 2H_2O$	1.37	-6.2	-6.6	-5.8	-4.8	-2.3	0.0	1.8	2.1	3.1	3.6	4.0	4.6	5.0	5.1	5.0	4.6	4.0
MgF_2	$MgF_2 \leftrightarrow Mg^{+2} + 2F^-$	-8.13	1.5	1.9	2.1	2.3	1.7	0.9	0.3	-0.1	0.2	0.2	-0.2	-0.1	-1.2	-1.0	-0.3	-0.4	-1.0
Strengite	$FePO_4 \cdot 2H_2O \leftrightarrow Fe^{+3} + PO_4^{-3} + 2H_2O$	-26.4	-2.3	-3.0	-2.8	-2.3	-0.4	1.1	2.4	2.3	2.5	2.3	2.0	0.5	0.1	-1.3	-2.9	-4.9	-7.5

Table AP2.6. Theoretical reactions, equilibrium constants and saturation indices (SI) for treated process water with respect to some minerals according to PHREEQC simulations using the MINTEQ database. Negative and positive SI values indicate undersaturation and oversaturation, respectively.

Mineral	Reaction	Saturation index																		
		pH / LogKeq	1.5	2.0	2.5	3.0	3.6	4.0	4.6	5.0	5.5	6.0	6.5	7.1	7.5	8.1	8.5	9.0	9.5	10
Brushite	$CaHPO_4 \cdot 2H_2O \leftrightarrow Ca^{+2} + H^+ + PO_4^{-3} + 2H_2O$	-19.0	-2.3	-2.1	-2.1	-1.6	-1.1	-0.7	-0.1	0.3	0.6	1.0	0.5	0.5	0.4	0.0	-0.3	-0.5	-1.1	-1.9
Cryolite	$Na_3AlF_6 \leftrightarrow 3Na^+ + Al^{+3} + 6F^-$	-33.8	5.2	3.3	0.6	0.1	-0.2	-0.2	-0.7	-1.1	-2.7	-3.5	-4.6	-5.2	-6.4	-9.0	-12	-14	-16	-18
Fluorite	$CaF_2 \leftrightarrow Ca^{+2} + 2F^-$	-10.5	3.3	3.2	2.8	3.1	3.0	3.0	2.9	2.7	2.4	2.2	1.6	1.0	0.5	0.1	-0.3	-0.3	-0.6	-0.3
Hydroxylapatite	$Ca_5(PO_4)_3OH + H^+ \leftrightarrow 5Ca^{+2} + 3PO_4^{-3} + H_2O$	-44.3	-18	-16	-14	-10	-6.9	-3.9	0.1	2.9	5.8	8.9	8.8	11	12	13	13	15	15	14
MgF_2	$MgF_2 \leftrightarrow Mg^{+2} + 2F^-$	-8.13	0.9	0.6	-0.2	0.0	-0.1	-0.1	-0.3	-0.4	-0.7	-0.9	-1.2	-1.6	-2.1	-2.4	-3.1	-3.0	-3.4	-3.0
Strengite	$FePO_4 \cdot 2H_2O \leftrightarrow Fe^{+3} + PO_4^{-3} + 2H_2O$	-26.4	-0.1	0.1	0.6	0.4	0.9	1.3	2.0	2.6	3.0	3.1	2.7	2.3	1.7	0.8	0.0	-1.3	-3.1	-5.5

Table AP2.7. Results of aqueous speciation (in percentage) according to PHREEQC for P and As (anions) and some metals such as Cu and Zn (cations) for the entire pH range in the neutralization experiment of edge outflow of zone 3.

		Distribution of species (%)									
	pH	$H_2PO_4^-$	H_3PO_4	HPO_4^{-2}	$MgHPO_4$	$CaPO_4^-$	Other species	$H_2AsO_4^-$	H_3AsO_4	$HAsO_4^{-2}$	AsO_4^{-3}
M0-EO-Z3	2.09	47.1	36.5	0.00	0.00	0.00	16.4	62.3	37.7	0.01	0.00
M1-EO-Z3	2.50	64.6	20.1	0.00	0.00	0.00	15.3	78.4	21.6	0.02	0.00
M2-EO-Z3	3.00	77.5	7.70	0.00	0.00	0.00	14.8	91.3	8.62	0.08	0.00
M3-EO-Z3	3.52	85.0	2.67	0.02	0.01	0.00	12.3	96.8	3.08	0.12	0.00
M4-EO-Z3	4.04	86.9	0.80	0.05	0.05	0.00	12.2	98.6	1.01	0.39	0.00
M5-EO-Z3	4.50	87.6	0.29	0.13	0.18	0.00	11.8	98.6	0.40	1.00	0.00
M6-EO-Z3	5.00	87.1	0.09	0.38	0.43	0.00	12.0	96.8	0.14	3.06	0.00
M7-EO-Z3	5.50	83.3	0.03	1.16	1.21	0.00	14.3	91.0	0.05	8.95	0.00
M8-EO-Z3	6.03	73.4	0.01	3.94	3.14	0.01	19.5	76.0	0.10	23.9	0.00
M9-EO-Z3	6.48	55.2	0.00	11.0	6.83	0.07	26.9	53.9	0.00	46.1	0.00
M10-EO-Z3	6.99	32.5	0.00	36.8	10.3	0.30	20.1	28.5	0.00	71.5	0.00
M11-EO-Z3	7.49	14.8	0.00	50.9	12.0	1.17	21.1	11.9	0.00	88.1	0.00
M12-EO-Z3	8.00	5.12	0.00	55.6	12.9	4.08	22.3	4.30	0.00	95.7	0.00
M13-EO-Z3	8.47	1.76	0.00	56.0	14.2	9.14	18.9	1.50	0.00	98.2	0.30
M14-EO-Z3	9.04	0.38	0.00	45.0	11.2	27.6	15.8	0.43	0.04	98.5	1.03
M15-EO-Z3	9.47							0.16	0.02	97.1	2.72
M16-EO-Z3	9.99							0.04	0.00	91.6	8.36

		Distribution of species (%)									
	pH	Cu^{+2}	$CuSO_4$	$CuCl^+$	CuF^+	Other species	Zn^{+2}	$ZnSO_4$	$Zn(SO_4)_2^{-2}$	$ZnCl^+$	Other species
M0-EO-Z3	2.09	63.8	21.8	7.19	6.96	0.25	53.5	17.7	15.4	9.69	3.71
M1-EO-Z3	2.50	62.1	19.3	4.65	13.8	0.15	60.7	18.3	8.44	7.31	5.25
M2-EO-Z3	3.00	57.6	17.6	3.22	21.5	0.08	62.0	18.4	6.05	5.59	7.96
M3-EO-Z3	3.52	67.4	17.4	2.54	12.6	0.06	70.7	17.7	2.79	4.30	4.51
M4-EO-Z3	4.04	77.2	16.5	2.61	3.69	0.00	76.9	15.9	1.67	4.18	1.35
M5-EO-Z3	4.50	78.6	16.3	2.56	2.50	0.04	77.7	15.7	1.53	4.08	0.99
M6-EO-Z3	5.00	77.6	16.5	2.48	3.28	0.14	77.2	16.0	1.56	3.98	1.26
M7-EO-Z3	5.50						77.4	15.8	1.48	3.90	1.42
M8-EO-Z3	6.03										
M9-EO-Z3	6.48										
M10-EO-Z3	6.99										
M11-EO-Z3	7.49										
M12-EO-Z3	8.00										
M13-EO-Z3	8.47										
M14-EO-Z3	9.04										
M15-EO-Z3	9.47										
M16-EO-Z3	9.99										

Table AP2.8. Results of aqueous speciation (in percentage) according to PHREEQC for P and As (anions) and some metals such as Cu and Zn (cations) for the entire pH range in the neutralization experiment of edge outflow of zone 4.

		Distribution of species (%)									
	pH	$H_2PO_4^-$	H_3PO_4	HPO_4^{-2}	$MgHPO_4$	$CaHPO_4$	Other species	$H_2AsO_4^-$	H_3AsO_4	$HAsO_4^{-2}$	AsO_4^{-3}
M0-EO-Z4	2.20	52.1	29.2	0.00	0.00	0.00	18.7	70.7	29.3	0.00	0.00
M1-EO-Z4	2.52	65.4	18.0	0.00	0.00	0.00	16.6	81.6	18.3	0.10	0.00
M2-EO-Z4	3.03	78.2	6.83	0.01	0.00	0.01	15.0	92.8	7.15	0.05	0.00
M3-EO-Z4	3.51	83.0	2.44	0.04	0.01	0.02	14.5	97.2	2.61	0.19	0.00
M4-EO-Z4	4.06	83.3	0.70	0.15	0.06	0.06	15.7	98.7	0.78	0.52	0.00
M5-EO-Z4	4.58	86.6	0.23	0.46	0.17	0.15	12.4	98.3	0.22	1.48	0.00
M6-EO-Z4	5.05	85.0	0.07	1.41	0.56	0.46	12.5	95.6	0.05	4.35	0.00
M7-EO-Z4	5.46	81.9	0.03	3.06	1.29	1.10	12.6	90.8	0.01	9.19	0.00
M8-EO-Z4	6.04	69.7	0.01	11.0	3.82	4.04	11.4	70.9	0.00	29.1	0.00
M9-EO-Z4	6.53	50.1	0.00	22.0	7.71	8.51	11.7	47.2	0.00	52.8	0.00
M10-EO-Z4	6.95	30.0	0.00	34.2	12.8	10.9	12.1	26.0	0.00	74.0	0.00
M11-EO-Z4	7.55	10.1	0.00	47.9	14.3	14.5	13.2	8.18	0.00	91.8	0.02
M12-EO-Z4	8.05							3.03	0.00	96.8	0.17
M13-EO-Z4	8.55							1.00	0.00	98.5	0.50
M14-EO-Z4	8.97							0.38	0.00	98.4	1.22
M15-EO-Z4	9.46							0.12	0.12	96.3	3.46
M16-EO-Z4	10.0							0.00	0.00	83.0	17.0

		Distribution of species (%)											
	pH	Cu^{+2}	$CuSO_4$	CuF^+	$CuOH^+$	$Cu(OH)_2$	Other species	Zn^{+2}	$Zn(SO_4)_2^{-2}$	$ZnSO_4$	$ZnCl^+$	ZnF^+	Other species
M0-EO-Z4	2.20	54.9	25.8	11.8	0.00	0.00	7.50	39.1	30.0	18.1	8.46	2.74	1.60
M1-EO-Z4	2.52	51.8	22.3	21.0	0.00	0.00	4.90	46.1	20.3	19.6	7.00	6.06	0.94
M2-EO-Z4	3.03	48.5	18.0	30.1	0.00	0.00	3.40	52.2	11.7	19.1	5.86	10.5	0.64
M3-EO-Z4	3.51	45.6	15.2	36.4	0.00	0.00	2.80	54.3	8.27	17.8	5.24	14.0	0.39
M4-EO-Z4	4.06	58.1	15.9	22.9	0.01	0.00	3.09	63.6	5.37	17.1	5.44	8.10	0.39
M5-EO-Z4	4.58	67.1	18.3	11.9	0.03	0.00	2.67	69.1	3.77	18.5	4.47	3.94	0.22
M6-EO-Z4	5.05	72.7	18.7	5.71	0.09	0.00	2.80	72.2	3.14	18.1	4.56	1.82	0.18
M7-EO-Z4	5.46	74.6	18.3	4.08	0.22	0.00	2.80	73.6	2.77	17.6	4.44	1.30	0.29
M8-EO-Z4	6.04	73.4	17.0	6.19	0.97	0.00	2.44						
M9-EO-Z4	6.53	72.4	16.5	6.01	2.75	0.02	2.32						
M10-EO-Z4	6.95	70.2	16.5	3.68	7.20	0.13	2.29						
M11-EO-Z4	7.55	56.2	11.9	3.90	23.8	2.16	2.04						
M12-EO-Z4	8.05	34.8	7.55	0.61	43.2	11.2	2.64						
M13-EO-Z4	8.55	11.4	2.44	0.27	46.0	37.4	2.49						
M14-EO-Z4	8.97	2.81	0.57	0.16	30.5	63.4	2.56						
M15-EO-Z4	9.46	0.37	0.08	0.02	12.1	80.7	6.73						
M16-EO-Z4	10.0	0.02	0.00	0.00	3.08	72.1	24.8						

Table AP2.9. Results of aqueous speciation (in percentage) according to PHREEQC for P and As (anions) and some metals such as Cu and Zn (cations) for the entire pH range in the neutralization experiment of process water.

		Distribution of species (%)								
	pH	$H_2PO_4^-$	H_3PO_4	HPO_4^{-2}	$CaPO_4^-$	Other species	$H_2AsO_4^-$	H_3AsO_4	$HAsO_4^{-2}$	AsO_4^{-3}
M0-PW	1.49	23.4	65.3	0.00	0.00	11.3	36.8	63.2	0.00	0.00
M1-PW	2.03	47.8	41.7	0.00	0.00	10.5	55.8	44.2	0.00	0.00
M2-PW	2.46	67.0	23.7	0.00	0.00	9.30	72.2	27.8	0.01	0.00
M3-PW	3.04	82.1	7.95	0.01	0.00	9.94	90.2	9.77	0.03	0.00
M4-PW	3.55	87.3	2.61	0.03	0.00	10.1	96.7	3.22	0.08	0.00
M5-PW	3.97	88.6	1.01	0.09	0.00	10.3	98.5	1.28	0.22	0.00
M6-PW	4.56	88.9	0.26	0.36	0.00	10.5	98.8	0.35	0.85	0.00
M7-PW	4.96	88.0	0.10	0.88	0.00	11.0	97.8	0.10	2.10	0.00
M8-PW	5.47	85.9	0.04	2.43	0.00	11.6	94.4	0.00	5.60	0.00
M9-PW	5.98	78.4	0.01	7.78	0.01	13.8	83.1	0.03	16.9	0.00
M10-PW	6.49	67.6	0.00	19.0	0.05	13.4	65.3	0.10	34.6	0.00
M11-PW	7.05	40.0	0.00	39.9	0.25	19.9	35.0	0.03	65.0	0.00
M12-PW	7.53	19.8	0.00	57.5	0.89	21.8	15.7	0.00	84.3	0.00
M13-PW	8.07	6.58	0.00	71.5	2.44	19.5	4.83	0.01	95.1	0.06
M14-PW	8.45	3.30	0.00	75.0	5.58	16.1	2.39	0.01	97.5	0.10
M15-PW	8.99	0.90	0.00	70.6	14.7	13.8	0.70	0.00	98.9	0.40
M16-PW	9.45	0.26	0.00	58.1	32.0	9.64	0.23	0.01	98.6	1.16
M17-PW	9.98	0.04	0.00	28.2	64.8	6.96	0.07	0.02	95.9	4.01

		Distribution of species (%)							
	pH	Cu^{+2}	$CuSO_4$	CuF^+	Other species	Zn^{+2}	$ZnSO_4$	$Zn(SO_4)_2^{-2}$	Other species
M0-PW	1.49	57.9	24.5	6.84	10.8	34.0	14.2	37.9	13.9
M1-PW	2.03	75.0	14.6	7.07	3.36	73.8	14.1	4.05	8.03
M2-PW	2.46	84.3	9.43	5.02	1.28	86.1	9.50	0.48	3.87
M3-PW	3.04	84.2	7.02	7.94	0.88	88.4	7.23	0.20	4.16
M4-PW	3.55	85.3	6.40	7.61	0.74	89.3	6.59	0.15	3.94
M5-PW	3.97	85.9	6.00	7.37	0.72	89.9	6.18	0.13	3.80
M6-PW	4.56	86.7	5.91	6.57	0.78	90.4	6.03	0.12	3.48
M7-PW	4.96	88.2	5.65	5.37	0.84	91.1	5.73	0.10	3.04
M8-PW	5.47	89.4	5.15	4.49	1.00	92.1	5.18	0.07	2.62
M9-PW	5.98	89.2	5.37	3.74	1.70	92.1	5.45	0.08	2.37
M10-PW	6.49								
M11-PW	7.05								
M12-PW	7.53								
M13-PW	8.07								
M14-PW	8.45								
M15-PW	8.99								
M16-PW	9.45								
M17-PW	9.98								

Table AP2.10. Percentages of the released elements with respect to the total composition for each leaching test.

		As	Ba	Cd	Cr	Cu	Mo	Ni	Pb	Sb	Se	Zn	V	Be	Tl	SO_4^-
Total solids (mg/kg)	EO-Z3	838	6.27	133	188	267	0.17	112	13.5	10.1	0.49	1076	305	2.65	0.32	19,452
	EO-Z4	330	9.63	105	369	744	0.21	112	12.2	15.2	0.20	2136	272	3.51	0.20	28,242
	PW	204	3.43	145	378	138	0.30	82.5	9.89	3.52	0.17	799	311	2.98	0.23	6410
EN-12457-2 leaching test (%)	EO-Z3	0.7	0.0	0.0	0.2	0.1	57	0.2	0.0	1.1	16	0.0	0.8	0.0	8.4	46
	EO-Z4	0.3	0.0	0.0	0.2	0.1	82	0.3	0.0	1.2	30	0.0	0.6	0.0	13	59
	PW	6.5	0.0	0.0	0.0	0.0	30	0.2	0.0	1.1	0.0	0.0	1.5	0.0	9.0	19
EN-12457-2 leaching test (%)	EO-Z3	14	0.4	0.3	0.3	0.1	4.0	10	0.0	2.9	29	0.0	1.5	0.0	27	69
	EO-Z4	12	0.0	0.7	0.1	0.2	3.6	15	0.0	2.2	42	0.0	0.8	0.0	48	85
	PW	38	2.0	6.5	0.0	0.6	4.0	94	0.0	10	21	0.3	12	0.0	74	16

AP3. CHAPTER 4 SUPPLEMENTARY INFORMATION

Table AP3.1. Bulk chemical and mineralogical composition of the biomass ash, fly ash and MgO.

Biomass ash				Fly ash				MgO			
Compounds (%)		Minerals (%)*		Compounds (%)		Minerals (%)		Compounds (%)		Minerals (%)*	
SiO_2	67.3	Quartz	100	SiO_2	41.3	Mullite	20.8	MgO	66.3	Periclase	70
Al_2O_3	11.3			Al_2O_3	27.5	Quartz	4.50	CaO	9.80	Dolomite	17
CaO	8.45			CO_2	16.4	Portlandite	4.10	SiO_2	3.09	Magnesite	<5
K_2O	4.83			CaO	5.30	Anhydrite	1.30	Fe_2O_3	2.45	Calcite	<5
Fe_2O_3	4.69			Fe_2O_3	3.28	Chalco-aluminosilicate glass phase	66.4	Al_2O_3	0.38	Lime	<5
MgO	1.47			TiO_2	1.41			SO_3	4.14	Quartz	<5
P_2O_5	0.93			P_2O_5	1.31						
Na_2O	0.67			MgO	1.31						
TiO_2	0.20			K_2O	0.82						
MnO	0.10			SO_3	0.54						
SO_2	0.04			Na_2O	0.33						
				MnO	0.04						

*Semi-quantitative mineralogical analysis of the crystalline phases

Table AP3.2. Ideal reactions, equilibrium constants and saturation indices (SI) for supersaturated minerals according to PHREEQC simulations from the database of MINTEQ model, for the solutions derived from the limestone-DAS treatment during the maximum effectiveness period. Negative and positive SI indicate undersaturation and oversaturation, respectively.

Mineral	Reaction	Saturation index									
		pH / LogKeq	4.24	4.81	4.63	4.64	4.38	4.53	4.31	4.06	3.62
Strengite	$FePO_4 \cdot 2H_2O \leftrightarrow Fe^{+3} + PO_4^{-3} + 2H_2O$	-26.4	1.5	1.8	0.8	1.1	1.0	0.6	0.9	0.4	0.1
Lepidocrocite	$FeOOH + 3H^+ \leftrightarrow Fe^{+3} + 2H_2O$	1.37	-0.3	0.5	-0.8	-0.6	-0.9	-1.2	-1.1	-1.8	-2.6
Goethite	$FeOOH + 3H^+ \leftrightarrow Fe^{+3} + 2H_2O$	0.49	0.6	1.3	0.1	0.4	0.0	-0.2	-0.3	-0.9	-1.7
$Fe(OH)_{2.7}Cl_{0.3}$	$Fe(OH)_{2.7}Cl_{0.3} + 2.7H^+ \leftrightarrow Fe^{+3} + 2.7H_2O + 0.3Cl^-$	-3.04	2.6	3.2	2.1	2.2	2.0	1.7	1.8	1.2	0.5
Hydroxylapatite	$Ca_5(PO_4)_3OH + H^+ \leftrightarrow 5Ca^{+2} + 3PO_4^{-3} + H_2O$	-44.3	-3.9	1.0	0.2	0.5	-1.3	-0.2	-1.8	-3.6	-6.7
Brushite	$CaHPO_4 \cdot 2H_2O \leftrightarrow Ca^{+2} + H^+ + PO_4^{-3} + 2H_2O$	-19.0	-1.0	-0.2	-0.3	-0.3	-0.5	-0.3	-0.5	-0.8	-1.2
Fluorite	$CaF_2 \leftrightarrow Ca^{+2} + 2F^-$	-10.5	3.1	3.3	2.8	2.4	2.2	2.1	2.0	2.0	2.3
Gypsum	$CaSO_4 \cdot 2H_2O \leftrightarrow Ca^{+2} + SO_4^{-2}$	-4.61	-0.1	0.1	0.2	0.2	0.2	0.2	0.2	0.2	0.1
Cryolite	$Na_3AlF_6 \leftrightarrow 3Na^+ + Al^{+3} + 6F^-$	-33.8	1.3	2.1	1.6	1.2	0.9	0.9	0.8	0.7	1.3
Diaspore	$ALOOH + 3H^+ \leftrightarrow Al^{+3} + 2H_2O$	6.87	-9.1	-7.4	-6.9	-6.0	-6.4	-6.0	-6.4	-7.2	-9.1

Table AP3.3. Ideal reactions, equilibrium constants and saturation indices (SI) for supersaturated minerals according to PHREEQC simulations from the database of MINTEQ model, for the solutions derived from the barium carbonate-DAS treatment during the maximum effectiveness period. Negative and positive SI indicate undersaturation and oversaturation, respectively.

Mineral	Reaction	Saturation index										
		pH / LogKeq	6.22	5.76	5.72	5.75	5.84	6.04	6.00	6.15	5.92	5.56	4.88
Strengite	$FePO_4 \cdot 2H_2O \leftrightarrow Fe^{+3} + PO_4^{-3} + 2H_2O$	-26.4	2.2	0.2	0.2	1.6	0.8	1.3	1.1	1.2	-0.4	-0.7	-2.3
Lepidocrocite	$FeOOH + 3H^+ \leftrightarrow Fe^{+3} + 2H_2O$	1.37	2.7	0.0	-0.2	1.2	0.5	1.3	1.0	1.3	-0.6	-1.4	-3.7
Goethite	$FeOOH + 3H^+ \leftrightarrow Fe^{+3} + 2H_2O$	0.49	3.6	0.8	0.7	2.2	1.5	2.1	1.8	2.2	0.3	-0.4	-2.8
$Fe(OH)_{2.7}Cl_{0.3}$	$Fe(OH)_{2.7}Cl_{0.3} + 2.7H^+ \leftrightarrow Fe^{+3} + 2.7H_2O + 0.3Cl^-$	-3.04	5.0	2.4	2.3	3.7	2.9	3.7	3.4	3.7	1.9	1.2	-0.9
Hydroxylapatite	$Ca_5(PO_4)_3OH + H^+ \leftrightarrow 5Ca^{+2} + 3PO_4^{-3} + H_2O$	-44.3	6.4	3.0	4.5	4.6	5.2	6.4	6.2	7.0	5.7	3.7	-0.8
Brushite	$CaHPO_4 \cdot 2H_2O \leftrightarrow Ca^{+2} + H^+ + PO_4^{-3} + 2H_2O$	-19.0	0.1	-0.3	0.1	0.1	0.1	0.3	0.3	0.4	0.2	0.0	-0.6
Fluorite	$CaF_2 \leftrightarrow Ca^{+2} + 2F^-$	-10.5	2.1	3.3	2.3	2.0	1.9	1.9	1.9	1.9	2.0	2.2	2.2
Gypsum	$CaSO_4 \cdot 2H_2O \leftrightarrow Ca^{+2} + SO_4^{-2}$	-4.61	-1.1	-0.9	-0.7	-0.8	-0.7	-0.7	-0.7	-0.7	-0.7	-0.7	-0.6
Cryolite	$Na_3AlF_6 \leftrightarrow 3Na^+ + Al^{+3} + 6F^-$	-33.8	-1.0	1.2	0.2	-0.1	-0.2	0.0	-0.1	-0.1	0.1	0.2	0.2
Diaspore	$ALOOH + 3H^+ \leftrightarrow Al^{+3} + 2H_2O$	6.87	-3.8	-7.8	-5.6	-4.9	-4.3	-3.9	-4.0	-3.6	-4.5	-5.7	-7.8
Barite	$BaSO_4 \leftrightarrow Ba^{+2} + SO_4^{-2}$	-9.98	0.9	2.9	1.1	0.9	1.0	1.0	1.0	1.2	1.2	0.9	0.8

Table AP3.4. Ideal reactions, equilibrium constants and saturation indices (SI) for supersaturated minerals according to PHREEQC simulations from the database of MINTEQ model, for the solutions derived from the biomass ash-DAS treatment during the maximum effectiveness period. Negative and positive SI indicate undersaturation and oversaturation, respectively.

Mineral	Reaction		Saturation index		
		pH	5.70	4.87	4.18
		LogKeq			
Strengite	$FePO_4 \cdot 2H_2O \leftrightarrow Fe^{+3} + PO_4^{-3} + 2H_2O$	-26.4	2.2	0.2	0.2
Lepidocrocite	$FeOOH + 3H^+ \leftrightarrow Fe^{+3} + 2H_2O$	1.37	2.7	0.0	-0.2
Goethite	$FeOOH + 3H^+ \leftrightarrow Fe^{+3} + 2H_2O$	0.49	3.6	0.8	0.7
$Fe(OH)_{2.7}Cl_{0.3}$	$Fe(OH)_{2.7}Cl_{0.3} + 2.7H^+ \leftrightarrow Fe^{+3} + 2.7H_2O + 0.3Cl^-$	-3.04	5.0	2.4	2.3
Hydroxylapatite	$Ca_5(PO_4)_3OH + H^+ \leftrightarrow 5Ca^{+2} + 3PO_4^{-3} + H_2O$	-44.3	6.4	3.0	4.5
Brushite	$CaHPO_4 \cdot 2H_2O \leftrightarrow Ca^{+2} + H^+ + PO_4^{-3} + 2H_2O$	-19.0	0.1	-0.3	0.1
Fluorite	$CaF_2 \leftrightarrow Ca^{+2} + 2F^-$	-10.5	2.1	3.3	2.3
Gypsum	$CaSO_4 \cdot 2H_2O \leftrightarrow Ca^{+2} + SO_4^{-2}$	-4.61	-1.1	-0.9	-0.7
Cryolite	$Na_3AlF_6 \leftrightarrow 3Na^+ + Al^{+3} + 6F^-$	-33.8	-1.0	1.2	0.2
Diaspore	$ALOOH + 3H^+ \leftrightarrow Al^{+3} + 2H_2O$	6.87	-3.8	-7.8	-5.6

Table AP3.5. Ideal reactions, equilibrium constants and saturation indices (SI) for supersaturated minerals according to PHREEQC simulations from the database of MINTEQ model, for the solutions derived from the fly ash-DAS treatment during the maximum effectiveness period. Negative and positive SI indicate undersaturation and oversaturation, respectively.

Mineral	Reaction	Saturation index			
		pH / LogKeq	7.01	6.34	5.37
Strengite	$FePO_4 \cdot 2H_2O \leftrightarrow Fe^{+3} + PO_4^{-3} + 2H_2O$	-26.4	1.3	1.9	0.7
Lepidocrocite	$FeOOH + 3H^+ \leftrightarrow Fe^{+3} + 2H_2O$	1.37	4.0	2.7	0.0
Goethite	$FeOOH + 3H^+ \leftrightarrow Fe^{+3} + 2H_2O$	0.49	4.9	3.5	0.9
$Fe(OH)_{2.7}Cl_{0.3}$	$Fe(OH)_{2.7}Cl_{0.3} + 2.7H^+ \leftrightarrow Fe^{+3} + 2.7H_2O + 0.3Cl^-$	-3.04	6.0	4.9	2.6
Hydroxylapatite	$Ca_5(PO_4)_3OH + H^+ \leftrightarrow 5Ca^{+2} + 3PO_4^{-3} + H_2O$	-44.3	10	9.6	4.7
Brushite	$CaHPO_4 \cdot 2H_2O \leftrightarrow Ca^{+2} + H^+ + PO_4^{-3} + 2H_2O$	-19.0	-0.1	0.6	0.2
Fluorite	$CaF_2 \leftrightarrow Ca^{+2} + 2F^-$	-10.5	2.8	2.5	2.6
Gypsum	$CaSO_4 \cdot 2H_2O \leftrightarrow Ca^{+2} + SO_4^{-2}$	-4.61	-0.2	-0.1	0.1
Cryolite	$Na_3AlF_6 \leftrightarrow 3Na^+ + Al^{+3} + 6F^-$	-33.8	-0.4	0.0	1.1
Diaspore	$ALOOH + 3H^+ \leftrightarrow Al^{+3} + 2H_2O$	6.87	-1.1	-2.4	-4.7

Table AP3.6. Ideal reactions, equilibrium constants and saturation indices (SI) for supersaturated minerals according to PHREEQC simulations from the database of MINTEQ model, for the solutions derived from the MgO-DAS treatment during the maximum effectiveness period. Negative and positive SI indicate undersaturation and oversaturation, respectively.

Mineral	Reaction		Saturation index														
		pH / LogKeq	8.76	8.70	8.49	8.39	8.19	7.69	7.84	7.41	7.28	7.12	7.06	7.00	6.86	6.72	6.73
Strengite	$FePO_4 \cdot 2H_2O \leftrightarrow Fe^{+3} + PO_4^{-3} + 2H_2O$	-26.4	-2.1	-1.9	-1.3	-0.9	-1.9	0.9	0.2	1.5	1.6	0.8	0.4	1.8	1.5	0.8	1.6
Lepidocrocite	$FeOOH + 3H^+ \leftrightarrow Fe^{+3} + 2H_2O$	1.37	4.9	4.8	4.8	4.9	3.4	4.8	4.4	4.7	4.3	3.0	2.5	3.6	3.1	2.0	2.8
Goethite	$FeOOH + 3H^+ \leftrightarrow Fe^{+3} + 2H_2O$	0.49	5.7	5.8	5.8	5.8	4.3	5.7	5.3	5.7	5.2	3.9	3.3	4.4	3.9	2.9	3.7
$Fe(OH)_{2.7}Cl_{0.3}$	$Fe(OH)_{2.7}Cl_{0.3} + 2.7H^+ \leftrightarrow Fe^{+3} + 2.7H_2O + 0.3Cl^-$	-3.04	6.4	6.4	6.5	6.6	5.2	6.7	6.3	6.7	6.3	5.1	4.5	5.7	5.2	4.2	5.0
Hydroxylapatite	$Ca_5(PO_4)_3OH + H^+ \leftrightarrow 5Ca^{+2} + 3PO_4^{-3} + H_2O$	-44.3	9.9	9.2	8.5	8.5	7.7	8.5	8.5	7.8	8.5	8.9	9.1	9.1	8.7	8.1	8.2
Brushite	$CaHPO_4 \cdot 2H_2O \leftrightarrow Ca^{+2} + H^+ + PO_4^{-3} + 2H_2O$	-19.0	-1.8	-1.9	-1.8	-1.6	-1.6	-0.9	-1.0	-0.7	-0.4	-0.1	0.0	0.1	0.2	0.1	0.2
Fluorite	$CaF_2 \leftrightarrow Ca^{+2} + 2F^-$	-10.5	-0.4	-0.6	-1.1	-1.1	-1.2	-0.1	-0.1	-0.5	0.5	1.1	1.5	1.6	1.7	1.6	1.7
Gypsum	$CaSO_4 \cdot 2H_2O \leftrightarrow Ca^{+2} + SO_4^{-2}$	-4.61	-1.1	-1.3	-1.4	-1.4	-1.4	-1.1	-1.2	-1.1	-1.0	-0.9	-0.8	-0.8	-0.8	-0.8	-0.8
Farringtonite	$Mg_3(PO_4)_2 \leftrightarrow 3Mg^{+2} + 2PO_4^{-3}$	-23.3	0.3	0.4	0.3	0.5	0.2	0.2	0.4	-0.2	0.0	0.1	0.0	0.0	-0.3	-0.6	-0.5
Cryolite	$Na_3AlF_6 \leftrightarrow 3Na^+ + Al^{+3} + 6F^-$	-33.8	-8.6	-8.5	-9.6	-9.1	-7.6	-3.2	-3.6	-3.3	-0.7	-0.1	0.7	1.0	0.9	0.7	0.8
Diaspore	$ALOOH + 3H^+ \leftrightarrow Al^{+3} + 2H_2O$	6.87	1.1	1.4	0.9	0.9	1.7	2.3	2.1	2.8	2.1	0.9	0.4	0.4	-0.4	-0.7	-0.8

Table AP3.7. Ideal reactions, equilibrium constants and saturation indices (SI) for supersaturated minerals according to PHREEQC simulations from the database of MINTEQ model, for the solutions derived from the $Mg(OH)_2$-DAS treatment during the maximum effectiveness period. Negative and positive SI indicate undersaturation and oversaturation, respectively.

Mineral	Reaction	Saturation index										
		pH / LogKeq	8.56	8.17	7.88	7.19	7.31	7.21	7.14	7.01	6.84	6.68	6.57
Strengite	$FePO_4 \cdot 2H_2O \leftrightarrow Fe^{+3} + PO_4^{-3} + 2H_2O$	-26.4	-1.2	-0.3	0.1	1.0	0.9	1.1	1.2	1.3	1.3	1.2	0.9
Lepidocrocite	$FeOOH + 3H^+ \leftrightarrow Fe^{+3} + 2H_2O$	1.37	4.4	4.3	4.1	3.5	3.6	3.5	3.4	3.2	2.8	2.4	1.8
Goethite	$FeOOH + 3H^+ \leftrightarrow Fe^{+3} + 2H_2O$	0.49	5.0	4.9	4.7	4.1	4.2	4.3	4.1	4.0	3.6	3.1	2.6
$Fe(OH)_{2.7}Cl_{0.3}$	$Fe(OH)_{2.7}Cl_{0.3} + 2.7H^+ \leftrightarrow Fe^{+3} + 2.7H_2O + 0.3Cl^-$	-3.04	5.9	6.0	5.9	5.5	5.6	5.5	5.5	5.3	5.0	4.6	4.1
Hydroxylapatite	$Ca_5(PO_4)_3OH + H^+ \leftrightarrow 5Ca^{+2} + 3PO_4^{-3} + H_2O$	-44.3	11	9.9	8.7	6.9	8.1	8.3	8.5	8.4	8.1	8.0	7.8
Brushite	$CaHPO_4 \cdot 2H_2O \leftrightarrow Ca^{+2} + H^+ + PO_4^{-3} + 2H_2O$	-19.0	-0.8	-0.7	-0.7	-0.5	-0.3	-0.2	-0.1	0.0	0.1	0.2	0.2
Fluorite	$CaF_2 \leftrightarrow Ca^{+2} + 2F^-$	-10.5	0.2	0.0	0.0	0.1	0.3	0.2	0.5	0.7	0.9	1.1	1.3
Gypsum	$CaSO_4 \cdot 2H_2O \leftrightarrow Ca^{+2} + SO_4^{-2}$	-4.61	-1.5	-1.4	-1.4	-1.2	-1.1	-1.1	-0.9	-0.9	-0.8	-0.7	-0.7
Farringtonite	$Mg_3(PO_4)_2 \leftrightarrow 3Mg^{+2} + 2PO_4^{-3}$	-23.3	1.4	1.1	0.9	0.0	0.4	0.3	0.2	0.0	-0.3	-0.5	-0.7
Cryolite	$Na_3AlF_6 \leftrightarrow 3Na^+ + Al^{+3} + 6F^-$	-33.8	-6.3	-4.8	-3.1	-1.4	-1.4	-1.7	-1.3	-1.1	-0.9	-0.7	-0.6
Diaspore	$ALOOH + 3H^+ \leftrightarrow Al^{+3} + 2H_2O$	6.87	1.0	1.4	1.7	0.9	1.2	1.3	0.7	0.2	-0.6	-1.2	-1.7

Table AP3.8. Ideal reactions, equilibrium constants and saturation indices (SI) for supersaturated minerals according to PHREEQC simulations from the database of MINTEQ model, for the solutions derived from the $Ca(OH)_2$-DAS treatment during the maximum effectiveness period. Negative and positive SI indicate undersaturation and oversaturation, respectively.

Mineral	Reaction		Saturation index					
		pH / LogKeq	12.4	12.7	12.4	12.4	12.5	12.2
Strengite	$FePO_4 \cdot 2H_2O \leftrightarrow Fe^{+3} + PO_4^{-3} + 2H_2O$	-26.4	-18	-18	-18	-17	-18	-16
Lepidocrocite	$FeOOH + 3H^+ \leftrightarrow Fe^{+3} + 2H_2O$	1.37	0.9	0.7	0.9	1.0	0.8	2.4
Goethite	$FeOOH + 3H^+ \leftrightarrow Fe^{+3} + 2H_2O$	0.49	1.6	1.3	1.5	1.6	1.4	3.2
$Fe(OH)_{2.7}Cl_{0.3}$	$Fe(OH)_{2.7}Cl_{0.3} + 2.7H^+ \leftrightarrow Fe^{+3} + 2.7H_2O + 0.3Cl^-$	-3.04	1.3	1.1	1.4	1.5	1.3	3.0
Hydroxylapatite	$Ca_5(PO_4)_3OH + H^+ \leftrightarrow 5Ca^{+2} + 3PO_4^{-3} + H_2O$	-44.3	20	20	20	19	19	18
Brushite	$CaHPO_4 \cdot 2H_2O \leftrightarrow Ca^{+2} + H^+ + PO_4^{-3} + 2H_2O$	-19.0	-4.4	-4.6	-4.3	-4.4	-4.5	-4.5
Fluorite	$CaF_2 \leftrightarrow Ca^{+2} + 2F^-$	-10.5	3.0	2.6	2.1	0.8	1.5	1.3
Gypsum	$CaSO_4 \cdot 2H_2O \leftrightarrow Ca^{+2} + SO_4^{-2}$	-4.61	0.2	0.3	0.4	0.4	0.4	0.4
Farringtonite	$Mg_3(PO_4)_2 \leftrightarrow 3Mg^{+2} + 2PO_4^{-3}$	-23.3	-19	-20	-20	-24	-22	-22
Cryolite	$Na_3AlF_6 \leftrightarrow 3Na^+ + Al^{+3} + 6F^-$	-33.8	-2.9	-3.1	-2.9	-2.9	-3.0	-2.9
Diaspore	$ALOOH + 3H^+ \leftrightarrow Al^{+3} + 2H_2O$	6.87	1.0	1.4	1.7	0.9	1.2	1.3

Table AP3.9. Phases identified during the mineralogical study by XRD of the precipitates collected from the different reactive columns.

	Minerals							
	Newly-formed phases				Phases inherited from the original material			
Treatment system	**Gypsum**	**Barite**	**Zhangpeishanite**	**Fluorite**	**Calcite**	**Whiterite**	**Quartz**	**Mullite**
Limestone-DAS								
0-5 cm	X	-	-	-	X	-	-	-
5-10 cm	X	-	-	-	X	-	-	-
10-15 cm	X	-	-	-	X	-	-	-
15-20 cm	X	-	-	-	X	-	-	-
Barium carbonate-DAS								
0-5 cm	-	X	X	-	-	X	-	-
5-10 cm	-	X	X	-	-	X	-	-
10-15 cm	-	X	X	-	-	X	-	-
15-20 cm	-	X	X	-	-	X	-	-
Biomass ash-DAS								
0-5 cm	-	-	-	-	-	-	X	-
5-10 cm	-	-	-	-	-	-	X	-
10-15 cm	-	-	-	-	-	-	X	-
15-20 cm	-	-	-	-	-	-	X	-
Fly ash-DAS								
0-5 cm	X	-	-	-	-	-	X	X
5-10 cm	X	-	-	-	-	-	X	X
10-15 cm	X	-	-	-	-	-	X	X
15-20 cm	X	-	-	-	-	-	X	X

	Minerals							
	Newly-formed phases				Phases inherited from the original material			
Treatment system	Gypsum	Barite	Zhangpeishanite	Fluorite	Calcite	Whiterite	Quartz	Mullite
MgO-DAS								
0-5 cm	X	-	-	X	-	-	X	-
5-10 cm	X	-	-	X	-	-	X	-
10-15 cm	X	-	-	X	-	-	X	-
15-20 cm	X	-	-	X	-	-	X	-
$Mg(OH)_2$-DAS								
0-5 cm	X	-	-	X	-	-	-	-
5-10 cm	X	-	-	X	-	-	-	-
10-15 cm	X	-	-	X	-	-	-	-
15-20 cm	-	-	-	X	-	-	-	-
$Ca(OH)_2$-DAS								
0-5 cm	X	-	-	X	-	-	-	-
5-10 cm	X	-	-	X	-	-	-	-
10-15 cm	X	-	-	X	-	-	-	-
15-20 cm	X	-	-	X	-	-	-	-

Table AP3.10. Chemical composition of the initial acid leachate and the solutions sampled at the output of the treatment systems (average values for the maximum effectiveness period), and comparison with the limit values established for metal and toxic element concentration in drinking water and the Criterion Continuous Concentration and Criterion Maximum Concentration limits established in the aquatic life criteria by the USEPA. Data in mg/L.

	Al	Cu	Fe	Mn	Zn	As	Cd	Cr	Ni	Pb	Se
WHO	0.2	2	0.3	0.4	3	0.01	0.003	0.05	0.07	0.01	0.04
CCC[1]	0.087*	1.3*	1	n.r.l	0.12	0.15	0.001	0.570	0.052	0.003	0.005*
CMC[1]	0.75*	n.r.l	n.r.l	n.r.l	0.12	0.34	0.002	0.074	0.470	0.082	n.r.l
CCC[2]	n.r.l	0.003	n.r.l	n.r.l	0.081	0.036	0.008	n.r.l	0.008	0.006	0.071
CMC[2]	n.r.l	0.005	n.r.l	n.r.l	0.090	0.069	0.033	n.r.l	0.074	0.14	0.29
Edge outflow	3.359	5.801	103.8	13.39	16.25	3.284	0.714	2.922	0.979	0.650	0.054
Treatment systems:											
Limestone-DAS	0.473	4.383	0.408	11.20	8.450	2.854	0.608	0.469	0.879	<l.d.	0.035
Barium carbonate-DAS	<l.d.	0.223	0.025	7.769	0.608	2.543	0.336	0.045	0.849	0.029	0.025
Biomass ash-DAS	1.674	2.403	0.359	10.64	5.644	1.873	0.404	0.352	5.644	<l.d.	0.018
Fly ash-DAS	0.080	0.735	<l.d.	4.467	0.749	1.560	0.188	0.103	0.481	<l.d.	0.098
MgO-DAS	0.066	0.651	0.025	0.986	0.061	1.585	0.051	0.017	0.292	<l.d.	0.033
$Mg(OH)_2$-DAS	<l.d.	0.904	<l.d.	1.035	0.082	2.556	<l.d.	<l.d.	0.367	<l.d.	<l.d.
$Ca(OH)_2$-DAS	<l.d.	0.717	<l.d.	0.013	0.088	<l.d.	<l.d.	<l.d.	<l.d.	<l.d.	<l.d.

[1]Freshwater
[2]Saltwater
*Macías et al., 2017a
n.r.l: no referenced limit
<l.d.: below detection limit

AP4. CHAPTER 5 SUPPLEMENTARY INFORMATION

Figure AP4.1. XRD spectra of the solid precipitates collected inside the decantation vessel of the $Ca(OH)_2$-DAS system; unwashed and washed with water.

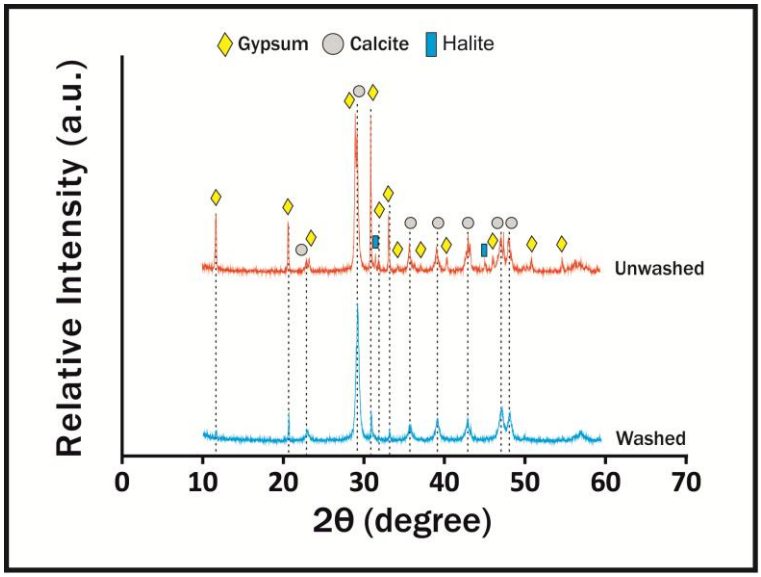

Table AP4.1. Mineralogical composition and bulk chemistry of MgO and $Ca(OH)_2$.

MgO				$Ca(OH)_2$			
Compounds (%)		Minerals (%)*		Compounds (%)		Minerals (%)*	
MgO	66	Periclase	71	$Ca(OH)_2$	> 95	Portlandite	100
CaO	9.8	Dolomite	15				
SiO_2	3.1	Lime	10				
Fe_2O_3	2.5	Magnesite	<5				
Al_2O_3	0.4	Quartz	<5				
SO_3	4.1						

***Semi-quantitative mineralogical analysis of the crystalline phases**

Table AP4.2. Hydrochemical characteristics of the contaminated acidic leachates from phosphogypsum stack.

Phosphogypsum leachates		
	pH	2.2
	CE (mS/cm)	39
	Eh (mV)	488
	Net acidity (mg/L as $CaCO_3$ equivalents)	6240
Anions (mg/L)	PO_4	2513
	SO_4	5321
	F	1328
	Cl	11,952
	Br	74
Cations (mg/L)	NH_4	160
	Fe	102
	Zn	16
	Cu	5.5
	As	3.0
	Al	2.8
	Cr	2.8
	U	1.8
	Cd	0.7
	Ni	0.8
	Co	0.4
	Sb	0.3

Table AP4.3. Ideal reactions, equilibrium constants and saturation indices (SI) for supersaturated minerals according to PHREEQC simulations from the database of MINTEQ model, for the solutions derived from the MgO-DAS treatment during the maximum effectiveness period. Negative and positive SI indicate undersaturation and oversaturation, respectively.

Mineral	Reaction	Saturation index														
		pH	9.65	9.60	9.50	9.55	9.64	9.63	9.56	9.48	9.50	9.47	9.54	9.29	9.22	7.65	7.48
		LogKeq															
Hydroxylapatite	$Ca_5(PO_4)_3OH+H^+ \leftrightarrow 5Ca^{+2}+3PO_4^{-3}+H_2O$	-44.3	8.5	5.2	4.8	4.7	4.6	4.4	4.2	3.7	4.0	8.8	3.9	8.0	10	10	9.2
Fluorapatite	$Ca_5(PO_4)_3F+3H^+ \leftrightarrow 5Ca^{+2}+3HPO_4^{-2}+F^-$	-25.0	10	6.6	6.3	6.2	5.9	5.8	5.6	5.2	5.5	10	5.3	12	15	15	16
Cattiite	$Mg_3(PO_4)_2 \cdot 22H_2O \leftrightarrow 3Mg^{+2}+2PO_4^{-3}+22H_2O$	-23.1	-5.3	-3.8	-3.9	-3.8	-3.6	-3.6	-3.8	-3.9	-3.9	-0.6	-3.8	0.3	0.2	0.1	0.5
Strengite	$FePO_4 \cdot 2H_2O \leftrightarrow Fe^{+3}+PO_4^{-3}+2H_2O$	-26.4	-8.1	-7.9	-7.6	-7.7	-8.0	-8.0	-7.8	-7.5	-7.6	-5.8	-7.7	-4.7	-4.5	0.1	0.6
Goethite	$FeOOH+3H^+ \leftrightarrow Fe^{+3}+2H_2O$	0.49	4.3	4.3	4.4	4.3	4.3	4.3	4.4	4.4	4.4	4.4	4.4	4.5	4.6	4.4	4.3
Lepidocrocite	$FeOOH+3H^+ \leftrightarrow Fe^{+3}+2H_2O$	1.37	3.7	3.7	3.8	3.8	3.7	3.7	3.7	3.8	3.8	3.8	3.8	4.0	4.1	4.0	3.8
$Fe(OH)_{2.7}Cl_{0.3}$	$Fe(OH)_{2.7}Cl_{0.3}+2.7H^+ \leftrightarrow Fe^{+3}+2.7H_2O+0.3Cl^-$	-3.04	4.9	5.1	5.2	5.1	5.0	5.0	5.1	5.2	5.2	5.2	5.1	5.5	5.5	5.9	5.8
Spertiniite	$Cu(OH)_2+2H^+ \leftrightarrow Cu^{+2}+2H_2O$	8.67	0.4	0.3	0.3	1.5	2.6	2.6	2.6	2.7	2.7	2.7	2.7	2.4	2.4	0.7	0.5
Diaspore	$ALOOH+3H^+ \leftrightarrow Al^{+3}+2H_2O$	6.87	-0.1	0.0	0.1	0.0	-0.1	0.0	0.0	0.1	0.0	0.1	0.0	0.4	0.4	1.7	1.3
Brucite	$Mg(OH)_2+2H^+ \leftrightarrow Mg^{+2}+2H_2O$	16.8	-0.5	-0.2	-0.4	-0.3	-0.1	-0.2	-0.2	-0.4	-0.3	-0.4	-0.3	-4.6	-0.9	-1.1	-4.3
Fluorite	$CaF_2 \leftrightarrow Ca^{+2}+2F^-$	-10.5	-5.4	-6.4	-6.4	-6.4	-6.6	-6.6	-6.6	-6.6	-6.6	-6.6	-6.6	-0.4	-0.2	0.6	0.7
Gypsum	$CaSO_4 \cdot 2H_2O \leftrightarrow Ca^{+2}+SO_4^{-2}$	-4.61	-0.5	-0.8	-0.8	-0.9	-1.0	-1.0	-1.0	-1.0	-1.0	-1.0	-1.1	-0.9	-0.9	-0.8	-0.8
Calcite	$CaCO_3 \leftrightarrow Ca^{+2}+CO_3^{-2}$	-8.48	-0.3	-0.6	-0.8	-0.8	-0.6	-0.7	-0.7	-0.8	-0.7	-0.7	-0.7	-0.8	-0.6	-0.5	-0.8

Table AP4.4. Ideal reactions, equilibrium constants and saturation indices (SI) for supersaturated minerals according to PHREEQC simulations from the database of MINTEQ model, for the solutions derived from the $Ca(OH)_2$-DAS treatment during the maximum effectiveness period. Negative and positive SI indicate undersaturation and oversaturation, respectively.

Mineral	Reaction	Saturation index															
		pH	12.6	12.5	12.4	12.5	12.4	12.3	13.0	12.5	12.4	12.7	12.6	12.4	12.3	12.4	12.3
		LogKeq															
Hydroxylapatite	$Ca_5(PO_4)_3OH+H^+ \leftrightarrow 5Ca^{+2}+3PO_4^{-3}+H_2O$	-44.3	19	20	20	20	20	19	20	20	20	19	20	19	19	19	20
Fluorapatite	$Ca_5(PO_4)_3F+3H^+ \leftrightarrow 5Ca^{+2}+3HPO_4^{-2}+F^-$	-25.0	21	21	22	22	22	21	21	21	21	21	21	21	21	18	18
Cattiite	$Mg_3(PO_4)_2 \cdot 22H_2O \leftrightarrow 3Mg^{+2}+2PO_4^{-3}+22H_2O$	-23.1	-14	-14	-14	-15	-15	-14	-16	-15	-15	-16	-15	-15	-14	-15	-14
Strengite	$FePO_4 \cdot 2H_2O \leftrightarrow Fe^{+3}+PO_4^{-3}+2H_2O$	-26.4	-17	-17	-16	-17	-17	-17	-19	-17	-17	-18	-18	-17	-16	-17	-17
Goethite	$FeOOH+3H^+ \leftrightarrow Fe^{+3}+2H_2O$	0.49	2.5	2.6	2.7	2.4	2.3	2.3	2.0	2.5	2.3	2.2	2.2	2.4	2.6	2.6	2.0
Lepidocrocite	$FeOOH+3H^+ \leftrightarrow Fe^{+3}+2H_2O$	1.37	1.9	2.0	2.1	1.8	1.7	1.7	1.5	2.0	1.7	1.6	1.6	1.8	2.0	2.0	1.5
$Fe(OH)_{2.7}Cl_{0.3}$	$Fe(OH)_{2.7}Cl_{0.3}+2.7H^+ \leftrightarrow Fe^{+3}+2.7H_2O+0.3Cl^-$	-3.04	2.3	2.4	2.6	2.2	2.2	2.2	1.8	2.5	2.2	2.0	2.1	2.3	2.6	2.5	2.0
Spertiniite	$Cu(OH)_2+2H^+ \leftrightarrow Cu^{+2}+2H_2O$	8.67	-1.0	-0.2	-0.1	-0.2	-0.1	0.1	-1.1	-0.2	0.1	-0.5	-0.2	0.3	0.3	0.3	0.4
Diaspore	$ALOOH+3H^+ \leftrightarrow Al^{+3}+2H_2O$	6.87	-3.0	-2.9	-2.9	-2.9	-2.8	-2.7	-3.3	-2.9	-2.9	-3.1	-2.9	-2.8	-2.7	-2.8	-2.7
Brucite	$Mg(OH)_2+2H^+ \leftrightarrow Mg^{+2}+2H_2O$	16.8	1.4	1.2	0.9	1.0	0.8	0.7	1.3	0.9	0.7	0.8	0.9	0.6	0.7	0.8	0.8
Fluorite	$CaF_2 \leftrightarrow Ca^{+2}+2F^-$	-10.5	1.4	1.4	1.2	1.4	1.1	1.1	1.0	1.1	0.8	0.7	0.7	0.3	0.2	-0.1	-0.1
Gypsum	$CaSO_4 \cdot 2H_2O \leftrightarrow Ca^{+2}+SO_4^{-2}$	-4.61	0.1	0.2	0.2	0.2	0.2	0.2	0.1	0.2	0.2	0.2	0.2	0.2	0.2	0.2	0.2
Calcite	$CaCO_3 \leftrightarrow Ca^{+2}+CO_3^{-2}$	-8.48	3.2	3.0	2.9	3.0	2.9	2.8	3.5	3.0	3.0	3.1	3.0	3.0	2.9	2.9	3.0

Table AP4.5. Percentages of the pollutants released during the simulated weathering processes with respect to the total composition of the solid wastes recovered from the MgO-DAS column.

		PO_4	SO_4	Fe	Zn	Cu	Al	As	Cr	U	Cd	Ni
Total solids (mg/kg)	**0-5 cm**	129,163	33,558	13,691	883	110	1113	76.1	234	165	33.0	32.5
	5-10 cm	153,675	14,238	8475	1443	127	695	77.7	194	117	50.3	44.4
	10-15 cm	178,713	7706	7343	923	211	593	156	71.2	25.5	55.6	73.3
	15-20 cm	80,010	11,244	7675	250	247	623	155	29.5	11.3	13.4	35.4
Rainwater (%)	**0-5 cm**	0.03	63.0	0.00	0.00	0.30	0.00	0.23	0.01	0.10	0.03	0.07
	5-10 cm	0.02	58.5	0.00	0.00	0.12	0.00	0.19	0.02	0.07	0.00	0.04
	10-15 cm	0.03	58.4	0.00	0.00	0.07	0.00	0.16	0.04	0.14	0.00	0.01
	15-20 cm	0.03	65.5	0.00	0.05	0.18	0.00	0.10	0.04	0.25	0.00	0.03
Reducing conditions (%)	**0-5 cm**	0.08	69.5	0.00	0.00	0.33	0.00	0.67	0.01	0.20	0.07	0.34
	5-10 cm	0.11	62.0	0.00	0.00	0.21	0.00	1.11	0.03	0.22	0.05	0.44
	10-15 cm	0.08	62.7	0.00	0.00	0.10	0.00	0.46	0.05	0.33	0.00	0.10
	15-20 cm	0.11	68.4	0.00	0.00	0.16	0.00	0.30	0.08	1.01	0.00	0.22

Table AP4.6. Percentages of the pollutants released during the simulated weathering processes with respect to the total composition of the solid wastes recovered from the $Ca(OH)_2$-DAS column.

		PO_4	SO_4	Fe	Zn	Cu	Al	As	Cr	U	Cd	Ni
Total solids (mg/kg)	**0-5 cm**	160,140	64,534	10,090	794	132	330	156	202	102	40.0	46.4
	5-10 cm	196,922	36,345	7762	1164	143	96.6	208	170	78.9	57.3	65.7
	10-15 cm	131,195	20,759	3221	545	160	49.3	149	53.1	12.3	34.6	47.7
	15-20 cm	12,130	6391	770	27.8	176	55.2	22.9	10.5	0.64	2.31	5.47
Rainwater (%)	**0-5 cm**	0.00	38.0	0.00	0.00	0.36	0.00	0.01	0.08	0.00	0.00	0.17
	5-10 cm	0.00	30.4	0.00	0.00	0.32	0.00	0.02	0.12	0.00	0.00	0.17
	10-15 cm	0.00	4.93	0.00	0.00	0.14	0.00	0.00	0.10	0.00	0.00	0.14
	15-20 cm	0.00	40.7	0.00	0.00	0.41	0.00	0.04	0.14	0.00	0.00	1.02
Reducing conditions (%)	**0-5 cm**	0.00	17.3	0.00	0.00	0.42	0.00	0.02	0.11	0.00	0.00	0.04
	5-10 cm	0.00	30.8	0.00	0.00	0.30	0.00	0.03	0.10	0.00	0.00	0.08
	10-15 cm	0.00	6.53	0.00	0.00	0.14	61.4	0.01	0.14	0.00	0.00	0.16
	15-20 cm	0.00	45.7	0.00	0.00	0.20	72.4	0.08	0.20	0.00	0.00	1.03

AP5. CHAPTER 6 SUPPLEMENTARY INFORMATION

Figure AP5.1. XRD spectra of original biomass ash (a) and of the newly-formed solids during the treatment of process water with biomass ash (b).

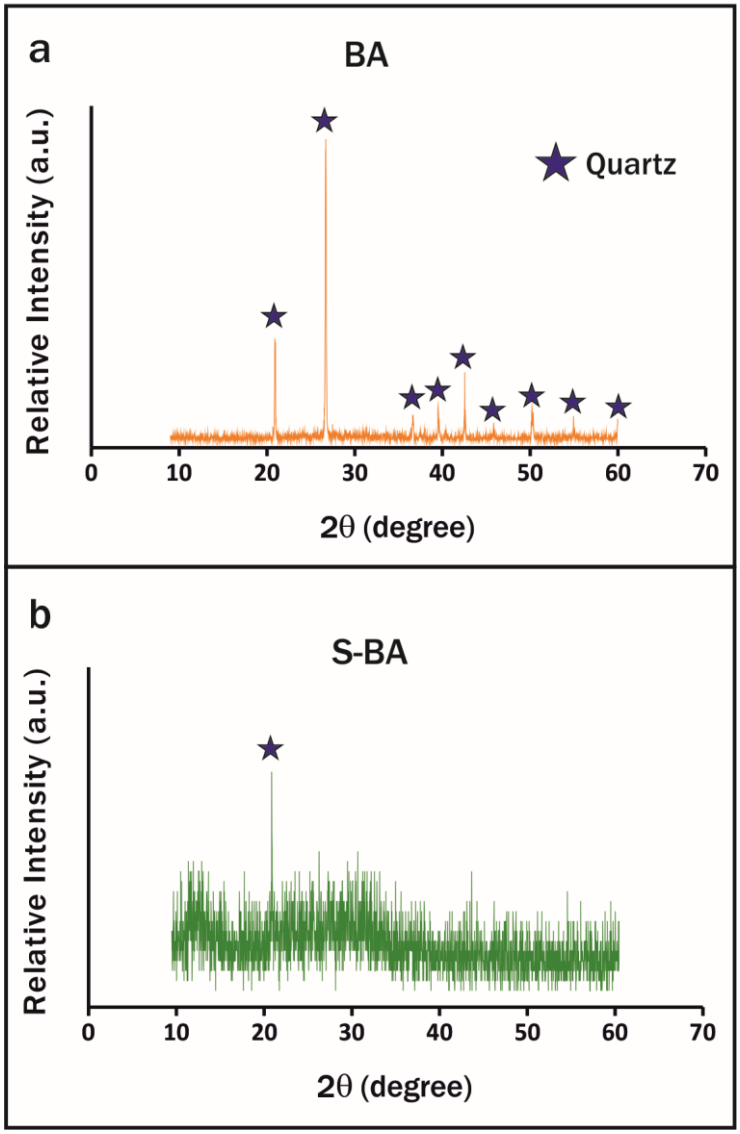

Table AP5.1. Results of the EN 12457-2 leaching test applied to biomass ash, and comparison with the regulatory limits for the acceptance of waste in landfills in the EU.

Landfill type	mg/kg											
	As	Ba	Cd	Cr	Cu	Mo	Ni	Pb	Sb	Se	Zn	SO_4^-
Inert Wastes	0.5	20	0.04	0.5	2	0.5	0.4	0.5	0.06	0.1	4	6000
Non-hazardous Wastes	2	100	1	10	50	10	10	10	0.7	0.5	50	20,000
Hazardous Wastes	25	300	5	70	100	30	40	50	5	7	200	50,000
Biomass ash	<l.d.	3.39	<l.d.	0.08	0.05	0.08	0.08	0.2	0.01	<l.d.	0.09	197

*<l.d. : below detection limit

Table AP5.2. Results of the TCLP leaching test (method 1311 of US EPA) applied to biomass ash.

Limits:	mg/L											
	As	**Ba**	**Cd**	**Cr**	**Ni**	**Pb**	**V**	**Zn**	**Se**	**Sb**	**Be**	**Tl**
TCLP	5	100	1	5	n.r.l	5	n.r.l	n.r.l	1	n.r.l	n.r.l	n.r.l
UTS	5	21	0.11	0.6	11	0.75	1.6	4.3	5.7	1.15	1.22	0.2
Biomass ash	<l.d.	0.398	<l.d.	0.014	0.115	0.005	0.027	0.093	<l.d.	0.004	<l.d.	<l.d.

*** n.r.l: no referenced limit**

<l.d. : below detection limit

Table AP5.3. Physicochemical parameters and contaminant concentrations of the solutions sampled during the treatment of the process water with biomass ash.

	Liquid-solid ratios	Reaction times	pH	CE (mS/cm)	Eh(mV)	mg/L			mg/L								
						PO_4	SO_4	F	Fe	Zn	Al	As	Cr	U	Cu	Cd	Sb
M0-PW/BE	-	0	1.07	54.4	645	65,220	5304	1134	116	105	60.0	47.9	47.8	33.4	18.9	13.7	0.78
M1-PW/BE	10:1	5 min	2.04	50.6	391	59,222	3334	874	141	94.8	501	46.3	26.1	26.8	19.1	12.3	0.50
M2-PW/BE	10:1	15 min	2.15	50.7	371	59,550	3434	682	96.7	97.2	455	47.0	21.8	26.4	20.0	12.5	0.38
M3-PW/BE	10:1	1 h	2.34	48.7	468	59,410	2800	467	27.7	90.2	326	43.6	15.4	22.7	18.6	12.8	0.27
M4-PW/BE	10:1	3 h	2.46	50.2	505	56,087	2709	176	9.90	92.3	221	45.7	10.3	19.7	18.9	12.4	0.24
M5-PW/BE	10:1	6 h	2.46	50.0	535	56,754	2625	76.2	7.06	91.6	194	44.8	9.5	19.8	18.6	12.8	0.19
M6-PW/BE	10:1	12 h	3.04	49.7	511	53,172	2461	29.2	4.17	84.9	107	44.0	5.94	16.2	18.3	12.6	0.14
M7-PW/BE	10:1	24 h	2.79	51.2	522	54,911	2643	30.9	5.36	90.6	173	44.8	7.22	19.8	18.3	12.8	0.13
M8-PW/BE	10:1	48 h	2.93	54.2	523	53,874	2547	29.5	2.95	88.2	108	45.1	4.80	17.1	17.7	12.8	0.11
M9-PW/BE	10:1	96 h	3.06	47.9	541	52,775	2514	29.0	2.06	83.8	66.7	45.5	2.52	14.1	16.1	12.0	0.11
M10-PW/BE	5:1	5 min	2.57	50.2	340	52,836	2533	161	40.9	67.9	112	45.0	11.4	15.3	20.4	12.4	0.28
M11-PW/BE	5:1	15 min	2.88	50.0	334	53,756	2386	48.8	14.4	60.2	42.8	44.1	7.30	11.2	19.4	11.8	0.28
M12-PW/BE	5:1	1 h	3.56	48.0	461	51,614	2319	11.4	1.09	37.2	11.7	44.4	4.16	5.01	12.7	11.8	0.48
M13-PW/BE	5:1	3 h	3.59	48.0	480	45,860	2537	12.0	0.90	16.5	13.0	44.5	1.70	0.10	7.24	11.2	0.45
M14-PW/BE	5:1	6 h	3.66	47.5	510	44,202	2723	10.7	0.63	7.79	12.4	44.1	0.57	<l.d.	3.90	10.3	0.40
M15-PW/BE	5:1	12 h	3.94	47.7	504	40,493	3043	8.84	0.46	6.11	12.6	43.2	0.36	<l.d.	2.98	9.84	0.38
M16-PW/BE	5:1	24 h	3.90	48.1	503	42,393	3344	10.2	0.49	8.03	10.6	43.3	0.12	<l.d.	2.91	9.50	0.18
M18-PW/BE	5:1	96 h	4.17	44.8	473	38,136	2676	10.1	0.28	4.00	2.67	42.8	<l.d.	<l.d.	1.60	7.98	0.09
M19-PW/BE	2.5:1	5 min	3.67	48.9	404	44,364	2585	18.3	0.82	13.5	8.17	44.6	2.48	1.70	9.32	7.66	0.33
M20-PW/BE	2.5:1	15 min	3.80	48.9	417	45,965	2649	10.9	1.01	6.85	9.58	44.5	1.66	0.75	7.56	7.88	0.43
M21-PW/BE	2.5:1	1 h	3.83	42.8	450	38,283	2930	10.3	1.22	2.57	12.0	44.4	1.01	0.02	4.43	8.73	0.49
M22-PW/BE	2.5:1	3 h	3.94	45.9	449	37,944	3865	8.26	1.01	1.01	18.5	44.0	0.23	<l.d.	2.59	7.20	0.45
M23-PW/BE	2.5:1	6 h	4.16	45.9	505	30,612	3723	9.49	0.21	0.60	23.8	42.0	0.07	<l.d.	1.08	5.28	0.40
M24-PW/BE	2.5:1	12 h	4.52	45.5	491	27,901	3780	8.76	0.19	0.42	29.1	42.7	0.03	<l.d.	0.57	4.43	0.37
M25-PW/BE	2.5:1	24 h	4.91	49.0	405	23,895	3947	8.70	1.75	0.21	21.7	41.4	0.03	<l.d.	0.30	1.96	0.21
M26-PW/BE	2.5:1	48 h	5.01	49.0	413	22,814	4042	8.62	0.30	0.34	0.65	41.8	0.11	0.02	0.22	1.78	0.12
M27-PW/BE	2.5:1	96 h	5.11	44.0	410	17,581	5208	8.54	0.06	0.24	0.42	42.1	<l.d.	<l.d.	0.18	1.15	0.09

<l.d.: below detection limit

Table AP5.4. Technology element concentrations of the solutions sampled during the treatment of the process water with biomass ash

			µg/L																	
	Liquid-solid ratios	Reaction times	Y	La	Ce	Pr	Nd	Sm	Eu	Gd	Tb	Dy	Ho	Er	Tm	Y	Lu	V[a]	Be	Sc	Ga
M0-PW/BE	-	0	475	321	135	56.7	182	48.7	13.4	62.7	<l.d.	72.9	19.2	44.8	11.1	38.1	<l.d.	66.3	334	279	59.8
M1-PW/BE	10:1	5 min	195	107	97.2	15.4	70.5	21.2	<l.d.	26.2	<l.d.	30.5	<l.d.	18.3	<l.d.	15.5	<l.d.	47.1	251	168	28.7
M2-PW/BE	10:1	15 min	74.5	21.1	21.5	<l.d.	17.3	<l.d.	<l.d.	10.5	<l.d.	11.5	<l.d.	<l.d.	<l.d.	<l.d.	<l.d.	45.8	215	101	11.0
M3-PW/BE	10:1	1 h	23.3	<l.d.	<l.d.	<l.d.	<l.d.	<l.d.	<l.d.	<l.d.	<l.d.	<l.d.	<l.d.	<l.d.	<l.d.	<l.d.	<l.d.	38.5	193	36.3	<l.d.
M4-PW/BE	10:1	3 h	11.0	<l.d.	<l.d.	<l.d.	<l.d.	<l.d.	<l.d.	<l.d.	<l.d.	<l.d.	<l.d.	<l.d.	<l.d.	<l.d.	<l.d.	32.3	183	15.2	<l.d.
M5-PW/BE	10:1	6 h	<l.d.	<l.d.	<l.d.	<l.d.	<l.d.	<l.d.	<l.d.	<l.d.	<l.d.	<l.d.	<l.d.	<l.d.	<l.d.	<l.d.	<l.d.	31.8	191	14.1	<l.d.
M6-PW/BE	10:1	12 h	<l.d.	<l.d.	<l.d.	<l.d.	<l.d.	<l.d.	<l.d.	<l.d.	<l.d.	<l.d.	<l.d.	<l.d.	<l.d.	<l.d.	<l.d.	24.6	134	<l.d.	<l.d.
M7-PW/BE	10:1	24 h	<l.d.	<l.d.	<l.d.	<l.d.	<l.d.	<l.d.	<l.d.	<l.d.	<l.d.	<l.d.	<l.d.	<l.d.	<l.d.	<l.d.	<l.d.	31.5	157	10.7	<l.d.
M8-PW/BE	10:1	48 h	<l.d.	<l.d.	<l.d.	<l.d.	<l.d.	<l.d.	<l.d.	<l.d.	<l.d.	<l.d.	<l.d.	<l.d.	<l.d.	<l.d.	<l.d.	26.0	130	<l.d.	<l.d.
M9-PW/BE	10:1	96 h	<l.d.	<l.d.	<l.d.	<l.d.	<l.d.	<l.d.	<l.d.	<l.d.	<l.d.	<l.d.	<l.d.	<l.d.	<l.d.	<l.d.	<l.d.	20.6	135	<l.d.	<l.d.
M10-PW/BE	5:1	5 min	<l.d.	<l.d.	<l.d.	<l.d.	<l.d.	<l.d.	<l.d.	<l.d.	<l.d.	<l.d.	<l.d.	<l.d.	<l.d.	<l.d.	<l.d.	22.5	130	20.3	<l.d.
M11-PW/BE	5:1	15 min	<l.d.	<l.d.	<l.d.	<l.d.	<l.d.	<l.d.	<l.d.	<l.d.	<l.d.	<l.d.	<l.d.	<l.d.	<l.d.	<l.d.	<l.d.	12.1	116	<l.d.	<l.d.
M12-PW/BE	5:1	1 h	<l.d.	<l.d.	<l.d.	<l.d.	<l.d.	<l.d.	<l.d.	<l.d.	<l.d.	<l.d.	<l.d.	<l.d.	<l.d.	<l.d.	<l.d.	2.77	26.6	<l.d.	<l.d.
M13-PW/BE	5:1	3 h	<l.d.	<l.d.	<l.d.	<l.d.	<l.d.	<l.d.	<l.d.	<l.d.	<l.d.	<l.d.	<l.d.	<l.d.	<l.d.	<l.d.	<l.d.	0.32	<l.d.	<l.d.	<l.d.
M14-PW/BE	5:1	6 h	<l.d.	<l.d.	<l.d.	<l.d.	<l.d.	<l.d.	<l.d.	<l.d.	<l.d.	<l.d.	<l.d.	<l.d.	<l.d.	<l.d.	<l.d.	0.13	<l.d.	<l.d.	<l.d.
M15-PW/BE	5:1	12 h	<l.d.	<l.d.	<l.d.	<l.d.	<l.d.	<l.d.	<l.d.	<l.d.	<l.d.	<l.d.	<l.d.	<l.d.	<l.d.	<l.d.	<l.d.	0.11	<l.d.	<l.d.	<l.d.
M16-PW/BE	5:1	24 h	<l.d.	<l.d.	<l.d.	<l.d.	<l.d.	<l.d.	<l.d.	<l.d.	<l.d.	<l.d.	<l.d.	<l.d.	<l.d.	<l.d.	<l.d.	0.15	<l.d.	<l.d.	<l.d.
M18-PW/BE	5:1	96 h	<l.d.	<l.d.	<l.d.	<l.d.	<l.d.	<l.d.	<l.d.	<l.d.	<l.d.	<l.d.	<l.d.	<l.d.	<l.d.	<l.d.	<l.d.	0.17	<l.d.	<l.d.	<l.d.
M19-PW/BE	2.5:1	5 min	<l.d.	<l.d.	<l.d.	<l.d.	<l.d.	<l.d.	<l.d.	<l.d.	<l.d.	<l.d.	<l.d.	<l.d.	<l.d.	<l.d.	<l.d.	0.72	<l.d.	<l.d.	<l.d.
M20-PW/BE	2.5:1	15 min	<l.d.	<l.d.	<l.d.	<l.d.	<l.d.	<l.d.	<l.d.	<l.d.	<l.d.	<l.d.	<l.d.	<l.d.	<l.d.	<l.d.	<l.d.	0.22	<l.d.	<l.d.	<l.d.
M21-PW/BE	2.5:1	1 h	<l.d.	<l.d.	<l.d.	<l.d.	<l.d.	<l.d.	<l.d.	<l.d.	<l.d.	<l.d.	<l.d.	<l.d.	<l.d.	<l.d.	<l.d.	0.09	<l.d.	<l.d.	<l.d.
M22-PW/BE	2.5:1	3 h	<l.d.	<l.d.	<l.d.	<l.d.	<l.d.	<l.d.	<l.d.	<l.d.	<l.d.	<l.d.	<l.d.	<l.d.	<l.d.	<l.d.	<l.d.	0.05	<l.d.	<l.d.	<l.d.
M23-PW/BE	2.5:1	6 h	<l.d.	<l.d.	<l.d.	<l.d.	<l.d.	<l.d.	<l.d.	<l.d.	<l.d.	<l.d.	<l.d.	<l.d.	<l.d.	<l.d.	<l.d.	0.05	<l.d.	<l.d.	<l.d.
M24-PW/BE	2.5:1	12 h	<l.d.	<l.d.	<l.d.	<l.d.	<l.d.	<l.d.	<l.d.	<l.d.	<l.d.	<l.d.	<l.d.	<l.d.	<l.d.	<l.d.	<l.d.	0.05	<l.d.	<l.d.	<l.d.
M25-PW/BE	2.5:1	24 h	<l.d.	<l.d.	<l.d.	<l.d.	<l.d.	<l.d.	<l.d.	<l.d.	<l.d.	<l.d.	<l.d.	<l.d.	<l.d.	<l.d.	<l.d.	0.07	<l.d.	<l.d.	<l.d.
M26-PW/BE	2.5:1	48 h	<l.d.	<l.d.	<l.d.	<l.d.	<l.d.	<l.d.	<l.d.	<l.d.	<l.d.	<l.d.	<l.d.	<l.d.	<l.d.	<l.d.	<l.d.	0.07	<l.d.	<l.d.	<l.d.
M27-PW/BE	2.5:1	96 h	<l.d.	<l.d.	<l.d.	<l.d.	<l.d.	<l.d.	<l.d.	<l.d.	<l.d.	<l.d.	<l.d.	<l.d.	<l.d.	<l.d.	<l.d.	0.21	<l.d.	<l.d.	<l.d.

<l.d.: below detection limit, [a]concentration in mg/L

Table AP5.5. Physicochemical parameters and contaminant concentrations of the solutions sampled during the treatment of the process water with $Ca(OH)_2$.

				mg/L			mg/L								
	pH	CE (mS/cm)	Eh(mV)	PO_4	SO_4	F	Fe	Zn	Al	As	Cr	U	Cu	Cd	Sb
M0-PW	1.48	57.4	700	69,513	5506	1136	118	105	60.7	48.2	46.9	34.7	18.3	16.8	0.79
M1-PW	1.98	16.1	637	15,815	1153	420	24.6	22.4	12.8	10.0	9.16	7.16	3.72	3.48	0.16
M2-PW	2.50	6.90	600	6339	433	173	8.38	8.63	4.87	3.85	3.53	2.69	1.36	1.32	0.06
M3-PW	2.98	4.74	570	4399	300	121	2.10	6.01	3.37	2.72	1.65	1.75	0.91	0.93	0.04
M4-PW	3.50	4.53	490	4179	291	108	0.84	5.71	3.18	2.51	1.20	1.64	0.88	0.88	0.04
M5-PW	4.06	4.24	444	3575	261	93.1	0.18	5.17	2.89	2.28	0.71	1.33	0.77	0.79	0.04
M6-PW	4.45	4.01	431	3421	262	86.0	0.12	4.80	2.69	2.18	0.59	1.13	0.68	0.74	0.03
M7-PW	4.99	3.63	427	3161	223	65.0	<l.d.	3.69	1.29	2.03	0.24	0.31	0.45	0.64	0.03

<l.d.: below detection limit

Table AP5.6. Technology element concentrations of the solutions sampled during the treatment of the process water with $Ca(OH)_2$.

	µg/L																		
	Y	La	Ce	Pr	Nd	Sm	Eu	Gd	Tb	Dy	Ho	Er	Tm	Yb	Lu	V[a]	Be	Sc	Ga
M0-PW	471	329	133	57.4	188	46.9	13.0	61.7	<l.d.	71.3	18.8	45.1	10.9	37.8	<l.d.	65.1	265	279	78.9
M1-PW	132	68.3	28.0	20.8	40.1	10.0	<l.d.	12.9	<l.d.	15.3	10.1	24.2	<l.d.	20.3	<l.d.	12.0	79.1	55.9	16.7
M2-PW	40.6	25.5	10.1	5.24	14.4	3.59	<l.d.	4.62	<l.d.	5.51	1.46	3.36	<l.d.	2.85	<l.d.	5.11	24.3	21.8	5.94
M3-PW	23.1	13.1	4.96	2.20	7.29	1.94	<l.d.	2.73	<l.d.	3.23	<l.d.	1.96	<l.d.	1.61	<l.d.	3.38	14.8	13.2	3.31
M4-PW	18.9	7.63	2.57	1.69	4.07	1.26	<l.d.	1.90	<l.d.	2.35	<l.d.	1.42	<l.d.	1.10	<l.d.	3.19	17.9	11.4	2.37
M5-PW	2.31	<l.d.	<l.d.	<l.d.	<l.d.	<l.d.	<l.d.	<l.d.	<l.d.	<l.d.	<l.d.	<l.d.	<l.d.	<l.d.	<l.d.	2.61	15.1	7.50	<l.d.
M6-PW	1.01	<l.d.	<l.d.	<l.d.	<l.d.	<l.d.	<l.d.	<l.d.	<l.d.	<l.d.	<l.d.	<l.d.	<l.d.	<l.d.	<l.d.	2.30	12.6	5.79	<l.d.
M7-PW	<l.d.	<l.d.	<l.d.	<l.d.	<l.d.	<l.d.	<l.d.	<l.d.	<l.d.	<l.d.	<l.d.	<l.d.	<l.d.	<l.d.	<l.d.	1.02	<l.d.	<l.d.	<l.d.

<l.d.: below detection limit, [a]concentration in mg/L

Table AP5.7. Ideal reactions, equilibrium constants and saturation indices (SI) for oversaturated phases according to PHREEQC simulations from the database of MINTEQ model, for the solutions derived from the biomass ash treatment with a solid:liquid ratio of 1:10. Negative and positive SI indicate undersaturation and oversaturation, respectively.

Mineral	Reaction		Saturation index									
		pH / LogKeq	1.07	2.04	2.15	2.34	2.46	2.46	3.04	2.79	2.93	3.06
Fluorapatite	$Ca_5(PO_4)_3F+3H^+ \leftrightarrow 5Ca^{+2}+3HPO_4^{-2}+F^-$	-24.9	-8.4	0.6	1.1	2.0	2.3	1.9	5.4	3.5	5.5	6.6
Strengite	$FePO_4 \cdot 2H_2O \leftrightarrow Fe^{+3}+PO_4^{-3}+2H_2O$	-11.3	1.8	0.5	0.3	1.7	2.0	2.1	2.5	2.3	2.2	2.3
Berlinite	$AlPO_4 \leftrightarrow Al^{+3}+HPO_4^{-2}$	-7.65	-7.4	-2.8	-2.0	-1.6	-0.4	0.0	0.1	0.1	0.0	0.1
Fluorite	$CaF_2 \leftrightarrow Ca^{+2}+2F^-$	-10.0	0.5	0.0	-0.6	-0.8	-2.3	-3.3	-3.0	-3.8	-1.0	-1.0
$LaPO_4 \cdot 10H_2O$	$LaPO4 \cdot 10H_2O \leftrightarrow La^{+3}+HPO_4^{-2}+10H_2O$	-12.4	-2.0	-0.3	-0.8	-1.8	-1.5	-1.4	-0.3	-0.8	-0.6	-0.3
$CePO_4 \cdot 10H_2O$	$CePO4 \cdot 10H_2O \leftrightarrow Ce^{+3}+HPO_4^{-2}+10H_2O$	-12.3	-2.3	-0.4	-0.8	-1.7	-1.5	-1.5	-0.3	-0.8	-0.6	-0.3
$PrPO_4 \cdot 10H_2O$	$PrPO4 \cdot 10H_2O \leftrightarrow Pr^{+3}+HPO_4^{-2}+10H_2O$	-12.3	-2.7	-1.0	-2.1	-1.7	-1.4	-1.4	-0.3	-0.8	-0.5	-0.3
$NdPO_4 \cdot 10H_2O$	$NdPO4 \cdot 10H_2O \leftrightarrow Nd^{+3}+HPO_4^{-2}+10H_2O$	-12.2	-2.5	-0.6	-0.9	-1.8	-1.5	-1.4	-0.3	-0.8	-0.6	-0.3
$SmPO_4 \cdot 10H_2O$	$SmPO4 \cdot 10H_2O \leftrightarrow Sm^{+3}+HPO_4^{-2}+10H_2O$	-12.2	-3.0	-1.1	-2.2	-1.8	-1.5	-1.4	-0.3	-0.8	-0.6	-0.3
$LaF_3 \cdot 0.5H_2O$	$LaF_3 \cdot 0.5H_2O \leftrightarrow La^{+3}+3F^-+0.5H_2O$	-18.7	-0.3	-2.4	-4.0	-5.6	-7.9	-9.5	-9.2	-10	-6.1	-6.1
$CeF_3 \cdot 0.5H_2O$	$CeF_3 \cdot 0.5H_2O \leftrightarrow Ce^{+3}+3F^-+0.5H_2O$	-18.8	-0.4	-2.2	-3.8	-5.4	-7.7	-9.3	-9.0	-10	-6.0	-5.9
$PrF_3 \cdot 0.5H_2O$	$PrF_3 \cdot 0.5H_2O \leftrightarrow Pr^{+3}+3F^-+0.5H_2O$	-18.7	-0.8	-2.9	-5.2	-5.5	-7.8	-9.4	-9.1	-10	-6.0	-5.9
$NdF_3 \cdot 0.5H_2O$	$NdF_3 \cdot 0.5H_2O \leftrightarrow Nd^{+3}+3F^-+0.5H_2O$	-18.6	-0.6	-2.5	-4.0	-5.6	-7.9	-9.4	-9.1	-10	-6.1	-6.0
$SmF_3 \cdot 0.5H_2O$	$SmF_3 \cdot 0.5H_2O \leftrightarrow Sm^{+3}+3F^-+0.5H_2O$	-17.5	-2.3	-4.1	-6.4	-6.7	-8.9	-11	-10	-11	-7.1	-7.0
Gypsum	$CaSO4 \cdot 2H_2O \leftrightarrow Ca^{+2}+SO_4^{-2}+2H_2O$	-4.48	-0.2	0.0	0.1	0.0	0.0	-0.1	0.0	0.0	0.0	-0.1

Table AP5.8. Ideal reactions, equilibrium constants and saturation indices (SI) for oversaturated phases according to PHREEQC simulations from the database of MINTEQ model, for the solutions derived from the biomass ash treatment with a solid:liquid ratio of 1:5. Negative and positive SI indicate undersaturation and oversaturation, respectively.

Mineral	Reaction		Saturation index								
		pH / LogKeq	1.07	2.57	2.88	3.56	3.59	3.66	3.94	3.90	4.17
Fluorapatite	$Ca_5(PO_4)_3F+3H^+ \leftrightarrow 5Ca^{+2}+3HPO_4^{-2}+F^-$	-24.9	-8.4	3.8	5.3	8.0	8.6	-2.7	-2.6	-2.6	-2.5
Strengite	$FePO_4 \cdot 2H_2O \leftrightarrow Fe^{+3}+PO_4^{-3}+2H_2O$	-11.3	1.8	0.3	0.4	2.4	2.4	2.4	2.5	2.5	2.5
Berlinite	$AlPO_4 \leftrightarrow Al^{+3}+HPO_4^{-2}$	-7.65	-7.4	-1.3	-0.5	0.1	0.2	0.3	0.2	0.1	-0.2
Fluorite	$CaF_2 \leftrightarrow Ca^{+2}+2F^-$	-10.0	0.5	-1.0	-1.7	-4.5	-3.3	-74	-75	-74	-74
Gypsum	$CaSO4 \cdot 2H_2O \leftrightarrow Ca^{+2}+SO_4^{-2}+2H_2O$	-4.48	-0.2	-0.1	-0.1	-0.1	-0.1	-0.1	0.0	0.0	-0.3

Table AP5.9. Ideal reactions, equilibrium constants and saturation indices (SI) for oversaturated phases according to PHREEQC simulations from the database of MINTEQ model, for the solutions derived from the biomass ash treatment with a solid:liquid ratio of 1:2.5. Negative and positive SI indicate undersaturation and oversaturation, respectively.

Mineral	Reaction		Saturation index									
		pH / LogKeq	1.07	3.67	3.80	3.83	3.94	4.16	4.52	4.91	5.01	5.11
Fluorapatite	$Ca_5(PO_4)_3F+3H^+ \leftrightarrow 5Ca^{+2}+3HPO_4^{-2}+F^-$	-24.9	-8.4	10	-25	-26	-26	-25	-24	-24	-24	-24
Strengite	$FePO_4 \cdot 2H_2O \leftrightarrow Fe^{+3}+PO_4^{-3}+2H_2O$	-11.3	1.8	1.9	2.4	2.7	2.9	2.5	2.4	3.9	3.2	-0.5
Berlinite	$AlPO_4 \leftrightarrow Al^{+3}+HPO_4^{-2}$	-7.65	-7.4	-0.1	0.4	0.4	0.8	1.1	1.2	1.5	0.0	0.1
Fluorite	$CaF_2 \leftrightarrow Ca^{+2}+2F^-$	-10.0	0.5	-1.3	-74	-74	-75	-74	-74	-74	-74	-74
Gypsum	$CaSO4 \cdot 2H_2O \leftrightarrow Ca^{+2}+SO_4^{-2}+2H_2O$	-4.48	-0.2	-0.1	-0.1	-0.1	0.0	-0.2	-0.3	-0.6	-0.7	-0.8

Table AP5.10. Ideal reactions, equilibrium constants and saturation indices (SI) for oversaturated phases according to PHREEQC simulations from the database of MINTEQ model, for the solutions derived from the $Ca(OH)_2$ treatment. Negative and positive SI indicate undersaturation and oversaturation, respectively.

Mineral	Reaction		Saturation index							
		pH / LogKeq	1.48	1.98	2.50	2.98	3.50	4.06	4.45	4.99
Fluorapatite	$Ca_5(PO_4)_3F+3H^+ \leftrightarrow 5Ca^{+2}+3HPO_4^{-2}+F^-$	-24.9	-4.8	-3.9	-1.4	1.5	4.9	8.3	10.4	13.3
Strengite	$FePO_4 \cdot 2H_2O \leftrightarrow Fe^{+3}+PO_4^{-3}+2H_2O$	-11.3	2.5	2.3	2.4	2.2	2.0	1.7	2.0	1.7
Berlinite	$AlPO_4 \leftrightarrow Al^{+3}+HPO_4^{-2}$	-7.65	-7.2	-8.1	-8.3	-8.2	-7.9	-6.9	-6.3	-5.3
Fluorite	$CaF_2 \leftrightarrow Ca^{+2}+2F^-$	-10.0	1.1	1.4	1.7	2.2	2.6	2.6	2.6	2.4
$LaPO_4 \cdot 10H_2O$	$LaPO4 \cdot 10H_2O \leftrightarrow La^{+3}+HPO_4^{-2}+10H_2O$	-12.4	-1.1	-0.6	0.0	0.3	1.1	1.2	1.9	3.1
$CePO_4 \cdot 10H_2O$	$CePO4 \cdot 10H_2O \leftrightarrow Ce^{+3}+HPO_4^{-2}+10H_2O$	-12.3	-1.5	-1.2	-0.8	-0.2	0.6	0.6	1.4	2.5
$PrPO_4 \cdot 10H_2O$	$PrPO4 \cdot 10H_2O \leftrightarrow Pr^{+3}+HPO_4^{-2}+10H_2O$	-12.3	-1.8	-1.3	-0.9	-0.2	0.5	0.5	1.3	2.4
$NdPO_4 \cdot 10H_2O$	$NdPO4 \cdot 10H_2O \leftrightarrow Nd^{+3}+HPO_4^{-2}+10H_2O$	-12.2	-1.5	-1.3	-1.1	-0.5	0.2	0.2	1.0	2.1
$SmPO_4 \cdot 10H_2O$	$SmPO4 \cdot 10H_2O \leftrightarrow Sm^{+3}+HPO_4^{-2}+10H_2O$	-12.2	-2.1	-1.9	-1.2	-0.6	0.1	0.1	0.9	2.0
$LaF_3 \cdot 0.5H_2O$	$LaF_3 \cdot 0.5H_2O \leftrightarrow La^{+3}+3F^-+0.5H_2O$	-18.7	0.3	1.0	1.3	1.4	1.7	0.8	0.8	0.6
$CeF_3 \cdot 0.5H_2O$	$CeF_3 \cdot 0.5H_2O \leftrightarrow Ce^{+3}+3F^-+0.5H_2O$	-18.8	0.1	0.7	0.7	1.1	1.3	0.4	0.4	0.3
$PrF_3 \cdot 0.5H_2O$	$PrF_3 \cdot 0.5H_2O \leftrightarrow Pr^{+3}+3F^-+0.5H_2O$	-18.7	-0.3	0.4	0.6	0.9	1.2	0.2	0.2	0.1
$NdF_3 \cdot 0.5H_2O$	$NdF_3 \cdot 0.5H_2O \leftrightarrow Nd^{+3}+3F^-+0.5H_2O$	-18.6	0.0	0.4	0.3	0.6	0.9	-0.1	-0.1	-0.2
$SmF_3 \cdot 0.5H_2O$	$SmF_3 \cdot 0.5H_2O \leftrightarrow Sm^{+3}+3F^-+0.5H_2O$	-17.5	-1.7	-1.3	-0.8	-0.5	-0.4	-1.3	-1.3	-1.4
Gypsum	$CaSO4 \cdot 2H_2O \leftrightarrow Ca^{+2}+SO_4^{-2}+2H_2O$	-4.48	0.2	-0.4	-0.7	-0.8	-0.7	-0.8	-0.8	-0.9

Table AP5.11. Calculation of the reserves of REE and Y contained in the solids originated during the treatments with both alkaline materials (i.e., biomass ash (BA) and $Ca(OH)_2$).

	Rare earth elements plus Y (mg/kg)																	
	Y	La	Ce	Pr	Nd	Sm	Eu	Gd	Tb	Dy	Ho	Er	Tm	Yb	Lu	ΣLREE	ΣHREE	REY
S-BA	105	59.1	67.3	10.5	43.5	9.56	2.57	13.0	2.03	14.0	3.34	10.7	1.48	9.53	1.64	190	163	353
S-$Ca(OH)_2$	1347	732	490	116	493	104	28.4	142	22.7	158	39.9	133	20.7	141	23.9	1935	2057	3992

AP6. PUBLISHED ARTICLES

Assessment of metals mobility during the alkaline treatment of highly acid phosphogypsum leachates

Ricardo Millán-Becerro[a], Rafael Pérez-López[a], Francisco Macías[a], Carlos R.Cánovas[a], Evgenia-Maria Papaslioti[a,b], M. Dolores Basallote[a]

[a] Department of Earth Sciences & Research Center on Natural Resources, Health and the Environment, University of Huelva, Campus 'El Carmen', 21071 Huelva, Spain

[b] Instituto Andaluz de Ciencias de la Tierra, CSIC & UGR, Avenida de las Palmeras 4, 18100 Armilla Granada, Spain

Published in: Science of The Total Environment

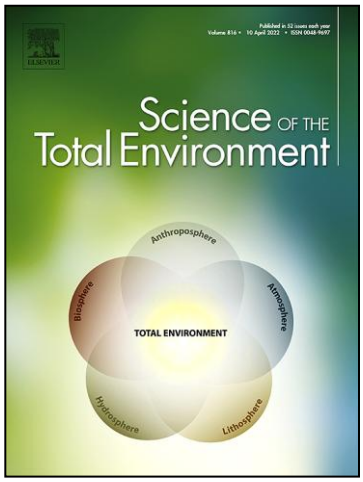

Publisher: ELSEVIER, RADARWEG 29, 1043 NX AMSTERDAM, NETHERLANDS

Co-Editors-in-Chief: Damià Barceló, PhD, Jay Gan, PhD, Philip Hopke, PhD, Elena Paoletti, PhD

ISSN: 0048-9697

EISSN: 1879-1026

DOI: org/10.1016/j.scitotenv.2018.12.305

Journals Metrics:

CiteScore: 10.5

Impact Factor (2020): 7.963

5-year Impact Factor:7.842

JCR® Category	Rank in Category	Quartile in Category
ENVIRONMENTAL SCIENCES	25 of 274	Q1

Science of the Total Environment 660 (2019) 395–405

Contents lists available at ScienceDirect

Science of the Total Environment

journal homepage: www.elsevier.com/locate/scitotenv

Assessment of metals mobility during the alkaline treatment of highly acid phosphogypsum leachates

Ricardo Millán-Becerro [a,*], Rafael Pérez-López [a], Francisco Macías [a], Carlos R. Cánovas [a], Evgenia-Maria Papaslioti [a,b], M. Dolores Basallote [a]

[a] Department of Earth Sciences & Research Center on Natural Resources, Health and the Environment, University of Huelva, Campus 'El Carmen', 21071 Huelva, Spain
[b] Instituto Andaluz de Ciencias de la Tierra, CSIC & UGR, Avenida de las Palmeras 4, 18100 Armilla Granada, Spain

HIGHLIGHTS

- Behaviour of pollutants during neutralization of phosphogypsum leachates is studied.
- Alkaline treatment removed around 90–100% of most pollutants from the leachates.
- Solids generated during the treatment host high pollutant concentrations.
- Treatment of leachates of unrestored zones generates hazardous wastes, and vice versa.
- Hazardousness of solids from industrial water depended on the applied normative.

GRAPHICAL ABSTRACT

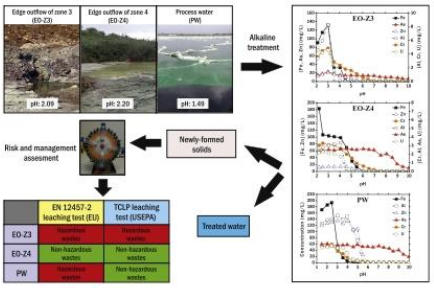

ARTICLE INFO

Article history:
Received 3 October 2018
Received in revised form 3 December 2018
Accepted 20 December 2018
Available online 21 December 2018

Editor: Daniel CW Tsang

Keywords:
Phosphogypsum
Acid leachates
Estuary of Huelva
Alkaline treatment
Leaching tests

ABSTRACT

This research evaluates the feasibility of an alkaline treatment system for highly acid leachates from a phosphogypsum stack located in an estuarine environment degraded by such pollution. The presented methodology consists of the addition of a $Ca(OH)_2$ solution to the different types of phosphogypsum-related acidic leachates with the aim to increase their pH and subsequently, to provoke the precipitation and immobilization of the dissolved contaminants. In fact, phosphates and fluorides reached removal of 100% and 90%, respectively. As regards metals, removal values close to 100% were reached for Fe, Al, Cr, Cd, U and Zn, whereas it did not seem to be totally effective for other elements such as As (removal of 57–82%) and Sb (4–36%). The decrease of contaminant concentrations was caused probably by co-precipitation and/or adsorption to phosphate phases, together with by fluoride precipitation. The solid phases formed during the treatment were subjected to two standard leaching tests (EN 12457-2 from the EU and TCLP from the US) in order to conduct a risk and management assessment. In this context, some of the precipitates formed during the treatment would be classified as hazardous wastes, due to the high concentration of As leached. Moreover, the potential economic costs of a convectional active treatment system were also explored. This study sets the basis for a new research line with the aim to minimise the impact of the phosphogypsum stacks worldwide to their adjacent environment.

1. Introduction

Phosphogypsum is a by-product generated during the manufacture of phosphoric acid (H_3PO_4) from the phosphate fertiliser industry. It is

* Corresponding author.
E-mail address: ricardo.millan@dct.uhu.es (R. Millán-Becerro).

https://doi.org/10.1016/j.scitotenv.2018.12.305
0048-9697/

Design and optimization of sustainable passive treatment systems for phosphogypsum leachates in an orphan disposal site

Ricardo Millán-Becerro, Rafael Pérez-López, Francisco Macías, Carlos R.Cánovas

Department of Earth Sciences & Research Center on Natural Resources, Health and the Environment, University of Huelva, Campus 'El Carmen', 21071 Huelva, Spain

Published in: Journal of Environmental Management

Publisher: ACADEMIC PRESS LTD- ELSEVIER SCIENCE LTD, 24-28 OVAL RD, LONDON NW1 7DX, ENGLAND

Co-Editors-in-Chief: Prof. Dr. Raf Dewil, Prof. Dr. Jason Evans, Prof. Dr. Lixiao Zhang

ISSN: 0301-4797

EISSN: 1095-8630

DOI: org/10.1016/j.jenvman.2020.111251

Journals Metrics:

CiteScore: 9.8

Impact Factor (2020): 6.789

5-year Impact Factor:6.914

JCR® Category	Rank in Category	Quartile in Category
ENVIRONMENTAL SCIENCES	34 of 274	Q1

Journal of Environmental Management 275 (2020) 111251

Contents lists available at ScienceDirect

Journal of Environmental Management

journal homepage: http://www.elsevier.com/locate/jenvman

Research article

Design and optimization of sustainable passive treatment systems for phosphogypsum leachates in an orphan disposal site

Ricardo Millán-Becerro *, Rafael Pérez-López, Francisco Macías, Carlos R. Cánovas

Department of Earth Sciences & Research Center on Natural Resources, Health and the Environment, University of Huelva, Campus 'El Carmen', 21071, Huelva, Spain

ARTICLE INFO

Keywords:
Highly polluted industrial waters
Dispersed alkaline substrate
Net acidity removal
eco-Friendly technology

ABSTRACT

The optimization of the dispersed alkaline substrate (DAS) technology was investigated to achieve the treatment of highly acidic and polluted effluents from a phosphogypsum pile in an orphan site of SW Spain. This phosphogypsum disposal area is located on the Tinto river marsh soils, where it acts as a source of pollution for the estuarine environment, releasing high concentrations of metal(loid)s and radionuclides, which degrade the surrounding waters. The methodology consists of flowing the leachates through columns loaded with a combination of a fine-grained alkaline reagent scattered in a non-reactive matrix to raise the water pH while decreasing the solubility of dissolved contaminants. Seven columns were built, one for each of the alkaline reagent used: limestone, barium carbonate, biomass ash, fly ash, MgO, $Mg(OH)_2$, and $Ca(OH)_2$. The $Ca(OH)_2$-DAS and MgO-DAS treatment systems showed the highest effectiveness, reaching near-total removal for PO_4, F, Fe, Zn, Cu, Al, Cr, and U with initial reagent mass:treated volume ratios of 36.3 g/L and 7.57 g/L, respectively. Total As removal was only achieved in the $Ca(OH)_2$-DAS treatment. Phosphate precipitation was the main mechanism responsible for pollutants removal. Geochemical modeling using PHREEQC code and mineralogical evidence confirmed the precipitation of these minerals. This study forms the basis of an effective and environmentally sustainable treatment system for phosphogypsum leachates to reduce the impact of the fertilizer industry worldwide.

1. Introduction

Phosphogypsum is an undesired residue derived from the production of phosphoric acid (H_3PO_4) by the phosphate fertilizer industry. Phosphogypsum is mainly composed of gypsum ($CaSO_4 \cdot 2H_2O$), which is generated during the chemical dissolution of phosphate ore (mainly fluorapatite, ($Ca_5(PO_4)_3F$)) with sulfuric acid (H_2SO_4), according to Eq. (1):

$$Ca_5(PO_4)_3F + 5H_2SO_4 + 10H_2O \rightarrow 3H_3PO_4 + 5CaSO_4 \cdot 2H_2O + HF \quad (1)$$

Phosphogypsum is highly acidic because it contains a residual fraction of acids from the industrial process trapped in its pores, including non-recoverable phosphoric acid, sulfuric acid and hydrofluoric acid (Lottermoser, 2010). During the industrial process, diverse impurities are released from the raw materials used (phosphate ore and sulfuric acid) and subsequently transferred to the generated products. Phosphogypsum also encloses high quantities of metal(loid)s (e.g., As and Cd) and radionuclides from the ^{238}U decay series (i.e., U, Ra, and Rn) (Rutherford et al., 1994; Macías et al., 2017). It is estimated that around five tons of phosphogypsum are produced for each ton of P_2O_5 manufactured by the fertilizer industry worldwide, and despite its hazardousness, most of the phosphogypsum produced worldwide is dumped close to coastal areas, suffering strong weathering (Tayibi et al., 2009).

Despite the cease of phosphogypsum generation in 2010, a legacy of waste piles after 40 years of fertilizer industry activities in the city of Huelva (SW Spain) continues to degrade the environmental quality of the surrounding waters (Pérez-López et al., 2016). In spite of being under the control of industry, these stacks can be considered an orphan site since their remediation seems to be impeded by financial constraints, uncertain liability, and the current legal status of lands. The waste piles are subject to strong social pressure and to an endless political and legislative disputes; meanwhile, highly-polluted acid leakages, known as edge outflows, continuously discharge large amounts of contaminants to the Ría de Huelva estuary, e.g., 42 t/yr of Fe, 12 t/yr of Zn, 6.9 t/yr of As, 4.2 t/yr of U, 3.5 t/yr of Cr, 1.8 t/yr of Cu, 1.6 t/yr of Cd, 1.2 t/yr of Ni, 0.10 t/yr of REE, and 0.04 t/yr of Sc and Y, among others (Pérez-López et al., 2016; Cánovas et al., 2018). These discharges,

* Corresponding author.
E-mail address: ricardo.millan@dct.uhu.es (R. Millán-Becerro).

https://doi.org/10.1016/j.jenvman.2020.111251
Received 17 April 2020; Received in revised form 31 July 2020; Accepted 15 August 2020
Available online 23 August 2020

Combined procedure of metal removal and recovery of technology elements from fertilizer industry effluents

Ricardo Millán-Becerro, Carlos R.Cánovas, Rafael Pérez-López, Francisco Macías, Rafael León

Department of Earth Sciences & Research Center on Natural Resources, Health and the Environment, University of Huelva, Campus 'El Carmen', 21071 Huelva, Spain

Published in: Journal of Geochemical Exploration

Publisher: ELSEVIER, RADARWEG 29, 1043 NX AMSTERDAM, NETHERLANDS

Editor-in-Chief: Professor Stefano Albanese

ISSN: 0375-6742

EISSN: 1879-1689

DOI: org/10.1016/j.gexplo.2020.106698

Journals Metrics:

CiteScore: 7.2

Impact Factor (2020): 3.746

5-year Impact Factor:4.362

JCR® Category	Rank in Category	Quartile in Category
GEOCHEMISTRY & GEOPHYSICS	25 of 88	Q2

Journal of Geochemical Exploration 221 (2021) 106698

Contents lists available at ScienceDirect

Journal of Geochemical Exploration

journal homepage: www.elsevier.com/locate/gexplo

Combined procedure of metal removal and recovery of technology elements from fertilizer industry effluents

Ricardo Millán-Becerro *, Carlos R. Cánovas, Rafael Pérez-López, Francisco Macías, Rafael León

Department of Earth Sciences & Research Center on Natural Resources, Health and the Environment, University of Huelva, Campus 'El Carmen', 21071 Huelva, Spain

ARTICLE INFO

Keywords:
Alkaline treatment
Phosphogypsum leachates
Pollutants removal
Valuable metals

ABSTRACT

This study focuses on the search for a sustainable treatment and metal recovery system for acid discharges from a fertilizer industry in SW Spain. The methodology proposed involves the addition of two types of alkaline materials (an industrial waste and a commercial reagent) to neutralize the acidity and remove dissolved elements. In the first case, the treatment consisted on batch reactions between biomass ashes and phosphogypsum leachates at different solid-liquid ratios (i.e. 1:2.5, 1:5, and 1:10). On the other hand, a 0.01 M solution of $Ca(OH)_2$ was used. The experiment with biomass ashes at a solid:liquid ratio of 1:2.5 showed a high effectiveness, reaching removal percentages close to 100% for F, Fe, Zn, Al, Cr, U, Cu and Cd. The depletion of contaminants from solutions during the alkaline treatments occurred mainly by co-precipitation and/or adsorption onto phosphate phases, in addition to precipitation of fluorides. Moreover, the solids precipitated during the alkaline treatments contain elements of high economic interest such as rare earth elements plus Y (353–3992 mg/kg), Sc (21–164 mg/kg), Be (5.0–7.0 mg/kg), V (1036–2974 mg/kg), Ga (16–40 mg/kg) or U (721–2963 mg/kg). These values could make this by-product a promising source of technology metals. This study proposes an environmentally-friendly solution for these industrial leachates, removing selectively impurities and target elements and producing a promising exploitable metal concentrate. This research could lay the foundations for an effective and sustainable treatment system for acid leachates from phosphogypsum stacks. Furthermore, the costs related with the treatments could be covered by recovering the valuable elements contained in the newly-formed precipitates during the treatments.

1. Introduction

The production of phosphoric acid (H_3PO_4) in the phosphate fertilizer industry generates a waste known as phosphogypsum (PG, mainly composed of gypsum, $CaSO_4{\cdot}2H_2O$). This by-product is generated during the wet chemical digestion of phosphate ore (i.e. fluorapatite, $Ca_5(PO_4)_3F$) with sulphuric acid (H_2SO_4). The industrial process is summarized in the following reaction (Eq. (1)):

$$Ca_5(PO_4)_3F + 5H_2SO_4 + 10H_2O \rightarrow 3H_3PO_4 + 5CaSO_4{\cdot}2H_2O + HF \quad (1)$$

The raw phosphate ore contains high amounts of metallic impurities and radionuclides from the decay series of ^{238}U such as uranium, radium and radon, which are released during the industrial process and subsequently transferred to the generated by-products, according to their chemical behavior (Rutherford et al., 1994; Pérez-López et al., 2010; Macías et al., 2017). The PG is highly acidic due to the presence of residual acids (i.e. phosphoric-sulphuric-hydrofluoric) from the manufacturing process (Bolívar et al., 2009; Lottermoser, 2010). The PG is usually piled in stacks near coastal areas exposed to weathering conditions (Tayibi et al., 2009). Nevertheless, this is not the only waste derived from the manufacture of phosphoric acid. The industrial process requires a large volume of water, known as process water (PW), which is employed for slurry and transport the PG to the stack in a closed-circuit system. Thus, the continuous reuse of PW in the closed-loop system yields a wastewater characterized by extremely low pH values and very high concentrations of fluoride, sulfate, phosphate, radionuclides, and metal/loids (Lottermoser, 2010). Such waters require storage and isolation within the waste repository in central or lined ponds, and must be neutralized before their discharge to the surrounding water bodies. The neutralization process, for example with $Ca(OH)_2$, implies that contaminants pass from their soluble forms to an insoluble solid waste composed of phosphates and to a lesser extent fluorides (Fuleihan and Werner, 2011; Millán-Becerro et al., 2019). Therefore, this highly-polluted sludge requires isolation, usually in the PG stack (Ericson

* Corresponding author.
E-mail address: ricardo.millan@dct.uhu.es (R. Millán-Becerro).

https://doi.org/10.1016/j.gexplo.2020.106698
Received 26 May 2020; Received in revised form 16 September 2020; Accepted 11 November 2020
Available online 14 November 2020

Environmental management and potential valorization of wastes generated in passive treatments of fertilizer industry effluents

Ricardo Millán-Becerro, Francisco Macías, Carlos R.Cánovas, Rafael Pérez-López, José M. Fuentes-López

Department of Earth Sciences & Research Center on Natural Resources, Health and the Environment, University of Huelva, Campus 'El Carmen', 21071 Huelva, Spain

Published in: Chemosphere

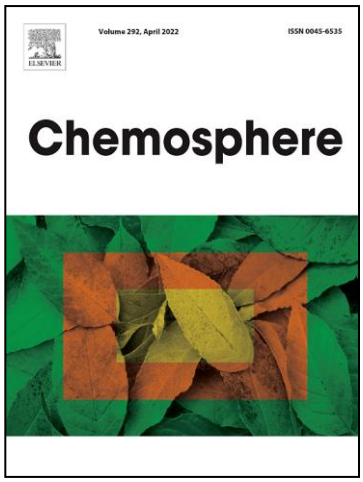

Publisher: PERGAMON-ELSEVIER SCIENCE LTD, THE BOULEVARD, LANGFORD LANE, KIDLINGTON, OXFORD OX5 1GB, ENGLAND

Co-Editors-in-Chief: Jacob de Boer, Prof.dr., Tamara Galloway, Yeomin Yoon, PhD

ISSN: 0045-6535

EISSN: 1879-1298

DOI: org/10.1016/j.chemosphere.2022.133876

Journals Metrics:

CiteScore: 10.1

Impact Factor (2020): 7.086

5-year Impact Factor: 6.956

JCR® Category	Rank in Category	Quartile in Category
ENVIRONMENTAL SCIENCES	30 of 274	Q1

Chemosphere 295 (2022) 133876

Contents lists available at ScienceDirect

Chemosphere

journal homepage: www.elsevier.com/locate/chemosphere

Environmental management and potential valorization of wastes generated in passive treatments of fertilizer industry effluents

Ricardo Millán-Becerro *, Francisco Macías, Carlos R. Cánovas, Rafael Pérez-López, José M. Fuentes-López

Department of Earth Sciences & Research Center on Natural Resources, Health and the Environment, University of Huelva, Campus 'El Carmen', 21071, Huelva, Spain

HIGHLIGHTS

- Highly polluted phosphogypsum leachates were effectively treated with DAS technology.
- The MgO-DAS and $Ca(OH)_2$-DAS removed around 100% of PO_4, F, Fe, Zn, Al, Cd, U and As.
- The hazardousness of DAS wastes was depth-dependent according to the EU legislation.
- A low mobility of Cd and As was found in wastes upon different weathering scenarios.
- Solids from DAS systems could be considered a secondary source of P and calcite.

GRAPHICAL ABSTRACT

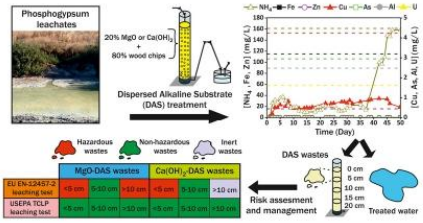

ARTICLE INFO

Handling Editor: Tsair-Fuh

Keywords:
Phosphogypsum leachates
Dispersed alkaline substrate technology
Column experiments
Metal-rich wastes
Leaching tests

ABSTRACT

A phosphogypsum stack located in SW Spain releases highly acidic and contaminated leachates to the surrounding estuarine environment. Column experiments, based on a mixture of an alkaline reagent (i.e., MgO or Ca$(OH)_2$) dispersed in an inert matrix (dispersed alkaline substrate (DAS) technology), have shown high effectiveness for the treatment of phosphogypsum leachates. MgO-DAS and $Ca(OH)_2$-DAS treatment systems achieved near total removal of PO_4, F, Fe, Zn, Al, Cr, Cd, U, and As, with initial reactive mass:volume of leachate treated ratios of 3.98 g/L and 6.35 g/L, respectively. The precipitation of phosphate (i.e., brushite, cattiite, fluorapatite, struvite and $Mn_3Zn(PO_4)_2{\cdot}2H_2O$) and sulfate (i.e., despujolsite and gypsum) minerals could control the solubility of contaminants during the treatments. Therefore, the hazardousness of these wastes must be accurately assessed in order to be properly managed, avoiding potential environmental impacts. For this purpose, two standardized leaching tests (EN-12457-2 from the European Union and TCLP from the United States) were performed. According to European Union (EN-12457-2) regulation, some wastes recovered from DAS treatments should be classified as hazardous wastes because of the high concentrations of SO_4 or Sb that are leached. However, according to United States (US EPA-TCLP) legislation, all DAS wastes are designated as non-hazardous wastes. Moreover, the solids generated in the DAS systems could constitute a promising secondary source of calcite and/or P. This research could contribute to worldwide suitable waste management for the fertilizer industry.

* Corresponding author.
E-mail address: ricardo.millan@dct.uhu.es (R. Millán-Becerro).

https://doi.org/10.1016/j.chemosphere.2022.133876
Received 12 July 2021; Received in revised form 24 November 2021; Accepted 2 February 2022
Available online 4 February 2022

Phosphogypsum weathering and implications for pollutant discharge into an estuary

Ricardo Millán-Becerro, Rafael Pérez-López, Carlos R.Cánovas, Francisco Macías, Rafael León

Department of Earth Sciences & Research Center on Natural Resources, Health and the Environment, University of Huelva, Campus 'El Carmen', 21071 Huelva, Spain

Submitted to: Journal of Hydrology

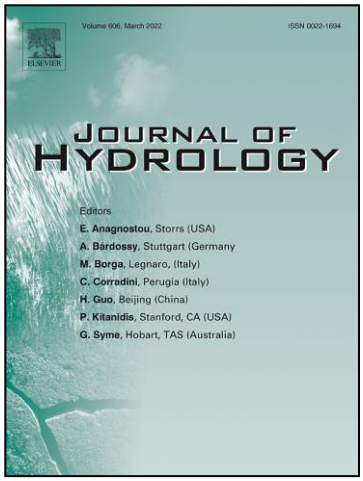

Publisher: ELSEVIER, RADARWEG 29, 1043 NX AMSTERDAM, NETHERLANDS

Editors-in-Chief: Professor Emmanouil Anagnostou, Professor András Bárdossy, Professor Nandita Basu…

ISSN: 0022-1694

EISSN: 1879-2707

Journals Metrics:

CiteScore: 7.8

Impact Factor (2020): 5.722

5-year Impact Factor: 6.033

JCR® Category	Rank in Category	Quartile in Category
WATER RESOURCES	8 of 98	Q1
GEOSCIENCES, MULTIDISCIPLINARY	18 of 200	Q1
ENGINEERING, CIVIL	11 of 137	Q1